New Dynamical Monte Carlo Renormalization Group Method

by

Martin Daniel Lacasse

Department of Physics, McGill University

Montréal, Québec

Canada

A Thesis submitted to the

Faculty of Graduate Studies and Research

in partial fulfillment of the requirements for the degree of

Master in Science

À Isabel,

Linda,

et Germaine

Abstract

The kinetics of a phase transition has been studied by using a new dynamical Monte Carlo renormalization group method. Using a majority rule block-spin transformation in both space and contiguous times, we numerically renormalized the evolving configurations during the phase separation of a kinetic Ising model with spin-flip dynamics. We find that, in the scaling regime, the average domain size $R(t)$ grows in time consistently with the $R \sim t^{1/2}$ Allen-Cahn antiphase boundary motion theory, although some correcting factors may exist. The same procedure has also been applied to the corresponding equilibrium critical system in order to find the critical exponent z. Our method yields values that are consistent with the ones obtained from a finite-size scaling analysis applied on the same data, thus showing that, in principle, this method can be successfully used to determine z in a more precise and consistent way.

Résumé

La cinétique d'une transition de phase a été étudiée à l'aide d'une nouvelle méthode dynamique Monte Carlo du groupe de renormalisation (MCRG). En utilisant une règle de majorité afin de réduire à un seul spin des cellules de spins formées de spins contigus dans le temps et l'espace, nous avons renormalisé les configurations successives d'évolution d'une séparation de phase simulée par un modèle Ising cinétique à excitation locale (*spin-flip*). Nos résultats indiquent que dans la région dite d'échelle de la courbe de croissance, la grandeur moyenne des domaines $\bar{R}(t)$ croît dans le temps en accord avec la loi de croissance $R \sim t^{1/2}$ prévue par la théorie du mouvement des antiphases de Allen et Cahn, quoique l'existence d'un facteur de correction ne soit pas exclue.

Le même procédé a aussi été appliqué au problème correspondant de dynamique critique à l'équilibre afin de déterminer la valeur de l'exposant critique z. La méthode utilisée donne des résultats qui sont en parfait accord avec une analyse de taille finie effectuée sur les mêmes données. Ceci nous porte donc à croire que cette méthode pourrait, en principe, être utilisée pour déterminer z avec plus de précision.

Contents

List of Figures

List of Tables

Acknowledgements

It is with great pleasure that I thank Jorge Viñals and Martin Grant, without whom this thesis would not have been possible. Not did only Jorge make Tallahassee more than what it really is by being a wonderful host, but working with him was a real everyday pleasure throughout my stay at SCRI. Also, I cannot forget Martin's patience, and the conviction he surely needed to have that I would end up doing something. Working with him has been an experience which I am ready to renew. I would also like to mention the admiration and the gratitude I have for Betty Pedersen and Diane Koziol for keeping on being so happy while doing so many things at the same time.

Moreover, I would like to thank Eugenia Corvera and Karen Pflug with whom I shared my first year sufferings and for nevertheless staying good friends afterwards. Special thanks to my *dear friend* Yao Jian Hua and also to Ren Hong with whom I learnt and shared the moment of a too short chinese revolution, to Ahmed Houari and Bruno Grossmann for their everyday kindness, to Loki Jörgenson for being what he, and nobody else, is and for pushing me forwards in the UNIX's Gods and Daemons realm, to Ross Thompson for special lessons of *everyday English*, Diane Fraser for making LaTeX still more accessible, Sun Tao for his sunny smile, Mohamed Laradji for his unforgettable cracking shoes, and to all the others who made my stay at McGill enjoyable, Tony Yang, Mao Ming, Steve Brauer, Jacques Mainville, Yi Zhao, all the others I might have forgotten, and last but not least Ricardo Ignacio Alvarez del Castillo Astiazarán.

Through this work, it has been a pleasure to work with good reference post doctoral fellows, in particular Emilio Hernández-García for a nice cooperation and

helpful suggestions, Ken Elder who has always been keen to teach the art of Langevin equations, and the eternal Ian Graham who, among many things, changed the life of the department by spreading the Iris virus. It has also been a pleasure to learn from McGill professors in particular Martin Zuckermann, Martin Grant, Robert Sharp and Hong Guo who all are exceptional persons of their kind.

I cannot forget to mention the patience Linda demonstrated during these years and for having given more than her share of care to our son Isabel. I also have to express my gratitude to Geoff Soga for the calming effect he exerts on his surroundings and for untangling the grammatical part of this thesis.

Finally, I would like to thank the Natural Sciences and Engineering Research Council which provided financial support during these two years. Part of the calculations reported in this thesis have been performed at the Supercomputer Computations Research Institute. This work has been supported in part by SCRI, which is partially funded by the U.S. Department of Energy, contract No. DE-FC05-85ER25000.

Chapter 1

Introduction

It has been a long way from the origin of the world to the way things look today. Throughout the evolution of matter, transformations involving less and less energy were involved. As a result, most of the transformations that can be observed from our tiny space-time scale point of view are due to electromagnetic forces.[1] This is the case, for example, in chemical reactions and, at an even lower energy level, in phase transformations.

Most of these transformations are characterized by some sort of discontinuity. Unfortunately, the idea of continuity is embedded in the major part of the physics developed in the last centuries. The invention and the success of calculus in physics has put this constraint on most representative functions. An even stronger conceptual problem arises when one considers the time-reversal symmetry of all classical and quantum theories in opposition to the second law of thermodynamics. This suggests that these theories are still incomplete and that some cosmological factor might have to be considered (Landau and Lifshitz 1981). These remarks show, however, that the theory of phase transitions is one of the most challenging problems nowadays.

The present century has seen the birth of various new techniques and major dis-

[1]The effects of gravitation on usual phase transitions are still not well understood. Most of the experiments conducted under microgravity yield unexpected results. The explanation of this failure may reside in the presence of residual effects from the environment (Viñals 1990). Only a few treatments (e.g. (Siggia 1979)) take gravity into account in the analysis of phase transitions. Phase transitions resulting from gravitation only (cosmological) will not be considered in this work.

coveries, from cryogenics to nuclear reactions, that permitted the exploration of new regions of the temperature spectrum. New classes of interesting phenomena were discovered and that added more complexity to the existing problem. As a result, more attention has been given to the topic and important progress in understanding equilibrium critical phenomena has been made. Good (but old) reviews can be found in articles by Fisher (1967) for the theoretical side and Heller (1967) for the experimental counterpart.

The main difficulty in the study of static critical phenomena is that the existing "mean field" approximation theories cannot be improved without yielding a problem more difficult than the original one. A way to get around this difficulty is to use a symmetry approach. One important step in this direction was made by the renormalization group[2] (RG) theory. This theory tackles the problem by analyzing the renormalized free energy resulting from an interaction scale transformation. Combined with Monte Carlo techniques, this new tool gave valuable results as first shown by Ma (1976a). The resulting Monte Carlo Renormalization Group (MCRG) theory has been applied to many problems since then. A brief review will be presented.

Comparatively little is known about the dynamics of phase transformations. Very long relaxation times and the divergence of some of the macroscopic variables near the critical point make the subject even more difficult. However, because of the great interest from metallurgy and the material sciences, there have been many encouraging attempts to understand the dynamics of some phase transitions. In addition, the success of the RG methods in the static case justified their extension to dynamics, and their application has yielded interesting results. Nonetheless, the mathematical foundations of these techniques is still an open problem.

[2]Formally, it is a semi group.

1.1 Description of the problem

If a system is suddenly cooled down, from a temperature at which it is normally found to be in a disordered state, to a temperature at which it is normally found to be in an ordered state, then order starts to develop in time. It is well known that the rate of cooling, as well as the temperature of the final state, have a determinant effect on the way order is set up.[3] In a binary substance[4] , domains of two different compositions will start to form and grow in time, thus forming a pattern that can sometimes be interpreted as the signature of the transition that occurred.

Experiments on Cu-Au[5] and Al-Zn[6] binary alloys for example, as well as computer simulations, show that at "late" times, i.e. times for which the ordering involves long range order rather than ordering in the vicinity of a point, the average domain size $\bar{R}$ fits a power law with respect to time. The growth exponent n in $\bar{R}(t) \sim t^n$ is believed to be one of the characteristics that can be used to separate these phase transitions into universality classes. Moreover, when the distances over the system are measured in units of $\bar{R}(t)$, then the time dependence of certain functions involving space and time disappears. For example, the order parameter correlation function[7] g often "scales" as $g(\boldsymbol{r}, t) \sim f(\boldsymbol{r}/\bar{R}(t))$.

The problem of such an order-disorder or phase transition is of fundamental interest in the field of statistical mechanics of non-linear phenomena far from equilibrium. Moreover, this problem is of practical interest in metallurgy and surface science

In this thesis, we shall be concerned with aspects of growth and scaling in order-disorder transitions during which the order parameter does not follow any conservation law. For such systems, theoretical models have been proposed on the basis of various approaches. Considering the movement of the interfaces, Allen and Cahn

[3]For example, there exist millenial Japanese ceremonies that specifically show, to the samurai, how to harden his sword.

[4]A lot of "hands on" science exhibitions contain a binary fluid system of aniline and cyclohexane that becomes immiscible in all proportions below a certain temperature

[5]This system tends to order in an .. $ABABA$... fashion below a certain temperature

[6]These two metals become immiscible below a certain temperature and start to separate in two distinct phases. This process has a signature different from the preceding one

[7]The definition of this function will be found in Chapter 2

(1979) proposed an antiphase boundary motion theory, that had partly been developed earlier by Lifshitz (1962), which predicts a value of $n = 1/2$. Similarly, phenomenological studies (Valls and Mazenko 1986) involving stochastic equations for the relaxation of the system lead to the same prediction.

Much effort has been devoted to developing new computer simulation techniques and models. The advent of more powerful computers, as well as the ease with which the various microscopic-mesoscopic discrete models can be implemented on any of these number-crunching machines, strongly contributed to this state of fact. Moreover, only a few of the models used have a complete analytical solution, so that the results obtained from numerical studies are of prime importance in the development of this field. One of these models, the Ising model, has been thoroughly investigated since it undergoes a "real" phase transition in two dimensions and above.

The numerical *Monte Carlo* techniques, employed in different models, involve the generation of random numbers which are then used to perform the integration of a function that involves a huge number of variables (static model) or to generate successive states in a probabilistic way which can then be mapped to a real time evolution of the physical phenomenon (dynamical model). In practice, these two cases are very similar and the main difference remains in interpretation. Dynamic investigations of the Ising model are more recent than the static ones and have been carried out using different techniques including RG, finite-size scaling, spreading damage algorithms, conformational invariance mapping, series expansions, MCRG and matching algorithms, among others. Some of these approaches will be described further on.

Working from the Ising model, a new dynamical Monte Carlo renormalization group method will be presented. Results obtained from a two-dimensional — square lattice, periodic boundary conditions — model undergoing phase transitions far from its critical temperature T_c will be given and analyzed. The problem of critical slowing down, as well as the concept of scaling in dynamic phenomena, will be presented in order to pave the way for the straightforward extension of the method to critical dynamic phenomena.

1.2 Outline of the thesis

The structure of the following chapters is as follows. Chapter 2 will give a brief overview of phase transitions as well as a short description of critical phenomena. The standard thermodynamic approaches will be presented, including some approximation methods referred to as mean field theories. Scaling relations, both for critical phenomena and first-order phase transitions will be described on the basis of the scaling hypothesis or self-similarity.

Chapter 3 will be a thorough presentation of both the theoretical and practical aspects of a computer simulation study of the Ising model. Monte Carlo methods will be formally described and finite-size effects briefly summarized. The concept of *blocking*, in view of the application of RG methods, as well as the phenomenological approaches given by Langevin equations, will be discussed in the framework of the kinetic interpretation of the Ising model.

Real space renormalization group methods will briefly be explained in Chapter 4, starting from the standard one- and two-dimensional Ising models. Although very descriptive, this formal presentation will lead the way to the Monte Carlo RG techniques that will be used in subsequent chapters.

Chapter 5 will give a short theoretical description of critical dynamics by describing the conventional theory of critical dynamics as well as the dynamic scaling hypothesis. The remaining part of this chapter will serve to present the most recent developments in the evaluation of the critical exponent z.

The following chapter will deal with the kinetic aspects of first order phase transitions. Chapter 6 will concentrate on the theories of growth for a order-disorder transition where the order parameter is not conserved. The technical aspects of such computer simulations will also be introduced.

Original results made in the framework of this research will be presented in Chapter 7. A new MCRG method involving blocking both space and time will be described and applied to the two problems presented in Chapter 5 and 6. The method will first

be applied to the dynamics involved in a quench and comparisons will be made with the predictions of the Allen-Cahn antiphase boundary motion theory. The technical aspects of numerical simulations, as well as preliminary results for the value of the critical exponent z, will be given.

Lastly, Chapter 8 will evaluate the scope of this method and discuss its validity in comparison to other standard techniques. Some theoretical questions concerning the foundations of this process will also be discussed. New avenues of analysis, concerning the probabilistic aspects of a quench and special symmetries found at early and medium times of a quench, will also be presented.

For the sake of completeness, a detailed description of the algorithms as well as a *C* version of the code have been included as an Appendix. I hope this inclusion, as well as the complete thesis, may be of some help or some inspiration to new students starting numerical simulations from scratch.

Chapter 2

General Overview of Phase Transitions

The idea of a what a phase transition is evolved during the last century, as new developments occurred in the field of critical phenomena. This chapter will give a general overview of phase transitions and critical phenomena. The major characteristics of the conventional approaches will be briefly described in connection with the contents of subsequent chapters.

2.1 Thermodynamics of phase transitions

This section will give a brief outline of the standard equilibrium treatment of a phase transition. We first give the general classification of phase transformations. [1]

Phase transformations, undertaken at a temperature T and a pressure P, which can be characterized by a latent heat $T\Delta S$ and a sudden specific volume[2] change are said to be of the first order. Since the volume V and the entropy S can be obtained from the Gibbs potential G as $V = (\partial G/\partial P)_T$ and $S = (\partial G/\partial T)_P$, Ehrenfest first

[1] A complete description of the specific nomenclature of phase transformations between different phases is given in (Doremus 1985).

[2] Or the equivalent parameter. Note that the whole treatment can describe a magnetic system by the usual change $P \rightarrow -h$ and $V \rightarrow M$, where h is the magnetic field, and M the magnetization

proposed to classify phase transitions according to the order of the derivative(s) of the thermodynamic potential that has a discontinuity (a jump). However, we now know that critical transformations involve some higher derivatives which are infinite rather than discontinuous. Moreover, the intrinsic nature of the singularity is part of the central problem of the theory of critical phenomena. These phenomena have, nevertheless, all been included in second-order phase transitions and this wider classification, according to Fisher (1967), now means "not of the first order".[3] Some typical diverging second order derivatives are the compressibility or susceptibility, the specific heat, the expansion coefficient, and so on.

Consider now an A-B mixture (e.g. liquid-gas) of given chemical potential μ and at pressure P. At a first order phase transition, this system will be characterized by the equilibrium condition of the two phases, i.e.

$$\mu_A(P,T) = \mu_B(P,T).$$

This equation implies there exists an equilibrium coexistence curve $P = P(T)$. The possible existence of an equilibrium allows us to write

$$d\mu_A(P,T) = d\mu_B(P,T)$$

from which one can obtain the Clausius-Clapeyron equation by expanding the differentials:

$$\frac{dP}{dT} = \frac{s_A - s_B}{v_A - v_B} = \frac{\Delta H}{T(v_A - v_B)}$$

where s and v are respectively the entropy and the volume per particle and ΔH is the latent heat of the transformation. More generally, for a system under an intensive force X coupled to a parameter x, one has

$$\frac{dX}{dT} = \frac{\Delta s}{\Delta x}. \tag{2.1}$$

An important application of this equation is the determination of the dependence of the pressure on the transition temperature.

[3] We exclude, of course, the infinite-order Kosterlitz-Thouless transition.

Unlike first-order transitions, second-order transitions have no volume or entropy discontinuity. They are therefore reversible. The belief that the thermodynamic functions were continuous throughout, except for a jump at the transition point, was used by Ehrenfest to derive equations relating the finite discontinuities of the derivatives among themselves. This is done using l'Hopital rule with respect to both T and V on the indeterminate form 0/0 of equation (2.1). This approach is however obsolete in view of the nature of some of the singularities found.

Thermodynamics[4] deals with system in equilibrium. For example, the general condition for stable equilibrium for a closed system at T, P constant is to be in its state of minimum Gibbs potential.[5] Therefore, for any small fluctuation in $G = U - TS + PV$, where U is the internal energy, we must have,

$$G' - G = U' - U - T(S' - S) - P(V' - V) > 0.$$

Now assume we change T and P to T' and P' in order to get a state G' for which we have S' and V'. Since this state must be stable too, we must have, for the state G close to G'

$$G - G' = U - U' - T'(S - S') - P'(V - V') > 0.$$

Adding term by term

$$\Delta T \Delta S - \Delta P \Delta V > 0. \tag{2.2}$$

At fixed T and P, this merely says that the heat absorbed must always be greater than the work done. This last equation suffices to fix the stability of a system. At constant T and constant P, one gets respectively

$$\begin{aligned} (\partial P/\partial V)_T &< 0, \\ (\partial T/\partial S)_P &= T/C_P > 0. \end{aligned} \tag{2.3}$$

Since equation (2.2) is of general validity, it can also be divided by ΔV^2 at constant

[4]Despite its name... Historically, *dynamics* was justified from the movement induced by steam engines.

[5]The same derivation can be made with any two constant parameter and the corresponding thermodynamic potential

S and vice-versa yielding

$$\begin{aligned} (\partial P/\partial V)_S &< 0, \\ (\partial T/\partial S)_V &= T/C_V > 0. \end{aligned} \tag{2.4}$$

The thermodynamic approach to critical phenomena involves considering the limit of stability when, for a homogeneous system, the two phases become identical. Formally, this can be taken as the case of equality of the above equations and a set of equations characterizing the critical point can thus be obtained.

2.2 Further stability considerations

Gases are among the substances which were thoroughly investigated during the last centuries but, even if their behaviour at high T was well understood[6] , a complete theory explaining their behaviour at a phase transition was not developed. The van der Waals theory of phase transition had a strong influence on the subsequent theories.[7] His famous equation

$$\left(P + \frac{a}{V^2}\right)(V - b) = RT,$$

where a and b are constants, can be related to an elementary cusp catastrophe (Pippard 1985), because of the instability loop it produces. It could be derived rigorously in one dimension by assuming a hard-sphere repulsive potential and an attractive potential of the form $-a\gamma e^{-\gamma r}$. The result comes out in the $\gamma \to 0$ limit, i.e. for a

[6] Avogadro hypothesis, Boyle-Mariotte, Gay-Lussac, Dalton laws, etc...

[7] In fact, a myriad of other PV state equations appeared in the last century and, among the most useful, are:

$\left(P + \frac{a}{V^2 T}\right)(V - b) = RT$ Berthelot equation,
$P(V - b) = RT \exp^{-a/RTV}$ first and
$\left(P + \frac{a}{V^{5/3}}\right)(V - b) = RT$ second Dieterici equations,

to which enumeration one must add the exact phenomenological virial expansion in $1/V$ and in P. In addition to the description in the text, the previous success of the van der Waals equation came from the fact that it can be related to, say, the Lennard-Jones potential coefficients. Those can later be used to predict the non-universal critical parameters yielding a unique law of corresponding states in terms of reduced state variables (e.g $P/P_c, V/V_c, \ldots$). This assumption is verified by some gases as Guggenheim has shown This was one of the first manifestations of the universality concept

weak interaction of infinite range. See (Hemmer and Lebowitz 1976) and references therein for more details.

On this PV curve, Maxwell's construction (e.g. (Kadanoff et al. 1967)) defines two isobaric points, for each isotherm, such that the integral of $V\,dP$ vanishes for this interval. A complete numerical treatment in *FORTRAN* of this procedure can be found in (Schmid, Spitz and Lösch 1988). The locus of all these points forms the *binodal*. Inside this region is the locus of all points such that the isothermal compressibility $K_T = -V^{-1}(\partial V/\partial P)_T$ is infinite. Following Gibbs' interpretation, this defines the *spinodal* curve. It delineates two regions different by the sign of the compressibility. The region inside the spinodal is called unstable since, by (2.3) and (2.4), no stable state can have a negative compressibility. The other region is called *metastable* and represents an extension of the stable homogeneous state into the heterogeneous region.

As an example, consider a very poetic phase transition: the morning dew. The air, containing water vapour, gently cools down to a temperature at which it becomes saturated. At this point microscopic droplets start to form and slowly fall down under gravity. As shown by the usual PV diagram, the vapour would continuously condense by further reducing the partial volume (along the horizontal line) or by further cooling (down to another isotherm), both processes yielding portions of different phases according to the phenomenological lever rule.

This is, however, a particular case. In fact, in view of nucleation theory, when the condensing constituent is pure[8] nothing instantaneous happens (within a certain range) but a supersaturated or undercooled state forms respectively.[9] Thus, the behaviour of a phase transition is intimately bound to its dynamics and any attempt based on finding the right form of the free energy neglects this aspect. In fact, the major weakness of these theories is the absence of fluctuations. These play an important rôle in any transformation. If one brings a system to the metastable region then

[8]No wettable walls, ions, interfaces ..

[9]For example, metastable states having a pressure of 5 times the condensation pressure can be obtained experimentally for water vapour at $373K$ (Abraham 1974)

the relaxation process —it is now in a state out of equilibrium— will depend on local and finite fluctuations. These latter will help to form droplets that may continue to grow if fluctuations could drive them beyond a critical size. The characteristics of this critical droplet are related to the dimensionality and topology of the problem considered. This will be considered in Chapter 6. On the other hand, if one brings a system in the spinodal region, then the whole system will evolve in a continuous series of intermediate states, each of which is thermodynamically more favoured than the preceding one. Because of the very nature of such a mechanism, fluctuations must be infinitesimal and spread out over large regions. This difference is seen experimentally and gives distinct phenomena known as nucleation and spinodal decomposition respectively. See (Doremus 1985) for a good experimental treatment.[10] However, the distinction is not as sharp as one might expect and there is expected to be a transition region where both processes occur (Heermann 1984). The sharpness of the cut is related to the range of the interaction. Moreover, the shape of the pattern formed is not sufficient to make the distinction, since a spinodal pattern can be formed out of overlapping droplets.

2.3 The mean field approach

One main and important contribution from older theories has been the introduction of an order parameter. This is used to express the free energy of a system in a phenomenological form.[11] The principal approach consists in minimizing this phe-

[10] And pictures too!

[11] We have to stress here that this free energy *is not* the true free energy. Recall that in statistical mechanics, the latter is defined as $F(M,T) = -k_B T \log Z(M,T)$ where Z is the partition function and k_B is the Boltzmann constant, whereas it is defined as $E - TS$ in standard thermodynamics. The variable E represents the energy of the system while the others have been defined earlier. These definitions are consistent since they can theoretically be related one to the other.
When Legendre transformations are used for passing from, say, Helmholtz free energy $F(M,T)$ to Gibbs free energy $G(h,T)$, the number of thermodynamical variables required to describe the thermodynamics of the system remains constant. However, the introduction of a phenomenological free energy is generally one of the form $F(M,h,T)$. Therefore, although the same symbol has been used for both forms of free energy, it must be clear that the phenomenological form represents something different.

nomenological free energy with respect to this order parameter while including the interactions in a mean field term acting over a non-interacting system. In view of completeness and for further reference, we shall present a form of the Ginzburg-Landau free energy. The treatment given here follows the one given in Cahn (1958).

For this, assume a continuous model of a scalar field $\psi(\boldsymbol{x})$, where $\boldsymbol{x}$ is the spatial position vector. It may be thought of as the magnetization or concentration. It is further assumed that the free energy density, f, can be expressed as a sum of two contributions which are functions of the local composition and the local composition derivatives respectively. Providing f is also continuous[12] , it can be expanded about the value f_o representing a homogeneous substance. If one considers the isotropic case, then f is a scalar that must be invariant with respect to rotation. Thus only even powers of the gradient can appear. Therefore, the leading terms of the expansion are

$$f(\psi, \nabla\psi, \nabla^2\psi, ...) = f_o(\psi) + c\nabla^2\psi + d(\nabla\psi)^2 + \ldots$$

where c and d are tensors resulting from the expansion, i.e.

$$c_{ij} = \left(\frac{\partial f}{\partial \left[\partial^2\psi / \partial x_i \partial x_j \right]} \right)_o$$

and

$$d_{ij} = \left(\frac{\partial^2 f}{\partial(\partial\psi/\partial x_i)\partial(\partial\psi/\partial x_j)} \right)_o$$

that become, under the symmetry requirements,

$$c_{ij} = \begin{cases} \left(\frac{\partial f}{\partial \nabla^2\psi}\right)_o & \text{for } i = j \\ 0 & \text{otherwise} \end{cases}$$

and

$$d_{ij} = \begin{cases} \left(\frac{\partial^2 f}{\partial |\nabla\psi|^2}\right)_o & \text{for } i = j \\ 0 & \text{otherwise.} \end{cases}$$

[12]The most striking result of Onsager's solution is that the free energy has a $\ln|T - T_c|$ term when expanded, thus showing that the expansion is not possible about the singular point T_c. The fact that a first order transition point is also a singular point can be obtained by metastable nucleation arguments. See (Andreev 1964). Therefore, the assumption that the coefficients a and b are analytic in T in equation (2.6) is unjustified

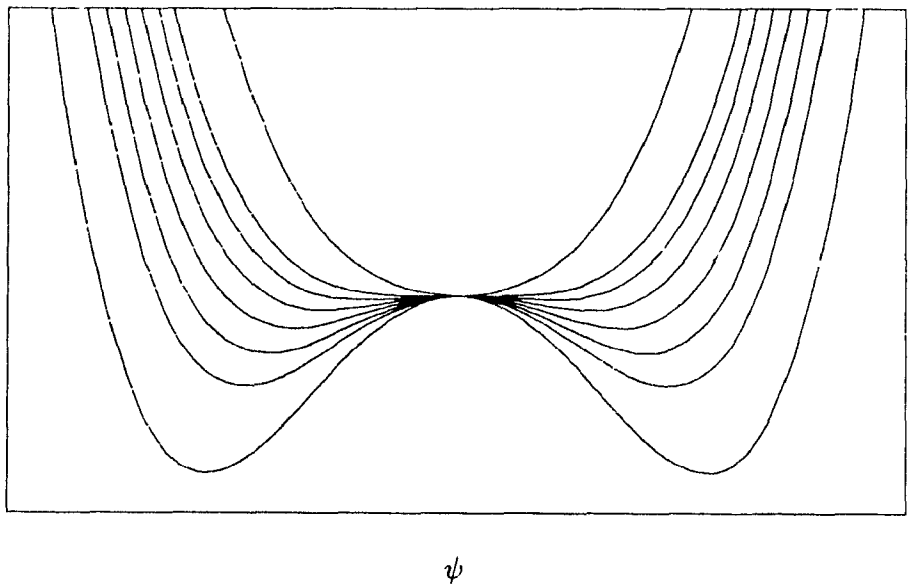

Figure 2.1: Representation of the free energy in the Landau theory of phase transitions. The second curve from the inside is at T_c.

When one integrates over the whole space, the second term can be integrated by parts and reduced, with the help of the divergence theorem, to a surface term and a $(\nabla\psi)^2$ term. The former is not relevant in the thermodynamic limit. This reduces the preceding equation to

$$F[\psi] = \int (f_o(\psi) + c(\nabla\psi)^2 + \ldots)d\boldsymbol{x} \tag{2.5}$$

where

$$c = -\frac{dc}{d\psi} + d.$$

Note that the value $F[\psi]$ depends on the form of the functions $f_o(\psi(\boldsymbol{x}))$ and $\psi(\boldsymbol{x})$ and is therefore a *functional*. The function f_o is assumed to be of the form guessed by Landau (Landau and Lifshitz 1981); i.e. an even power expansion in the order parameter with a linear coefficient $(T - T_c)$ for the ψ^2 term , thus changing its sign at T_c in order to from a double well potential. This is represented in figure 2.1. Formally,

$$f_o = \frac{a}{2}(T - T_c)\psi^2 + \frac{b}{4}\psi^4 \tag{2.6}$$

where a and b are positive constants and the numeric factors are there only to simplify the derivatives. See (Pippard 1985) for a nice analogy between equation (2.6) and el-

ementary catastrophe theory. Note that the symmetrical well implies the equivalence between the two states ψ and $-\psi$ coming out of the broken symmetry. This means that the theory is expected to be always valid near T_c where the two different phases cease to be distinct.

2.4 Critical phenomena, universality and scaling

With the help of the concept of an order parameter, all phase transitions can be described in similar terms. The order parameter takes on different values in coexisting phases and therefore jumps discontinuously in course of a phase transition. The magnitude of the jump is related to the difference between the coexisting phases, being finite for a first order transition and going to zero at a critical point. Formally, the order parameter ψ vanishes in the disordered state, and is non-zero in an ordered state, where its different values, say $\psi = \pm 1$, correspond to distinct ordered states. We shall first concentrate on critical phenomena.

2.4.1 Critical phenomena

Near the critical point, the qualitative similarity among the different phase transitions is even more apparent when one notes that the experimental results can all be written in terms of power law singularities and some critical exponents, once the order parameter is used as a descriptive variable. The similarity observed among exponents obtained from different physical phenomena suggests that all phase transitions can be divided into a small number of "universality" classes, depending upon the dimensionality of the system and the symmetries of the order states. For example, the critical exponents for a three-dimensional Ising model, which will be discussed in the next chapter, are the same no matter what the underlying lattice is.

The physical source of universality can be understood as follows. Consider, for example, a ferromagnetic system. The order parameter is proportional to the magnetization M, for which the magnetic susceptibility χ is related to the fluctuations of the

order parameter via the fluctuation-dissipation relation (e.g. (Landau and Lifshitz 1981)),

$$\chi = \beta\langle(\Delta M)^2\rangle. \tag{2.7}$$

By using the magnetic density,

$$M = \int d\boldsymbol{x}\; m(\boldsymbol{x}), \tag{2.8}$$

the susceptibility χ can be redefined as

$$\chi = \beta \iint d\boldsymbol{x}\; d\boldsymbol{x}'\; \langle \Delta m(\boldsymbol{x}) \Delta m(\boldsymbol{x}')\rangle = \beta V \int d\boldsymbol{x}\; \langle \Delta m(\boldsymbol{x}) \Delta m(\mathbf{o})\rangle, \tag{2.9}$$

where we have used translational invariance,[13] and the standard definition $\beta = 1/k_B T$, where k_B is Boltzmann's constant. It is found experimentally (Heller 1967) that the susceptibility diverges at the Curie temperature, i.e. as the system goes from a paramagnetic to a ferromagnetic state. The divergence of the susceptibility then shows, by (2.9) and the fact that $\Delta m(\boldsymbol{x})$ is bounded, that correlations must involve larger and larger regions while approaching T_c. A way to postulate universality is as follows. As the system goes to its critical point, the thermodynamic potential derivatives diverge *because* of the diverging correlation length ξ. Critical phenomena are therefore dominated by fluctuations in M which appear on scales much larger than the force range. Consequently, these fluctuations can only see certain gross features of the interatomic potential. Therefore, the determinant features of the process will be quantities such as dimensionality and symmetry.

This description leads to the idea of scaling. Since most critical phenomena can be classified into a small set of classes, the main characteristics of the transition can then be thought of as being related to common features of the models. For example, if one measures the linear dimensions of the system in units of ξ, then a "universal function" could be obtained, since the same diverging length, ξ, is responsible for all the divergences. The study of the characteristics that the free energy functional, or the equation of state, should have in order to produce the correct critical exponents leads

[13] Note that for an isotropic system the correlation function forming the last integrand would read $4\pi r^2 \langle \Delta m(r) \Delta m(0)\rangle$.

to the conclusion that it should asymptotically behave like a homogeneous function of its arguments as it gets near to the critical temperature T_c. Thus, the critical exponent inequalities, both observed and predicted from thermodynamics arguments, would be followed as equalities.

In order to illustrate this idea, we shall continue the above example for a magnetic system (Plischke and Bergersen 1989). Given a thermodynamic potential Φ which depends on the field $h = H - H_c$, and a reduced temperature defined as

$$\theta = \frac{T - T_c}{T_c}, \tag{2.10}$$

we assume that the singular part behaves like

$$\Phi(\theta, h) = \lambda \Phi(\lambda^x \theta, \lambda^y h).$$

It follows from standard thermodynamics relations (Pippard 1957) that

$$\begin{aligned} m(\theta,h) &= -\left(\frac{\partial \Phi}{\partial h}\right)_\theta = \lambda^{y+1} m(\lambda^x\theta, \lambda^y h), \\ \chi(\theta,h) &= \left(\frac{\partial m}{\partial h}\right)_\theta = \lambda^{2y+1} \chi(\lambda^x\theta, \lambda^y h), \\ C_h(\theta,h) &= -T\left(\frac{\partial^2 \Phi}{\partial \theta^2}\right)_h = \lambda^{2x+1} C_h(\lambda^x\theta, \lambda^y h). \end{aligned} \tag{2.11}$$

If one selects the special scale change $h = 0$ and $\lambda = |\theta|^{-1/x}$, then one can write, according to the previous equations and the definition of critical exponents (Stanley 1971),

$$\begin{aligned} m(\theta,0) &= (-\theta)^{-(y+1)/x} m(-1,0) \sim (-\theta)^\beta \\ \chi(\theta,0) &= |\theta|^{-(2y+1)/x} \chi(\pm 1,0) \sim |\theta|^{-\gamma} \\ C_h(\theta,0) &= |\theta|^{-(2x+1)/x} C_h(\pm 1,0) \sim |\theta|^{-\alpha} \end{aligned}$$

and similarly, with the choice $\theta = 0$ and $\lambda = |h|^{-1/y}$ get

$$m(0,h) = |h|^{-(y+1)/y} m(0,\pm 1) \sim |h|^{-\delta}\ \mathrm{sign}(h).$$

The critical exponents are therefore not all independent and they can be related by the following "scaling laws"

$$\alpha + 2\beta + \gamma = 2 \tag{2.12}$$

$$\beta(\delta - 1) = \gamma. \tag{2.13}$$

The fact that ξ diverges as $|\theta|^{-\nu}$ at T_c, combined with the hypothesis that ξ is the only characteristic length, leads to the conclusion that the system has to be scale invariant at this temperature. The application of the scaling hypothesis is facilitated by using the ideas of scale transformation and dimensional analysis.

As a last example, consider a scale change of a factor b. Because the system has to be scale invariant at T_c, we assume that the effective field h' and temperature θ' after the scale transformation will be given by

$$\begin{aligned} \theta' &= b^x\theta \\ h' &= b^y h \end{aligned}$$

for which scale invariance $(0 = 0)$ holds at T_c. Since the free energy is an extensive function, we must also have

$$\Phi(\theta, h) = \frac{1}{b^d}\Phi(b^x\theta, b^y h).$$

On the other hand, under the same scale change, the correlation length rescales as

$$\xi(\theta, h) = b\xi(b^x\theta, b^y h).$$

Now choose a factor $b = |\theta|^{-1/x}$ and $h = 0$ to obtain

$$\begin{aligned} \Phi(\theta, 0) &= |\theta|^{-d/x}\Phi(\pm 1, 0) \\ \xi(\theta, 0) &= |\theta|^{-1/x}\xi(\pm 1, 0) \sim |\theta|^{-\nu} \end{aligned}$$

from which follows $\nu = 1/x$. By using the last equation of (2.11) on the free energy we get $\alpha - 2 = d/x$. The relation thus obtained is called the hyperscaling relation and involves dimension

$$d\nu = 2 - \alpha. \tag{2.14}$$

A scaling relation also exists for the so-called correlation function

$$g(\theta, h, r) = \langle \sigma_o \sigma_r \rangle - \langle \sigma_o \rangle \langle \sigma_r \rangle$$

and has the functional form

$$g(\theta, h, r) = \frac{1}{b^{2-d-\eta}} g(b^x\theta, b^y h, r/b) \tag{2.15}$$

near T_c.

2.4.2 Scaling in first order phase transitions

The idea of scaling proved so useful in the study of critical phenomena that it has been extended to first order phase transitions. The central idea, equivalent to the notion of scale invariance at T_c in critical phenomena, is the concept of self-similarity. That is, we assume that all the parts of the system grow in the same ratio for all times within the scaling regime. Thus, a scale change will automatically induce a time rescaling in the case of dynamical growth phenomena. Figures 2.4.2 and 2.4.2 illustrate this idea.

As a measure of correlation, we shall use the time-dependent structure factor $S(k,t)$ which is simply the Fourier transform of the correlation function g. It is more convenient to use, since the wave regularity of the covariance between the local fluctuations over the whole space is thus extracted. The variable k is used as the wave number. In view of what has been said before, we assume that the structure factor can be expressed as a function of the wave number, the mean domain size R and the dynamic correlation length $\xi(t)$. By using the same scaling method and dimensional analysis we used before, we can write, after a scale change by a factor b,

$$S(k,t) = f(k,\bar{R}(t),\xi(t)) \tag{2.16}$$

$$= b^d f(bk,\bar{R}(t)/b,\xi(t)/b). \tag{2.17}$$

We now choose a scale change such that $b = \bar{R}(t)$ so that

$$S(k,t) = \bar{R}(t)^d f(k\bar{R}(t),1,\xi(t)/\bar{R}(t)).$$

The idea that the mean size of the domains will be the only dominant length eliminates the dependency of the last argument since it should be related to the former by some function, i.e.

$$S(k,t) = \bar{R}(t)^d f(k\bar{R}(t)). \tag{2.18}$$

This scaling law is different from the above scaling laws in two aspects. One is the time dependence of the characteristic length $\bar{R}(t)$. The other is the irrelevancy of the correlation length ξ of the order parameter fluctuations; equation (2.18) is only

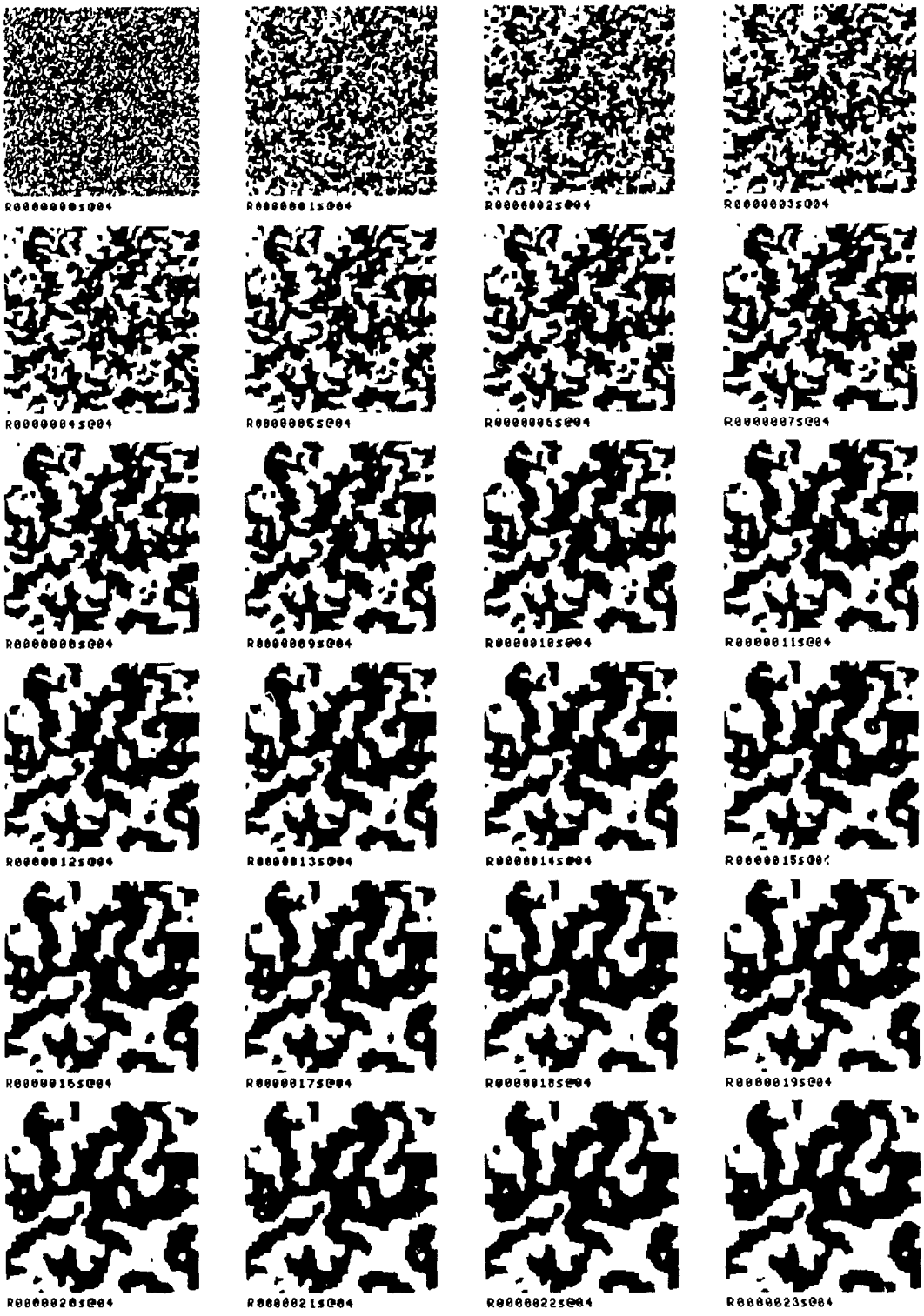

Figure 2.2: The time evolution of a bi-dimensional ferromagnetic Ising model. The system of size 128×128 was put in contact with a heat bath at $0.6T_c$. Note the similarity of a mentally enlarged piece of an early configuration with a later one. The time scale goes from 0 to 23 mcs.

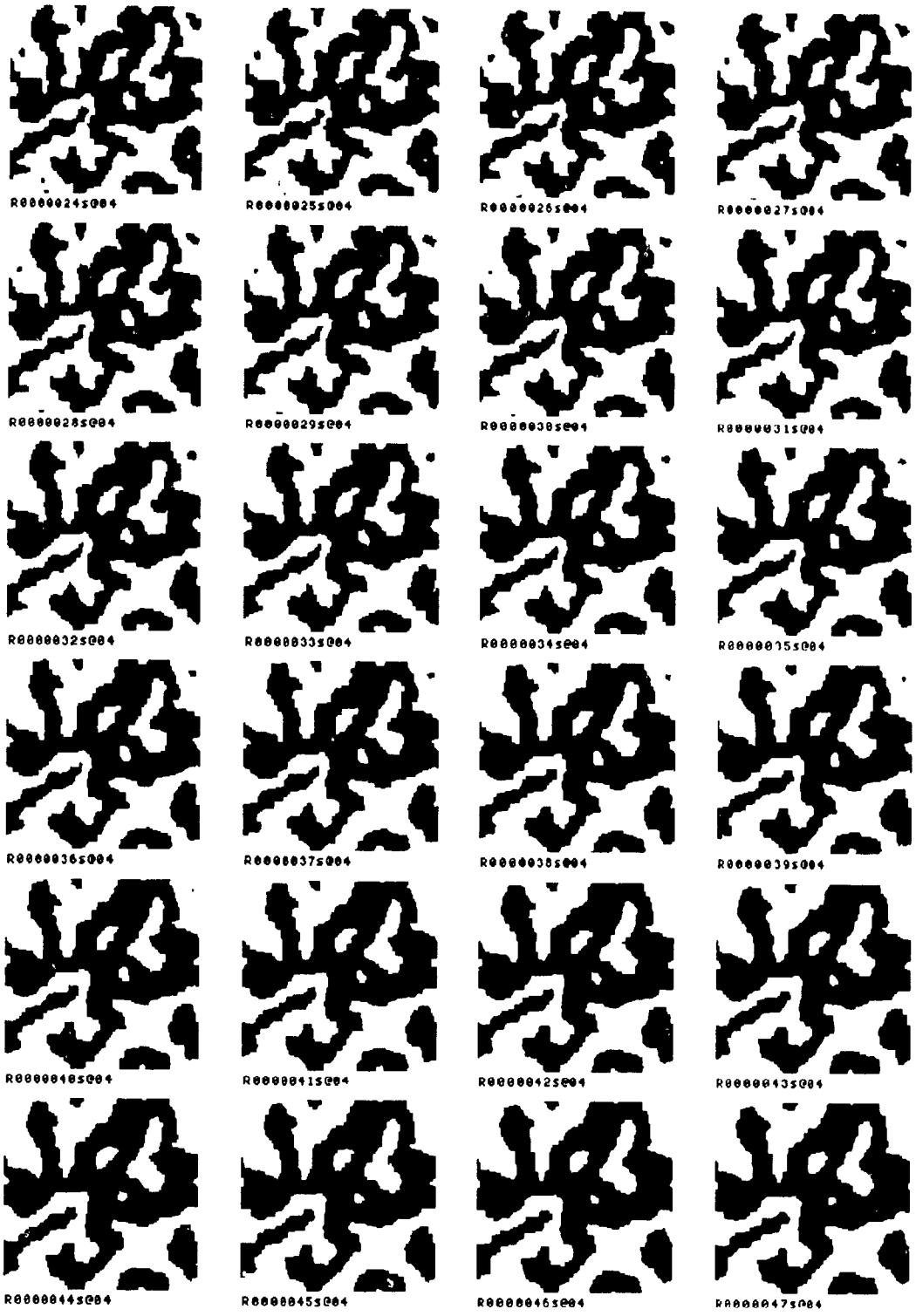

Figure 2.3: The same as the preceding figure. The time evolution is from 24 to 47 mcs. Note how the discreteness of a cubic lattice favors the creation of diagonal interfaces.

found to hold in a scaling region for which $k\xi << 1$, so that $\bar{R}(t) >> \xi$ is the only characteristic length of the problem.

This scaling law will serve as the main ingredient of the dynamic MCRG method used in the study of a first order transition. This will be presented in a following chapter.

Chapter 3

The Ising Model

The Ising model has been an important model in the study of critical phenomena. Indeed, it is the first non-trivial model to have been solved completely.[1] Its complete solution in two dimensions served as a reference result for all the subsequent approximation theories.

Lenz invented this model based on ferromagnetic considerations. Lenz' student, Ising (1925), published the solution of this model in one dimension, and concluded the model was not good enough to show a ferromagnetic behaviour... The complete history of the Lenz-Ising model as well as its developments can be found in (Brush 1967).[2]

Although the two-dimensional equilibrium Ising model can be a good approximation to some physical systems, the kinetic Ising models should not be regarded as models faithfully describing phenomena occurring on small and large length scale in real physical systems. Indeed, as some authors remarked (e.g. (Kawasaki 1972)), the value of those models lies in the fact that these provide us with precisely defined mathematical models in which no statistical approximation of cooperative effects enter. However, provided the universality hypothesis holds, the scope of applicability is large. The rareness of valuable experimental dynamic information from two

[1] Some other non-trivial systems to have a solution are the triple-spin triangular model and the symmetric 8-vertex model (Baxter) in 2D as well as the spherical model in 3D

[2] It also contains photographs of Ising and Lenz for your collection album .

dimensional systems (e.g. adatoms, surface science) and layers (e.g. films, interfaces) should also be noted.

3.1 Description of the model

In spite of its relative simplicity, the Ising model shows phase transformation behaviour. The basis of this model is a d-dimensional lattice having its topology given by the choice of the boundary conditions and the elementary cell. To each of the nodes is mapped a variable[3] that can take discrete values. The discreteness of this variable is intimately related to the modes involved in the transition. In particular, it is responsible for the fact that a discrete symmetry group (reflection) is broken at the transition point.[4]

In a general way, the exchange energy between the sites is included in a Hamiltonian of the form

$$\mathcal{H} = \frac{1}{2}\sum_{i}^{N}\sum_{j}^{N}\epsilon_{ij}(\sigma_i,\sigma_j)\ \sigma_i\sigma_j - h\sum_{i}\sigma_i \tag{3.1}$$

where the sum is over the N sites, $\sigma_i = \pm 1$, h is proportional to the external field and $\epsilon_{ij}(\sigma_i,\sigma_j)$ is the i-j interaction function. The latter can vary over the lattice thereby representing inhomogeneous cases.[5] However, we will mainly be concerned with the homogeneous case (i.e. $\epsilon_{ij} = \epsilon\ ,\forall i,j$). This way, the interaction may be thought of as a square well potential when, in addition, one only considers nearest neighbours. Thus, the model represents a domain of a strongly anisotropic homogeneous ferromagnetic substance.[6] This crude view seems nevertheless a good approximation to some other physical systems. The interaction function can also be taken as a "U" potential minimized when the spin are on the nodes so that continuous values for spin position

[3] Often called spin

[4] A broken symmetry involving a continuous symmetry group gives rise to a spectrum of zero energy collective modes such as spin waves for the Heisenberg model (rotation group), for example These are the so-called Goldstone excitation modes. See (Brout 1965) for example.

[5] E g spin glasses composed of some ferromagnetic and some antiferromagnetic sites.

[6] Note that a "real" ferromagnetic transition is also accompanied with a volume change called *magnetostriction* This is one more argument in favour of symmetry breaking in a transition. The crystal even looses its cubic symmetry in Fe, for example

can be used, thus allowing the use of an electronic probability density. See (Ma 1976b) for details.

This model has been studied in many dimensions (up to 7...) and over various lattices. These investigations found the lower and upper critical dimensions of the model. The former, i.e. the dimension below and at which no phase transition can occur is one. In fact, Landau (1981) showed, some time ago, that no phase transition can ever occur in one dimension. It turns out however that the lower critical dimension depends on the symmetry of the order parameter.[7] The upper critical dimension is the dimension beyond and from which the behaviour of the occurring phase transition can be exactly described in terms of mean field theories.

Even if the model can be seen as a nice and challenging mathematical problem, physicists are concerned with applicable models. The models in 1, 2 and 3 dimensions can serve as a representation, although sometimes crudely, of some specific physical systems. We shall concentrate on the homogeneous two-dimensional zero field model with a Hamiltonian given by

$$\mathcal{H} = \frac{\epsilon}{2} \sum_{i=1}^{N} \sum_{j=1}^{\gamma} \sigma_i \sigma_j \tag{3.2}$$

where the sum is carried out over the γ nearest neighbours. For the rest of this work, we shall assume a two dimensional model unless stated otherwise.[8]

Due to historical reason, the two cases $\epsilon < 0$ and $\epsilon > 0$ are called ferromagnetic and antiferromagnetic respectively. There is however a slight difference in the order parameter for these two cases. In the first place, it is defined as the average $\langle \sigma_i \rangle$ over the system whereas it is defined as the same average over different superlattices in the second.[9] The latter is sometimes referred to as the *staggered magnetization*. The same models can be used to represent other physical systems. For example, a crude liquid-gas transition model called *lattice gas* can be mapped to the first case or a $ABABA\ldots$ binary alloys can be mapped to the second. These homomorphisms

[7]The lower critical dimension is 1 for a system involving a discrete order parameter and at least 2 otherwise.

[8]Note that in this case and for $\epsilon = 1$, the value of the energy per spin $\langle \mathcal{H} \rangle / N$ is equivalent to the nearest neighbour correlation function estimated over the system.

[9]E.g. both even or both odd *row*, *column* for a 2-d square lattice.

are well described in (H ıang 1987) and (Gunton and Droz 1983) respectively.

Finally, note that the definition of such a Hamiltonian does not define any dynamical behaviour. This will be seen more formally in Section 3.4.

3.2 The equilibrium Ising model

This section shall be devoted to the investigation of the model with different approaches. A good and complete analysis of the Ising model under mean field theories can be found in (Plischke and Bergersen 1989). We will only consider here the cases relevant to the following chapters.

3.2.1 The exact solution

Since the Ising model is special in the sense that it has an exact solution, and also for completeness, we shall start by giving the results for the two-dimensional zero field case, as obtained for the first time by Onsager[10] (1944). Simpler and more elegant methods involving a transfer matrix have been published since and the curious reader will find all the details in the following references (Stanley 1971; Huang 1987; Plischke and Bergersen 1989). The solution of the 3-D model is still an open challenge.

The internal energy per spin $u(T)$ is found to be, using $\beta = 1/k_B T$, $K = \beta\epsilon$ and $q(K) = 2\sinh(2K)/\cosh^2(2K)$

$$u(T) = \epsilon \coth(2K)\left[1 + \frac{2}{\pi}(2\tanh^2(2K) - 1)K_1(q)\right] \tag{3.3}$$

where

$$K_1(q) = \int_0^{\pi/2} \frac{d\phi}{\sqrt{1 - q^2\sin^2\phi}}$$

is the complete elliptic integral of the first kind which may be evaluated numerically. Note that u is an even function with respect to ϵ. The spontaneous magnetization is

[10] As a counterpart to the cold fusion story, it may be worth noting that Onsager was a chemist.

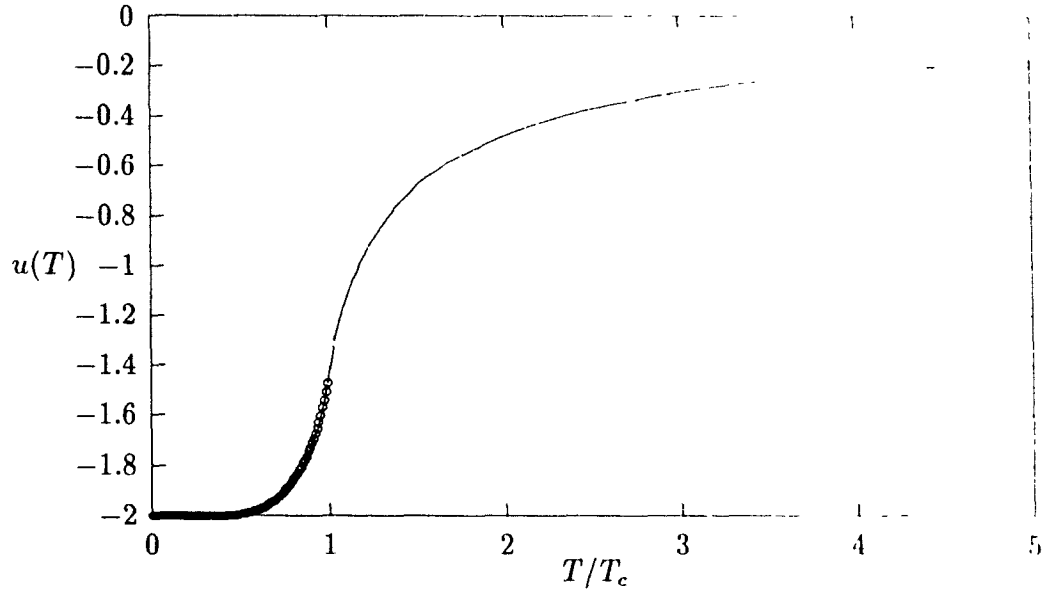

Figure 3.1: Energy per spin for the Ising model at different temperatures. The solid line is obtained from a numerical integration of equation (3.3). The data points correspond to a simulation on a ferromagnetic system of size 64 × 64

given by

$$m_0(T) = \begin{cases} [1 - (\sinh(K))^{-4}]^{1/8} & T < T_c \\ 0 & T > T_c \end{cases} \tag{3.4}$$

where

$$T_c = \frac{-2k_B}{\epsilon \ln(\sqrt{2}-1)} \simeq 2.2691 \frac{k_B}{\epsilon}. \tag{3.5}$$

The magnetization as well as the energy are shown on figures 3.2 and 3.1 respectively The solution itself is a mathematical tour de force, and is considered a landmark in the study of critical phenomena. This showed explicitly that a singularity in the free energy can emerge from a non-singular Hamiltonian. Since then, a major challenge has been to show how the non-analyticity develops in the course of a second-order phase transition.

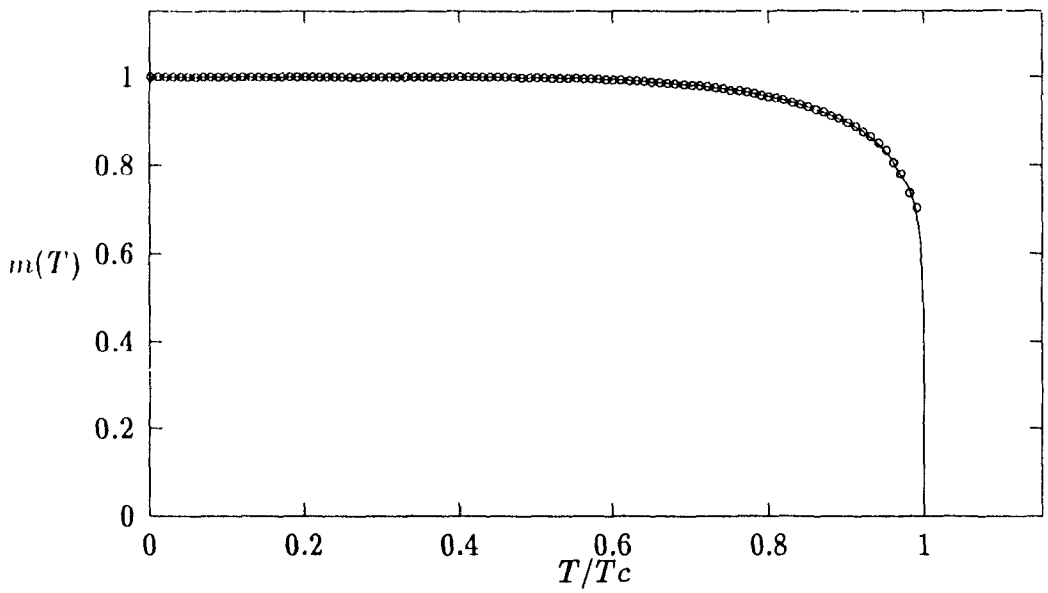

Figure 3 2. Magnetization of the Ising model. The solid line is obtained by plotting equation (3.4) The data points are extracted from the simulation mentioned in figure 3.1. They represent an average on 320 systems.

3.2.2 A continuum approximation

All materials possess magnetic behaviour due to the orbital and spin magnetic momenta of the electrons.[11] Although theories on ferromagnetism can involve band theory or Hartree-Fock approximation methods, the essentials of the cooperative behaviour can be explained by considering the coupling of only two electrons. In this regard, the Ising model, though it is in some sense a microscopic description, is already a rough approximation over the various degrees of freedom of the atom. But the details of the microscopic interactions are not the crucial point to cooperative phenomena. Therefore, one can go a little bit further by taking an arithmetic mean over small regions of space[12] , thus smoothing the discreteness of the model and "integrating out" the short wavelengths of spatial fluctuations. This method can be seen as a one way scale change operator and will be physically meaningful as long as the choice of the new block size is not larger than the correlation length. It has the ad-

[11]The nucleus magnetic momentum can be ignored since it is several order of magnitude smaller, though very important in NMR.

[12]This method is usually called *coarse graining*.

vantage that the resulting variable, say ψ_j, will be a smoother, or, as is said, a "slow" variable. Thus, one would be justified in using a continuous function to describe the block variables.

Formally, the new variable will be defined as

$$\psi_j^b = \frac{1}{b^d} \sum_{i \in j, i=1}^{b^d} \sigma_i \tag{3.6}$$

where d is the dimension, b the scaling factor, and j is the block index. We now ask Knowing the probability distribution (in the canonical ensemble) of the configuration ensemble $\{\sigma\}$, what is the resulting distribution of the new ensemble $\{\psi^b\}$? Using a Kronecker delta, one finds that the new probability must be proportional to

$$\propto \sum_{\sigma_N \pm 1} \cdots \sum_{\sigma_1 \pm 1} \left[e^{-\beta H(\sigma)} \prod_{j=1}^{N/b^d} \delta \left(\psi_j^b - \sum_{i \in j, i=1}^{b^d} \sigma_i \right) \right] \equiv e^{-\beta H'(\psi^b)} \tag{3.7}$$

where some of the explicit degrees of freedom of the σ_i 's have been included in greter freedom in the range of the less numerous ψ_j^b 's. H' also includes a degeneracy term that can be associated with an entropy. This equation defines a new Hamiltonian that has a coarser spatial resolution over our model. This last probability will be normalized by the partition function

$$Z = \sum_{\{\psi^b\}} e^{-\beta H'(\psi^b)}$$

where $\{\psi^b\}$ means the set of all possible configurations. From it, one would be able to find the free energy of the system.

Using arguments similar to those used in Section 2.3, one can approximate[13] the free energy by a spatially homogeneous part and a spatially inhomogeneous part describing the slow spatial variations. That is, the free energy density can be described by

$$f_i = f_o(\psi_i^b) + \sum_{j=1}^{\gamma} C_{ij} (\psi_i^b - \psi_j^b)^2 \tag{3.8}$$

[13]The reader can find in (Wegner 1976) a nice short derivation of a Ginzburg-Landau type free energy for the Ising model, derived directly from the Hamiltonian

where f_o is taken as in equation (2.6) and where the second term is analogous to the gradient term of (2.5). In fact, it can be demonstrated (Tartas 1988) that the sum above is equivalent to a $(\nabla\psi)^2$ term when integrating over the whole space in the continuum limit. We are then left with an equation similar to the Ginzburg-Landau free energy functional (2.5). By taking equation (3.8) to describe the system, we deliberately neglected the short-scale interactions. This approach is justified in view of the long-range order observed at the critical point. It is also justified if one wishes to isolate long-range effects from the short-range fluctuations of a system.

Equation (3.8), in relation to equations (3.6) and (3.7), is not directly evaluated by simulation techniques. Some estimations can be made by calculating the one- and two-point distribution functions. See (Gunton and Droz 1983; Gunton, San Miguel and Sahni 1983) and references therein.

Another technique of coarse graining consists in rewriting the Hamiltonian (3.2) in terms of Fourier transformed variables. Then, one can integrate all the spatial fluctuations on a scale smaller than a certain cut-off wavelength along a given dimension of linear size L. That is, for a hypercubic system of dimension L^d, we define[14]

$$\sigma_x = \frac{1}{L^{d/2}} \sum_{k=1}^{L} \sigma_k e^{i\boldsymbol{k}\cdot\boldsymbol{x}} \tag{3.9}$$

and

$$\sigma_k = \frac{1}{L^{d/2}} \sum_{x=1}^{L} \sigma_x e^{-i\boldsymbol{k}\cdot\boldsymbol{x}}, \tag{3.10}$$

where we used x and k indices for the real and transformed space respectively. In fact, it would be possible to express the Hamiltonian $\mathcal{H}$ in terms of these new variables. Now if we are interested in the probability distribution of long wavelengths, irrespectively of the value of short ones, it will be found to be proportional to

$$\propto \sum_{k_d>\Lambda} \cdots \sum_{k_1>\Lambda} e^{-\beta H_k(\sigma)} \equiv e^{-\beta H'_k(\sigma)}. \tag{3.11}$$

With this new Hamiltonian $\mathcal{H}'_k(\sigma)$, the short wavelengths (large k) have been integrated out in the probability distribution so that variations of spins over a scale

[14] As usual, the infinite volume continuum limit implies the replacement $\sum \to \frac{1}{(2\pi)^{d/2}} \int d^d x$.

shorter than $\sim \frac{2\pi}{\Lambda}$ will not be specified. That is, the spatial resolution $\frac{2\pi}{\Lambda}$ can be identified with the scaling factor b and an effect similar to equation (3.6) can be achieved. The new "blocked" configuration can be obtained from

$$\psi_x^{\Lambda} = \frac{1}{L^{d/2}} \sum_{k<\Lambda} \sigma_k e^{i\boldsymbol{k}\cdot\boldsymbol{x}}. \tag{3.12}$$

Lastly, we note that the process of blocking smears out the discreteness of the model and that the replacement of the sums by integrals can be perfectly justified This whole process is sometimes referred to as Kadanoff blocking and will be the starting point of Chapter 4.

3.3 Monte Carlo simulations

The advent of more powerful[15] computers in the last two decades has permitted the development of new numerical methods. These faster machines can perform simulations on systems of reasonable size which involve a huge number of elementary operations. One major task of statistical mechanics is the evaluation of the partition function. A possible numerical way to evaluate it is to choose a point at random in the phase space, calculate the energy and then weight it according to the corresponding distribution function. But, unlike common high-dimensional numerical integration, the evaluation of the energy over the lattice is still too time consuming. Another method is therefore necessary.

3.3.1 The Metropolis algorithm

At the dawn of computer age, Metropolis *et al.* (1953) invented a method that simplifies this calculation. [16] The main idea is that rather than generating states randomly

[15] For the time being...

[16] In a paper named *Equation of state calculations by fast computing machines* ... They reported a 3 min/mcs for a $N = 224$ rigid sphere model. Compared with the magnitude of 10^8 updates/sec that can be obtained from supercomputers nowadays (see (Wansleben 1987) and references therein) eight orders of magnitude has been gained since then.

and then weighting them with the distribution factor, one generates new configurations according to their distribution and weights them evenly.[17] Consider, for example, the N site two-dimensional Ising model we have been working with so far. The algorithm is as follows. Given a configuration, select a site i randomly, evaluate the energy ΔE to "flip" σ_i to $-\sigma_i$ and generate the new flipped state according to the probability $\min(1, e^{-\beta\Delta E})$.[18] This procedure can be used, for example, to represent the process of adsorption of an adatom onto a surface in equilibrium with the vapour. As can be seen, this process does not conserve the order parameter. A way to preserve it is to select two sites at random, evaluate the energy involved in interchanging these two sites and then proceed as above.[19] This last method is more representative of a physical phenomena involving a local diffusion process. Note that in both cases, the method only involves the local calculation of the energy of one or two spins. This is what makes this technique so advantageous.[20]

Since each site can be selected and flipped with a non-null probability, we expect that the system can (and should) access all of its states in time, so that the ergodic hypothesis holds.[21] This latter assumes that an average over time should be equivalent to an average over an ensemble of systems. This will only be true if the sampling period is longer that the relaxation time of the system of interest. This is why time correlation has to be considered in any Monte Carlo simulation.

---

[17] This process is sometimes known as *importance sampling* as opposed to *simple sampling*. See the book by Binder and Heermann (1988) for a clear and complete introduction to Monte Carlo methods in statistical physics.

[18] This way of proceeding is named after Metropolis The equivalent field dynamic model is known as *model A* (Halperin and Hohenberg 1977) (cf. Section 3.4 2). Note however, that *Glauber* (who solved the resulting stochastic dynamical problem in one dimension (Glauber 1963)), is sometimes used (Williams 1985a) to designate the same algorithm but with the transition probability (3.23).

[19] This way of proceeding is referred to as *Kawasaki* dynamics (Kawasaki 1972). The equivalent field dynamic model is called *model B*

[20] The *Metropolis* algorithm is also used, for example, to find a solution to the *traveling salesman problem* This is an example of *combinatorial minimization*. A path joining cities to be visited is randomly chosen and the distance traveled is minimized by allowing some restructuring of the path in a Maxwell-Boltzmann fashion. The solution is found by slowly adjusting a "temperature" parameter and the method is then called *simulated annealing* (Press et al. 1988). It is used, for example, for the arrangement of the circuit elements, in the design of integrated circuits.

[21] This is not true in some spin glasses where the existence of frozen spins can form a bottleneck to some regions of phase space.

For this, assume we consider two quantities A and B. The covariance for these two sets of values will be given by

$$\text{covar}(A,B) = \langle \Delta A \Delta B \rangle = \langle AB \rangle - \langle A \rangle \langle B \rangle$$

as well as the correlation

$$\text{corr}(A,B) = \frac{\text{covar}(A,B)}{\langle (\Delta A)^2 \rangle^{1/2} \langle (\Delta B)^2 \rangle^{1/2}}$$

so that for a time-displaced quantity evaluated with respect to an arbitrary time t_o, at which the system is in equilibrium, we can write the time-displaced correlation function $\varphi(t)$ as

$$\varphi_A(t) = \frac{\langle A(t_o)A(t_o+t)\rangle - \langle A(t_o)\rangle\langle A(t_o+t)\rangle}{\langle (A(t_o) - \langle A(t_o)\rangle)^2\rangle^{1/2} \langle (A(t_o+t) - \langle A(t_o+t)\rangle)^2\rangle^{1/2}}. \tag{3.13}$$

Typically, when the system is far from the critical temperature, the time correlation is negligible after a few *Monte Carlo steps*[22] (*mcs*). At T_c, it can be as large as thousands of *mcs*, being highly dependent on the system size. The decay can be described by a series of exponentials, one of which is dominant, with the largest relaxation time. This suggests a definition for a characteristic relaxation time

$$\tau_A = \int_0^\infty \varphi_A(t) dt. \tag{3.14}$$

This definition will yield the usual time constant if the relaxation is purely and simply exponential. This is found to be the case at T_c. See figure 3.3.

3.3.2 The Markov chain—a deeper look

Any process for which the probability of a future state is only function of the present one is said Markovian. The evolution probability of the present state is therefore not function of its history. Since the Metropolis algorithm satisfies this criterion, it allows us to use the theory of Markov processes.

[22] One Monte Carlo step is defined as N elementary processes, i.e. it defines a time scale that allows comparison between systems of different sizes.

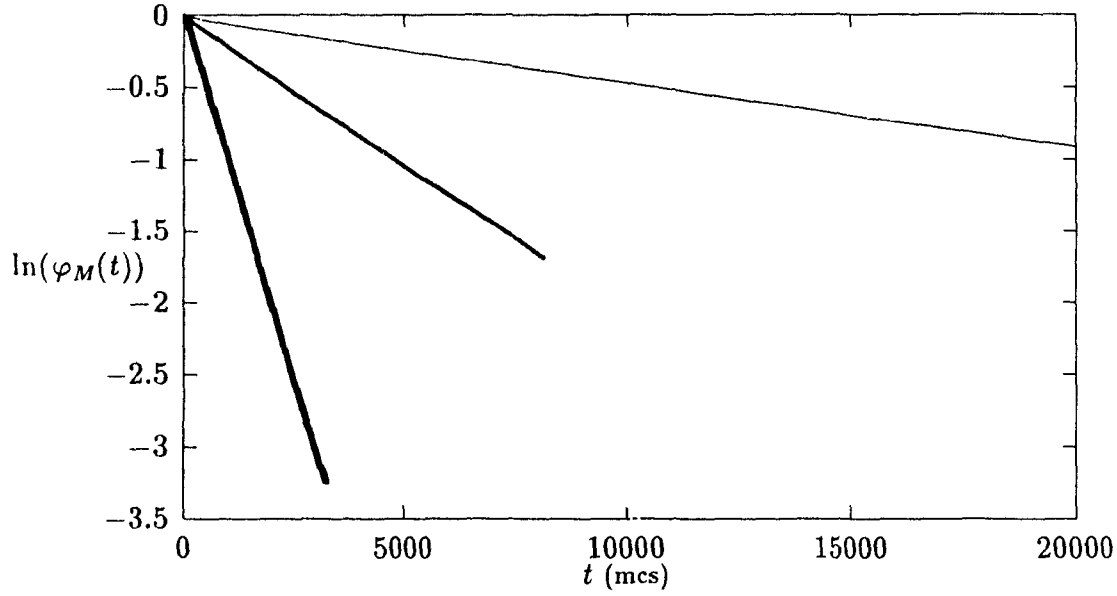

Figure 3.3: The time-displaced correlation function $\varphi_M(t)$ obtained from simulations over systems of $L = 64, 32, 16$, from top to bottom. Note the strong system size dependence which will be further exploited in Chapter 5. It also shows, by the slow decay of these correlations, how highly correlated in time is a system at T_c. A system at, say, $0.5T_c$ would ideally appear on the ordinate of this graph. However a real simulation shows noise that would appear on the lower part of the logarithmic scale.

Let us first note that the Ising model has a finite number of configurations, since the number of degrees of freedom is finite and those are discrete and bounded ($\sigma = \pm 1$). Consider now a statistical ensemble of configurations a represented by a probability distribution Q.[23] We can think of the probability of all the possible states in this finite ensemble grouped in a vector $Q(a)$.[24] An elementary process can thus be represented by a matrix $\mathcal{W}(b \leftarrow a)$ acting on the vector $Q(a)$ to give a vector $Q'(a)$. Thus

$$Q'(b) = \sum_a \mathcal{W}(b \leftarrow a) Q(a).$$

We would like this process to bring an initial ensemble Q_o to a desired ensemble

[23] If, for example, one starts a Markov chain from a known configuration a then Q will be zero everywhere and 1 for $Q(a)$. This distribution should spread out and converge to some desired probability distribution. This notation, from (Bhanot 1988), is similar to the ket vector introduced by Kadanoff (e g. (Kawasaki 1972)).

[24] A continuous distribution function can be thought of as an infinite vector and the extension becomes straightforward.

P.[25] This means that $\mathcal{W}$ must be such that[26]

$$\lim_{n\to\infty} \mathcal{W}^n Q_o = P. \tag{3.16}$$

This would be true if $P = \mathcal{W}P$ is the unique fixed point of the algorithm. We must therefore show that P is an eigenvector of $\mathcal{W}$ associated with an eigenvalue 1. Moreover $\mathcal{W}$ must satisfy the usual probability conditions

$$\sum_b \mathcal{W}(b \leftarrow a) = 1 \tag{3.17}$$

$$\mathcal{W}(b \leftarrow a) > 0 \tag{3.18}$$

where a stronger restriction (non-null probability) has been imposed by (3.18). These two conditions ensure that there is a non-vanishing probability to go from any initial configuration to any final one. This is called the strong ergodicity condition. In some cases, condition (3.18) can be relaxed and one can still have an ergodic process. Also note that

$$\sum_a Q(a) = 1 \tag{3.19}$$

holds at each step of the evolution. These three last equations are sufficient to define a Markov process.

If one chooses $\mathcal{W}(b \leftarrow a)$ such that it satisfies the detailed balance equation, i.e.[27]

$$\mathcal{W}(b \leftarrow a)P(a) = \mathcal{W}(a \leftarrow b)P(b), \tag{3.20}$$

then one can show that P is an eigenvector of $\mathcal{W}$. Indeed, it follows from (3.17) and (3.20) that

$$\sum_a \mathcal{W}(b \leftarrow a)P(a) = P(b)\sum_a \mathcal{W}(a \leftarrow b) = P(b).$$

[25] E g , $P(\sigma_1,\ldots,\sigma_N) = e^{-\beta H(\sigma_1, \ldots,\sigma_N)}$ for a canonical distribution or $\delta(H(\sigma_1, \ldots,\sigma_N) - E_o)$ for a microcanonical ensemble.

[26] This would also imply that, for an observable A estimated by $\langle A\rangle_P$ over the desired ensemble and by $\bar{A}$ over the Markov chain, one would have

$$\lim_{n\to\infty} \bar{A} = \langle A\rangle_P \tag{3.15}$$

[27] This is sometimes referred to as *microscopic reversibility*

This merely says that the probability of being in a state b after one evolution step from any possible existing states (including b itself) is equal to the present probability of being in b. The proof that P is unique is beyond the scope of this description and the reader is referred to a very comprehensive paper by Bhanot (1988). It has also been proven (Kennedy et al. 1986) that unity is the largest eigenvalue. This means that as long there exists some overlap between Q_o and P, the repeated action of $\mathcal{W}$ will damp out all eigenvectors except P.

Using the same notation we can define the Metropolis algorithm, as described above, by the following transition matrix

$$\mathcal{W}(b \leftarrow a) = \begin{cases} \frac{1}{\tau N} & \text{if } E_b < E_a \quad (P(b) > P(a)) \\ \frac{1}{\tau N}\frac{P(b)}{P(a)} & \text{if } E_b \geq E_a \quad (P(b) \leq P(a)) \end{cases} \quad (a \neq b) \tag{3.21}$$

where P is the temperature dependent Boltzmann probability factor ($e^{-\beta E}$) describing the canonical ensemble and τ fixes the time scale.[28] This latter is generally chosen to be unity. The factor N comes from the nature of the algorithm and the element $\mathcal{W}(a \leftarrow a)$ is determined from condition (3.17). In order to have size independent equations, it is common to work with a size normalized evolution probability matrix $\mathcal{W}'$ defined as

$$\mathcal{W}'(b \leftarrow a) = \mathcal{W}^N(b \leftarrow a). \tag{3.22}$$

This defines a normalized time scale having, as elementary unit, one Monte Carlo step per spin (*mcs*) on the average.

Another common way of defining the algorithm, especially for dynamics problems, is (Müller-Krumbhaar and Binder 1973; Binder 1974; Binder and Stauffer 1984) [29]

$$\mathcal{W}(b \leftarrow a) = \frac{1}{\tau N}\frac{P(b)}{P(a) + P(b)}, \tag{3.23}$$

[28] The factor τ can be seen as T dependent in order to describe the details of the interaction with the heat bath. However, a change in τ would break condition (3.17) and must be seen as a factor multiplying the whole matrix $\mathcal{W}$ in order to modify the transition probability per unit time. It would be simpler in this case to rescale time

[29] Note that the forms

$$\mathcal{W} = \frac{1}{2\tau N}\left[1 - \tanh\frac{\beta\Delta E}{2}\right] = \frac{1}{\tau N}\frac{e^{-\beta\Delta E}}{1 + e^{-\beta\Delta E}}$$

are equivalent to (3.23).

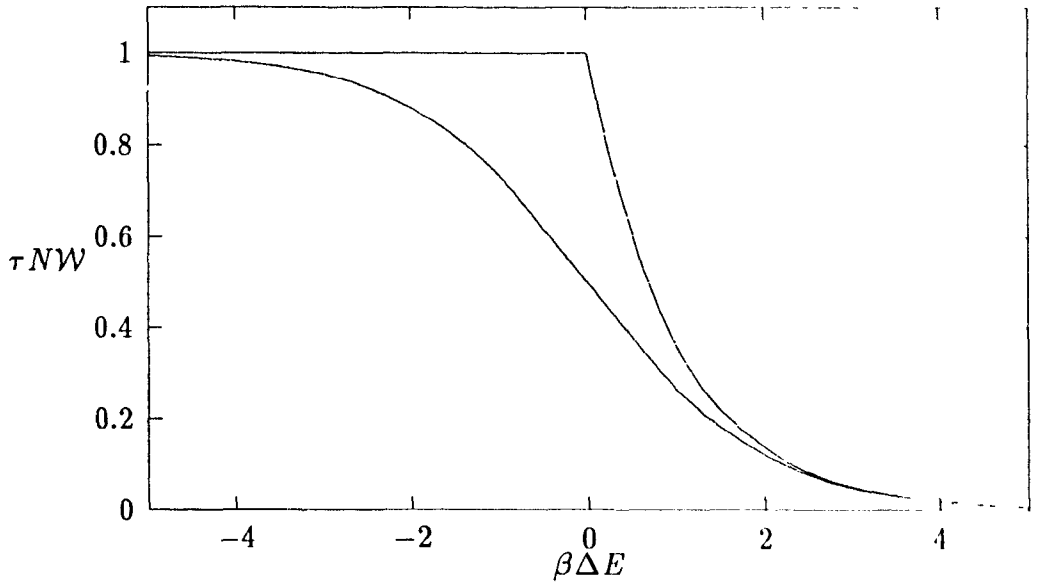

Figure 3.4: A comparative plot of the *Metropolis* and *Glauber* transition probabilities. The *Metropolis* (top) has a transition probability of 1 for any change having the net effect of lowering the energy of the system. *Glauber* algorithm (bottom) is softer with that respect. Note that both processes yield the same curve for $\beta \to \infty$, with the only difference that the transition probability τNW for $\beta\Delta E = 0$ is always 1 for the first case and always 1/2 for the second

which seems more natural in terms of transition probability. This is the form Glauber used for solving the one-dimensional dynamic problem (1963). This transition probability, by being softer, satisfies equation (3.18) even when rescaled according to (3.22). Indeed, after N elementary steps, there is a non-null probability of being in any state from any initial configuration. Thus, ergodicity follows. This is not the case for our first definition where one has to assume a longer time for ergodicity to be possible. On the other hand, one sure test to prove that a transition matrix is not ergodic is to check if the matrix can be put in a block-diagonal form. Figure 3.4 shows the probability behaviour for these two choices.

Computer simulations give the same results for either method when studying equilibrium properties. Method (3.21) goes faster to equilibrium though, due to the fact that no possible flip is rejected once considered (Binder and Stauffer 1984). We shall now consider, as an example of definition (3.21), the N site $\beta = 0$ matrix. In this case, $\mathcal{W}$ is a $2^N \times 2^N$ symmetric matrix of trace zero.[30] The off-diagonal part

[30]The singularity here is the symmetry of the matrix that would also be obtained with definition

consists of zeros and $1/N$ elements. The $\beta = \infty$ case has the singularity that one of its column is a null vector.[31] It would be justified then to suspect some sort of singularity, such as a strong instability, at T_c, where the convergence of $\mathcal{W}$ becomes a minimum (critical slowing down).

It can be proved that both definitions obey to the detailed balance equation (3.20). For (3.21), for example, we have if $E_a > E_b$, $a \neq b$,

$$\mathcal{W}(b \leftarrow a)P(a) = P(a)/N$$

$$\mathcal{W}(a \leftarrow b)P(b) = \frac{1}{N}\frac{P(a)}{P(b)}P(b) = P(a)/N$$

and the detailed balance follows. The same result comes out when $E_a \leq E_b$. The convergence of the algorithm is therefore ensured by these conditions.

Instead of defining the transition probability $\mathcal{W}$ over the configuration space, it is common to use the individual values of the spin variables. The probability distribution Q will then be a function of N variables taking two discrete values instead of one variable of 2^N possible values. With this notation, the transition probability (3.21) becomes

$$\mathcal{W}(-\sigma_i \leftarrow \sigma_i) = \begin{cases} \frac{1}{\tau N} & \text{if } E(\sigma_1, \ldots, \sigma_i, \ldots, \sigma_N) < E(\sigma_1, \ldots, -\sigma_i, \ldots, \sigma_N) \\ & (P(\sigma_1, \ldots, -\sigma_i, \ldots, \sigma_N) > P(\sigma_1, \ldots, \sigma_i, \ldots, \sigma_N)) \\ \frac{1}{\tau N}\frac{P(\sigma_1, \ldots, -\sigma_i, \ldots, \sigma_N)}{P(\sigma_1, \ldots, \sigma_i, \ldots, \sigma_N)} & \text{if } E(\sigma_1, \ldots, -\sigma_i, \ldots, \sigma_N) \geq E(\sigma_1, \ldots, \sigma_i, \ldots, \sigma_N) \\ & (P(\sigma_1, \ldots, -\sigma_i, \ldots, \sigma_N) \leq P(\sigma_1, \ldots, \sigma_i, \ldots, \sigma_N)) \end{cases} \tag{3.24}$$

This definition has the weakness that the mode of spin selection is not implicitly taken into account as will be seen in the next section. Actually, the selection of the site only has importance when the dynamical characteristics of the model are considered. In view of the static case, most of the choices are equivalent and yield the same results, although requiring different amounts of computer time. The more usual selection algorithms are sequential, random, or the so-called *checker-board* algorithm. This latter consists in going in a sequential way over one of the l super-lattices of the

(3.23)

[31] For a degenerate case, there should be as many null column vectors as ground states.

system at the time. On parallel machines,[32] this way of proceeding has the advantage that N/l flips can be done in only one parallel step. On the other hand, random selection necessitates a good random number generator for otherwise some site might never be visited due to pair[33] coupling among the numbers generated. This would then break the ergodicity because some states will be forbidden and as a result the phase space may be split in separated independent domains.[34]

3.4 The kinetic Ising model

The following will be concerned with the technical aspects of a simulated quench i.e. the action of suddenly changing the heat bath from a hot temperature to a much colder one — whereas Chapter 6 will present growth in a more general context.

Let us first mention that kinetic simulations on the various models allow us to calculate the values of different time correlations which are not accessible experimentally, but which can be of some theoretical interest. The lack of intrinsic dynamics of the model has already been discussed. This can be seen formally by using the classical mechanics formalism of Poisson brackets or the formalism of commutators for a quantum system. Unlike the Ising model, most of the other models (Heisenberg, fluids, ...) do have time evolution in terms of deterministic kinetic equations. On the other hand, the dynamic evolution, according to stochastic methods, is not consistent with the actual physical time evolution of these systems (Binder and Stauffer 1984).[35] In the Ising model however, the Monte Carlo process could be interpreted as a simulation of the real kinetics of the system. Moreover, some direct applications have been made in the last years. For example, some related models were used by Safran *et al.* to represent adsorption of oxygen on a tungsten surface (1983). For this

[32] Where one processor can be assigned to each lattice site

[33] Or triplet, depending on the dimension of the lattice

[34] As mentioned before, the same thing can happen in the study of spin glasses, where some *frustrated* spin may hinder the probability flow from going in certain region of phase space

[35] For the Heisenberg model for example, Monte Carlo simulations only show a relaxational behaviour, despite the spin wave dynamics predicted by the analysis of the Hamiltonian

purpose, they used a model having three possible values for the σ_i's instead of two.[36]

Here are some examples showing how a kinetic Ising model can be used to simulate various physical systems.

- A ferromagnetic model with spin-flip dynamics. This is the standard treatment of a ferromagnet. This is also the kinetic lattice gas representation. The order parameter is not conserved.

- An antiferromagnetic model with spin-flip dynamics. This can be used, for example, to represent a surface adsorption or a similar process on a lattice that permits only two equivalent choices for the forming superlattice. The order parameter is not conserved.

- A ferromagnetic model with spin-exchange dynamics. This is, among other applications, the standard representation of the spinodal decomposition process. The order parameter is conserved.

- An antiferromagnetic model with spin-exchange dynamics. This represents the usual AB binary alloy system simulation. The order parameter is not conserved.

The concept of universality classes has also been extended to dynamical models. For example, all the combinations above are thought to involve only two classes governed by conservation laws. These latter thus play an important rôle. Lastly, it should be noted that the only exact solution existing at the present time, for any kinetic model, is Glauber's solution for the spin-flip one-dimensional Ising model (Glauber 1963).

3.4.1 The master equation

Let us return to the probability distribution Q of the preceding section. If one takes an evolution step, as defined in (3.22), as the evolution time, then one can write the

[36] Those models are then called Q-state Potts models.

master equation valid at any discrete time t [37]

$$Q(a,t+1) - Q(a,t) = \sum_b [\mathcal{W}(b \to a)Q(b,t) - \mathcal{W}(a \to b)Q(a,t)] . \qquad (3.25)$$

When Q has converged to P and if $\mathcal{W}$ and P have been chosen such that they satisfy the detailed balance equation (3.20) then a stationary state follows.

Now assume that we have a system at equilibrium at some high T and that we quench it. This is usually done by starting from a random configuration representing a $\beta = 0$ temperature. The stress given to a system at time t_o can be seen as a step function so that no explicit time dependence comes in $\mathcal{W}$. This is valid as long as the process involved has a relaxation time scale much longer than the assumed phonon-type energy diffusion. We are only interested in the $t > t_o$ region so that we consider a stationary transition probability matrix. Because of that, and the associative property of matrices, one can define a new time scale by redefining the matrix $\mathcal{W}$ as any power of itself.[38]

We can see, however, that the master equation is crucially related to the chosen algorithm. For the two transition probabilities presented above for example —cf. (3.21), and (3.23)—, it has been argued that the dynamical properties could be rescaled to match, simply by using a temperature dependent factor (Müller-Krumbhaar and Binder 1973). This latter is calculated as the ratio of the mean successful spin flips per Monte Carlo step for each method.

If one puts the additional condition of updating the spins in a particular way, then the master equation will no longer be valid, as pointed out by Gawlinski *et al.* (1985) Indeed, their results showed substantial discrepancies between different methods of updating the spins. They argued that the main condition in this situation is that the time scale chosen must be such that there is no significant evolution during one mcs They studied a sequential updating method that changes the nature of the transition matrix. Indeed, in this case, a discrete time dependence is imposed, as one considers

[37]The prime is dropped on $\mathcal{W}$.

[38]Note that the property 3.17 still remains valid for any power of $\mathcal{W}$

the elementary processes made over the configuration distribution.[39] Suppose, for example, one updates the spins in a "disordered" sequential fashion. Then, the net effect will be the same as if one uses a poor, strongly correlated, short period ($\sim N$) random number generator. If N is large, this effect can be seen to vanish as if the randomness of the "generator" was improved. Therefore the question this problem raises is still the same old one: What is the freedom one has on a real random number generator before effects start to be seen? Or, equivalently, what is an ideal random number generator for the problem considered?

The problem of parallel processing has also been investigated by Williams (1985a) and by Viñals *et al.* (1986). At this point, the studies seem to conclude that the dynamical results obtained from a parallel (multi-spin-flip) algorithm are consistent with the one obtained from a single-spin-flip updating scheme under certain conditions only. In other words, the two algorithms are thought to be in the same dynamical universality class. However, further investigations are still required in order to know the degree of equivalence between these different algorithms.

3.4.2 A phenomenological approach

Suppose one can find some sort of smooth variable(s) that would contain the principal (macroscopic) information about the system. The forgotten degrees of freedom could then be expressed as a random term, selected according to the expected response of the system. One sometimes calls these variables *slow* and and *fast* respectively. In general, the order parameter ψ and some hydrodynamic variables are chosen as slow variables. The derivation of dynamic equations, expressed in terms of these new variables, depends on whether or not the order parameter is conserved.

Before presenting the phenomenological equations describing the relaxation of the Ising model described above, let us consider the formalism developed earlier, in the framework of Brownian motion. The latter was one of the first direct applications

[39]The transition probability for each spin will behave like the valves of an engine, being on and off cyclicly for each N flip turn.

of the theory of Markov processes in physics. The study of this phenomena involves a set of stochastic equations defined over continuous space variables, of which the famous example is the random walk problem.

Consider the equation of motion of a particle i, of given mass m_i, in suspension in a fluid

$$-h\dot{x}_i + f_i + f_i^r = m_i\ddot{x}_i,$$

where h is the coefficient of friction, f_i is an external driving force and f_i^r is a random force due to the collisions of the molecules with the particle. If one neglects the inertial force and takes f_i as a conservative force that can be derived from a potential $\mathcal{V}$, then

$$\dot{x}_i = -\Gamma\frac{\partial\mathcal{V}}{\partial x_i} + \eta_i, \tag{3.26}$$

where $\eta_i = f_i^r/h$ is a random force such that its average over an ensemble of particles is null and uncorrelated in both space and time, i.e. such that

$$\begin{aligned} \langle\eta_i(t)\rangle &= 0, \\ \langle\eta_i(t)\eta_j(t')\rangle &= B\delta(t-t')\delta_{ij} \end{aligned} \tag{3.27}$$

where $B = 2\Gamma k_B T$ is a constant, a consequence of the fluctuation-dissipation relation. This type of equation is called a Langevin equation.[40]

Now, consider the spin-flip Ising model described by equations (3.2) and (3.21) or (3.23) dynamics. Assume that the discreteness of the model has been smoothed out by using the technique described in Section 3.2.2, for example. Then, by taking the free energy functional as the driving force, one can write, in a way similar to the one considered above,

$$\frac{\partial\psi_i^b}{\partial t} = -\Gamma_o\frac{\delta F[\psi_i^b]}{\delta\psi_i^b} + \eta_i \tag{3.28}$$

where any "inertial term" $\ddot{\psi}$ has been neglected. Here Γ_o is the coefficient[41] that causes ψ to relax towards a configuration which minimizes the functional F and η_i is

[40]For Brownian motion, by using the equipartition theorem and the diffusion equation $\langle x^2\rangle \quad Dt$, B is found to be equal to hk_BT, from which one finds Einstein's equation for diffusion $D \quad (k_BT/h)$ See (Léontovitch 1986) for example.

[41]This coefficient is sometimes called *Onsager* kinetic coefficient since this equation has also been developed in the context of the thermodynamics of irreversible processes

a random force term, as in (3.26), such that

$$\begin{aligned} \langle \eta_i(x,t) \rangle &= 0, \\ \langle \eta_i(x,t)\eta_j(x',t') \rangle &= 2\Gamma_o k_B T \delta(x-x')\delta(t-t')\delta_{ij}. \end{aligned} \tag{3.29}$$

Because ψ_i^b is not restricted by the value of any other cell, no conservation law holds in this model. In the case of a spin-exchange dynamics, the coefficient Γ_o of the driving force will have to be changed to $-\Gamma_o \nabla^2$.[42] Note that these models only describe the relaxation of a system towards equilibrium.[43]

There exists no real physical derivation, from first principles, of equation (3.28). One derivation of the above Langevin equation was made by Langer (Langer 1971) who makes plausible assumptions and obtains the non-linear equation (3.28) from the master equation. However, the validity of this derivation is sometimes questioned for its lack of rigour (Gunton 1984).

Much of the literature has been devoted to this approach. A summary and classification of the different models, as well as their applicability, have been made by Halperin and Hohenberg (1977). All these models use a Ginzburg-Landau free energy functional F as described in equation (2.5) and, for this reason, are often called time-dependent Ginzburg-Landau (TDGL) models. The models described above are designated as model A (non-conserved) and model B (conserved) respectively.

These non-linear equations may be solved numerically. This is generally done by using a lattice on which continuous ψ_i are defined. This requires the use of a discrete form of the Laplacian over the nearest neighbours in order to calculate the free energy functional. For example, a numerical solution of the Langevin equation (3.28) can be found in a paper by Valls and Mazenko (1986).

[42] In analogy with Brownian motion, this would correspond to a system of interacting particles with a fixed center of mass at all time.

[43] Consistency with equilibrium is enforced by the fluctuation-dissipation relation for η.

3.5 Finite-size effects and scaling

Although the size of today's computers allows us to perform work on larger and larger systems, they still remain finite. However, a sharp phase transition can only occur in the thermodynamic limit. This obliges us to understand how the size of the system can affect the results.

One of the direct consequence of the finiteness of the system is the fact that for any non-zero temperature there exists a finite probability for the whole system to flip from near $|\psi|$ to near $-|\psi|$. In other words the two identical probability "pockets" located near $\pm|\psi|$ in the phase space are connected. This means that any importance sampling as taken by equation (3.15) will eventually yield a zero value for the order parameter. Formally

$$\langle\psi\rangle_{T,N} = \langle\sum_{i=1}^{N}\sigma_i\rangle_{T,N} = 0, \ \forall \text{ finite } N \tag{3.30}$$

and the only formal way to get around this difficulty is to define the order parameter by taking the thermodynamic limit as follows

$$\psi_{TD} = \lim_{H\to 0}\lim_{N\to\infty}\langle\psi\rangle_{N,H,T}. \tag{3.31}$$

The possibility of observing the order parameter comes mainly from the fact that each of the state located around $\pm|\psi|$ are metastable with a characteristic time τ_e called the *ergodic time* (Binder and Heermann 1988). For systems of reasonable size (i.e. $L > 10$), this "flipping" period is large enough to allow valuable observation simply by storing the absolute value. The relatively small value of the energy required to form a band crossing the entire system, which is generally precursive to a global change, is also responsible for the formation of a "slab", obtained when one cools a system from a high temperature to a very low ($\lesssim 0.4T_c$) one. Because the fluctuations are then too weak, the system freezes in this metastable state, which forms a local minimum [44]

A survey of finite-size scaling techniques is found in the following references (Binder 1979; Binder and Stauffer 1984; Binder and Heermann 1988). This method

[44]This would not be true if the whole (straight) interface were allowed to move

simply consists in doing simulations on systems of various sizes, and see if there is a trend that develops in the results. One then tries to find a scaling form, similar to those explained in the context of second-order phase transitions, that would contain the size as a scaling factor. Because the scaling form often has an asymptotic behaviour, the result for an infinite system can be obtained by extrapolating the size of the system to infinity. This kind of scaling regime is only valid when the correlation length is much smaller than the linear size of the system. One direct manifestation of finite-size effects is the spread of the transition point. For example, the magnetization curve will not go sharply to zero at T_c as in figure 3.2, but will have a tail near $T > T_c$.

The effects of the boundary conditions used are also important. Analysis on models at equilibrium with free surfaces have shown that the critical behaviour can be shifted to a lower temperature and smeared out. When periodic boundary conditions are used to eliminate free surfaces then the shift is smaller but in the other direction (i.e. $T_c' > T_c$). In this case it has been suggested that finite-size effects on the critical temperature can be described by an equation of the type

$$T_c' = T_c\left(1 - \frac{a}{L^\lambda}\right),$$

where L is the linear dimension of the system and a and λ are parameters.[45] See (Binder 1974) and references therein for more details. We used periodic boundary conditions.

Some other types of finite-size effects will be observed when one studies dynamics. Beyond a certain size, the growth of a "droplet" will start to perturb itself because it can loop across the periodic boundary conditions. Based on Monte Carlo simulations, this effect is usually seen when the typical size of the domains is of the order of $\sim 0.4L$ (Viñals et al. 1985; Sadiq and Binder 1984). Therefore late time studies require very large systems.

[45] λ can be related to some critical exponents

Chapter 4

Renormalization Group Methods

During the last decades, renormalization group methods (RG) have played an important rôle in statistical mechanics. They have been widely used with great success for a variety of many-body calculations. Given a system with a large number of degrees of freedom whose statistical state is described by a Boltzmann distribution related to the Hamiltonian in the usual way, the basic idea consists in integrating some of the degrees of freedom, typically those associated with a small wavelength, and describing the probability of the remaining degrees of freedom in terms of a Hamiltonian which involves these latter only. At the same time, the system is rescaled in terms of its linear dimensions so that it has the same set of dynamical variables, the same number of degrees of freedom, as the original system, though it is now described by a new Hamiltonian. This approach has been developed in the context of static critical phenomena but generalization to growth problems and critical dynamics, for example, have been made in the recent years.

There exist different operators that can do this transformation on the degrees of freedom of the system. They can be divided in two groups depending on whether they are performed in real or Fourier space. We have already seen some of them, such as blocking in real space or introducing a cut-off in Fourier space (cf. Section 3.2.2) Wilson (1971) has shown that an equivalent method is to perform an incomplete integration by expanding the dimension of the integral (!) about the upper critical

dimension (4) of a Ginzburg-Landau free energy functional. Despite the success of this approach, there still remain questions about the mathematical foundations of the method. See (Griffith 1981) for a comprehensive presentation of these problems. We shall now consider some simple but interesting real space RG examples.

4.1 Real space RG — some examples

The following applications are different from the usual theoretical field RG, but they are closely related to the kind of RG that can numerically be done during a computer simulation. Moreover, although the primary goal of the RG theory is the calculation of critical exponents, it proved to give much more information than expected in one dimension. For this reason, it may be worthwhile to consider that case too.

4.1.1 The one-dimensional case

Consider first the one-dimensional nearest-neighbour Ising model. To simplify the notation, it is common to use a coupling constant $K = \beta\epsilon$ (cf. Section 3.2.1). The partition function is then written

$$Z(N,K) = \sum_{\sigma_N=\pm 1} \cdots \sum_{\sigma_2=\pm 1} \sum_{\sigma_1=\pm 1} e^{K\sum_{i=1}^{N}\sum_{j=nn}\sigma_i\sigma_j}, \tag{4.1}$$

where nn stands for nearest neighbours according to periodic boundary conditions. By expanding the sum in the exponent,

$$Z = \sum_{\sigma_N=\pm 1} \cdots \sum_{\sigma_2=\pm 1} \sum_{\sigma_1=\pm 1} \cdots e^{K(\sigma_1\sigma_2+\sigma_2\sigma_3)} e^{K(\sigma_3\sigma_4+\sigma_4\sigma_5)} \cdots .$$

If the sum is performed on all even indices, then the same partition function can be rewritten, assuming N is odd, as

$$Z = \sum_{\sigma_N=\pm 1} \cdots \sum_{\sigma_3=\pm 1} \sum_{\sigma_1=\pm 1} \cdots [e^{K(\sigma_1+\sigma_3)} + e^{-K(\sigma_1+\sigma_3)}][e^{K(\sigma_3+\sigma_5)} + e^{-K(\sigma_3+\sigma_5)}] \cdots .$$

One would like to have an equation of a form similar to (4.1). If, by matching term by term, one tries to have an equality such as

$$e^{K(\sigma_1+\sigma_3)} + e^{-K(\sigma_1+\sigma_3)} = f(K) e^{K'\sigma_1\sigma_3}, \tag{4.2}$$

then it would be possible to rewrite (4.1) as

$$Z = f(K)^{N/2} \sum_{\sigma_{N/2}=\pm 1} \cdots \sum_{\sigma_2=\pm 1} \sum_{\sigma_1=\pm 1} e^{K' \sum_{i=1}^{N/2} \sum_{j=nn} \sigma_i \sigma_j}$$

or, more simply,

$$Z(N, K) = f(K)^{N/2} Z(N/2, K'). \tag{4.3}$$

This is possible if

$$\begin{aligned} K' &= \tfrac{1}{2} \ln \cosh(2K), \\ f(K) &= 2 \cosh^{1/2}(2K), \end{aligned} \tag{4.4}$$

which are solution of equation (4.2).

Equation (4.3) relates a partition function of N sites with coupling constant K to a similar one having $N/2$ sites and coupling constant K'.

If the free energy is proportional to N then we must have[1]

$$\ln Z(N, K) = N\zeta(K), \tag{4.5}$$

where ζ *does not* depend on N.

Using this last equation along with (4.3), we obtain

$$\zeta(K) = \frac{1}{2} \ln f(K) + \frac{1}{2} \zeta(K') \tag{4.6}$$

or, by (4.4),

$$\zeta(K') = 2\zeta(K) - \ln[2 \cosh^{1/2}(2K)]. \tag{4.7}$$

Equations (4.4) and (4.7) will allow us to know the partition function at any T (or K) once one of these is known. One can see from relation (4.4) that K' is always smaller than K. It is possible to rewrite the transformation such that it will go in the opposite direction. That is, by inverting the transformations above, one can get the following set of equations that goes from K' to a larger K,

$$\begin{aligned} K &= \tfrac{1}{2} \cosh^{-1}(e^{2K'}), \\ \zeta(K) &= \tfrac{1}{2} \ln 2 + \tfrac{1}{2} K' + \tfrac{1}{2} \zeta(K'). \end{aligned} \tag{4.8}$$

[1]This will hold whenever the interactions are saturated or, equivalently, whenever we have an extensive variable, in the thermodynamic limit. In this case, the chemical potential $\mu = (\partial F/\partial N) = f(N)$. This implies that (still in the thermodynamic limit) the partition function may be expressed as a product of N identical factors.

A direct application of this last transformation is to start from a small value K'_o (high T_o) and to assume that the partition function is given by 2^N (N independent spins), so that

$$\zeta(K'_o) \approx \ln 2.$$

So, by using K'_o in transformations (4.8), one can generate the value of the partition function at smaller T. The transformation has the following properties:

- The transformation (4.4) has two points for which $K = K'$. These fixed points are: $K = 0$ and $K = \infty$.
- The convergence is such that a small error in the first value of ζ leads to smaller and smaller errors only when one goes from high T to low T.

This defines a "flow diagram" that goes from $K = 0$ to $K = \infty$.

So what has been done above? We tried to express the partition function as the product of a temperature dependent function and a similar partition function defined over a superlattice of the system. This latter can then be rescaled in terms of its linear dimensions. What matters here is how the coupling constants, in the Hamiltonian, changed in such a transformation. At $T = \infty$, the correlation length is zero and we found $K = K'$. At $T = 0$, the correlation length is also zero and still the transformation did not change the coupling constants. This shows how closely related are the correlation length and this kind of transformation.

4.1.2 The two-dimensional case

The two-dimensional problem is a bit more complicated because coupling constants of second, third, ... neighbours start to appear in a real space transformation. When one considers a coupling constant space $(K_1, K_2, \ldots)$ for first, second, ..., and a combination of different neighbours, then one can say that the one-dimensional case transformation is along an axis in the K space whereas it moves differently in the two-dimensional case. In fact, the same transformation can be shown to yield (Maris

and Kadanoff 1978)

$$Z = f(K)^{N/2} \sum e^{\left[K_1 \sum_{nn} \sigma_i\sigma_j + K_2 \sum_{nnn} \sigma_k\sigma_l + K_3 \sum_{square} \sigma_i\sigma_j\sigma_k\sigma_l\right]}, \qquad (4.9)$$

where

$$f(K) = 2\cosh^{1/2}(2K)\cosh^{1/8}(4K)$$

and where *nn*, *nnn*, *square* stand for nearest-, next nearest- and square-nearest-neighbours. The transformation has been done on a square lattice such that we summed on all $i + j$ even. The resultant lattice is still square but diagonal with respect to the original. The explicit form of the K's is

$$\begin{aligned} K_1 &= \frac{1}{4}\ln\cosh(4K), \\ K_2 &= \frac{1}{2}K_1, \\ K_3 &= K_2 - \frac{1}{2}\ln\cosh(2K). \end{aligned}$$

It is therefore impossible to get a Hamiltonian of the same form. If one makes the approximation of neglecting both K_2 and K_3, then no phase transition occurs since a pattern similar to the one-dimensional case is obtained.[2] A better approximation is to include the alignment tendency from the next-nearest neighbours in the K_1 constant That is, each transformation carries K to $K_1 + K_2$. This way, an unstable point appears in the flow diagram, located at $K_c = 0,506$. This is surprisingly close to the Onsager value of 0,44069 (cf. equation (3.5)) when one considers the roughness of this approximation.

4.2 Real space RG formalism

A real space renormalization group (RSRG) transformation can be seen as a transformation, characterized by a factor b, that maps a "site" system to an isomorphic "cell" system. Because the transformation leaves the system isomorphic to itself, iteration is possible and we are interested in non-trivial ($K \neq 0, K \neq \infty$) fixed points

[2]The action of neglecting interaction constants generated by this RG method is referred to as *truncation*.

The transformation mapping the sites variables to the cell variables is generally non-linear. For example, a commonly used mapping transformation is the majority rule, where even (tie) situations are broken up randomly or by following a "fair" sequence.[3] Using Niemeijer *et al.* terminology (1976), we say that the site spin voters σ_i of a cell district determine a cell delegate s_j of one of two parties. Another common procedure is to install an internal hierarchy in the cell, so that one spin is automatically the delegate because of its respective position within the cell.[4]

The RG transformation will generate effective interactions between more distant neighbours, as well as many-spin couplings. It is possible to write a very general Hamiltonian in terms of any spin combination a by

$$\mathcal{H}(s) = \sum_a K_a \prod_{i \in a} s_i \tag{4.10}$$

as the one we obtained in the last section. The vector $\boldsymbol{K}$ will denote the entire set of coupling constants K_a. Representing by S_a the various neighbour interdependencies (cf. various combinations in eq. (4.9)) we can write

$$\mathcal{H}(s) = \sum_a K_a S_a. \tag{4.11}$$

Because the process is iterative, we shall denote by s_i and s_i' the cell variable and the transformed cell variable respectively. If the energy is adjusted so that its first moment is null, i.e.

$$\langle \mathcal{H}(s) \rangle = \sum_{\{s\}} \mathcal{H}(s) = 0, \tag{4.12}$$

then one can retrieve the coupling constants from the Hamiltonian. Indeed, we have for a particular combination of spin a

$$\langle S_a \mathcal{H}(s) \rangle = \sum_{\{s\}} S_a \mathcal{H}(s) = \sum_{\{s\}} S_a \sum_b K_b S_b$$

[3] Only when the blocking factor b and the lattice are such that the number of spins is even, obviously There also exists star-triangle transformation on triangular lattices A theoretical solution involving such a transformation can be found in (Hilhorst, Schick and van Leeuwen 1979).

[4] This procedure is called *decimation*. In terms of P as defined by equation (4.13) this process is represented by

$$P(s_j \leftarrow \sigma_i) = \prod_{i \in j} \delta(s_j - \sigma_{n_i}) \delta_{i,n_i}$$

where n_i is the i^{th} cell delegate's address.

$$= \sum_b K_b \sum_{\{s\}} S_a S_b = 2^N \sum_b K_b \delta_{ab}$$
$$= 2^N K_a.$$

If we represent by $P(s' \leftarrow s)$ the mapping probability factor, then, after a transformation, the new Hamiltonian will be given by

$$e^{\mathcal{H}'(s')+G} \equiv \sum_{\{s\}} P(s' \leftarrow s) e^{\mathcal{H}(s)} \tag{4.13}$$

where the factor $G(\boldsymbol{K})$ is introduced only to keep condition (4.12) valid. This is the renormalization transformation.

The probability P must follow the two usual probability conditions (3.17) and the "soft" ($\geq$) version of (3.18). Moreover, it must be such that the transformed Hamiltonian can still be written in a form similar to (4.11), i.e. such that the factor K_a for a given spin product S_a is the same constant for all of those. This can be seen as a symmetry requirement. Any mapping transformation P following these requirements is allowed in view of this theory. The probability condition (3.17), when applied to equation (4.13), leads to an important relation among free energies. That is, with F defined as

$$F = \ln \sum_{\{s\}} e^{\mathcal{H}(s)},$$

one gets

$$F' + G = F. \tag{4.14}$$

In the thermodynamic limit, we still assume that the free energy F will be represented by a function of the form (4.5). If furthermore we use $G(\boldsymbol{K}) = Ng(\boldsymbol{K})$ then equation (4.14) can be written as

$$\zeta(\boldsymbol{K}) = g(\boldsymbol{K}) + \frac{1}{b^d}\zeta(\boldsymbol{K}'). \tag{4.15}$$

We are interested in the $N \to \infty$ thermodynamic limit. Therefore, relation (4.13), via (4.14), can be looked at as a mapping of an infinite dimensional space of coupling

constants onto itself, i.e.[5]

$$\boldsymbol{K}' = \hat{T}\boldsymbol{K}. \tag{4.16}$$

The strategy of RG is to obtain the singularity of the free energy $\zeta(\boldsymbol{K})$ from the operator $\hat{T}\boldsymbol{K}$ and the function $g(\boldsymbol{K})$ which are assumed regular in the neighbourhood of a fixed point $\boldsymbol{K}^*$. This latter is characterized by

$$\boldsymbol{K}^* = \hat{T}\boldsymbol{K}^*. \tag{4.17}$$

Near this fixed point, equation (4.16) can be linearized about $\boldsymbol{K}^*$, i.e. we define a matrix $\mathcal{T}$ such that

$$\mathcal{T}_{\alpha\beta} = \frac{\partial K'_\alpha}{\partial K_\beta} \tag{4.18}$$

and a transformation near the fixed point $\boldsymbol{K}^*$ will then be written

$$K'_\alpha - K^*_\alpha = \sum_\beta \mathcal{T}_{\alpha\beta}(K_\beta - K^*_\beta). \tag{4.19}$$

The linear operator $\mathcal{T}$ can be simplified by using an eigenvector coordinate system. For this, assume that $\{\boldsymbol{\phi}^i\}$ is the set of left eigenvectors of the matrix $\mathcal{T}$ associated with the eigenvalue λ_i, that is

$$\boldsymbol{\phi}^i\mathcal{T} = \lambda_i\boldsymbol{\phi}^i. \tag{4.20}$$

Therefore, by using a new coordinate vector $\boldsymbol{w}$, describing the displacement $\boldsymbol{K} - \boldsymbol{K}^*$ from the fixed point in terms of the eigenvector basis, we can write the following projection

$$w_i = \boldsymbol{\phi}^i \cdot (\boldsymbol{K} - \boldsymbol{K}^*) \tag{4.21}$$

so that one must have, for each component of the vector $\boldsymbol{w}$,

$$w'_i = \boldsymbol{\phi}^i \cdot (\boldsymbol{K}' - \boldsymbol{K}^*) = \boldsymbol{\phi}^i \cdot \mathcal{T}(\boldsymbol{K} - \boldsymbol{K}^*) = \lambda_i\boldsymbol{\phi}^i \cdot (\boldsymbol{K} - \boldsymbol{K}^*) = \lambda_i w_i. \tag{4.22}$$

Note that the expansion (4.19) can be extended to second order to allow investigation further from the linear regime located around the fixed point.

[5]The set of the operators $\{\hat{T}(b)\}$ obeys associativity, has the closure property $(\hat{T}(b_1)\hat{T}(b_2) = \hat{T}(b_3)$, with $\hat{T}(b_3) \in \{\hat{T}\}$), and has the neutral element $\hat{T}(1)$. There exists no inverse element (except for the trivial identity case) so that it forms a semi group.

Because the eigenvectors are characterized by the transformation equations (4.21) and (4.22), this allows us to write

$$w_i(\boldsymbol{K}') = \lambda_i w_i(\boldsymbol{K})$$

or, similarly, for a series of transformations

$$w_i(\boldsymbol{K}^{(n)}) = \lambda_i^n w_i(\boldsymbol{K}). \tag{4.23}$$

The whole process of RSRG is thus strongly dependent on this eigenvalue equation and, depending on the value of the eigenvalue, the corresponding eigenvector will be named:

- *relevant*: if the eigenvalue is larger than 1. This means that iteration of the process makes the renormalized point moving away from $\boldsymbol{K}^*$. Clearly, the larger the eigenvalue, the more relevant it is. The associated field is obtained by determining the symmetry response (e.g. odd for h, even for T) to a global spin change.

- *irrelevant*: if the eigenvalue is smaller than 1. In this case iteration will move towards the fixed point so that the effect of these variables disappear after some iterations.

- *marginal*: if the corresponding eigenvalue is 1. Renormalization has no effect on these variables and the procedure fails.

The critical exponents are extracted from the eigenvalues of the matrix. In addition, it is possible to determine the critical temperature, the free energy, and the spontaneous magnetization. Because this analysis is not directly pertinent to our work, we prefer to skip it and refer the reader to a very good review given in (Niemeijer and van Leeuwen 1976).

The main problem with this method is that the matrix $\mathcal{T}$ is infinite in the thermodynamic limit so that one has to arbitrarily truncate all but a finite number of the

coupling constants. Sometimes, equivalently plausible selections can lead to different values. For example, in Section 4.1.2, an improvement of the method, by taking care of the forgotten third coupling constant, leads to results further from the known value of the critical point (Maris and Kadanoff 1978). The most systematic way to implement the real-space renormalization group is the Monte Carlo renormalization group. This numerical method incorporates all interactions commensurate with the system size studied.

4.3 Monte Carlo RG

Monte Carlo renormalization group was invented by Ma (1976a) and further developed by Swendsen (1979; 1984). It consists in generating a renormalized lattice without doing any analytical work on the Hamiltonian. For example, a sequence of configurations is generated according to one of the Monte Carlo algorithms defined in Section 3.3. Then a transformation is made on all these configurations in order to reduce the number of degrees of freedom of the system. The most common mapping between the spin sites to the cell variable is the majority rule where "ties" are broken randomly.[6] The assumption that the renormalized Hamiltonian will "fit" the smaller lattice reduces the number of possible coupling constants and, in this regard, truncates the Hamiltonian. For this truncation to be harmless, the effective range of the Hamiltonian must be smaller than the smallest linear size of the renormalized system. However, if two different renormalization series are started from systems differing in their linear dimensions by a factor b, then these finite-size effects will be eliminated (at least reduced) by comparing systems of equal size but differing only by the number of times they have been renormalized. As a consequence, the two systems may be related on the basis of their iteration numbers only.

The matrix $\mathcal{T}$ can then be calculated numerically by solving the set of chain rule

[6] It is very common to have $b = 2$ on a square lattice. An equivalent method consists in selecting randomly three voters out of four (Ma 1976a).

equations obtained after m and $m+1$ iterations

$$\frac{\partial\langle S_\gamma^{(m+1)}\rangle}{\partial K_\beta^{(m)}} = \sum_\alpha \frac{\partial K_\alpha^{(m+1)}}{\partial K_\beta^{(m)}} \frac{\partial\langle S_\gamma^{(m+1)}\rangle}{\partial K_\alpha^{(m+1)}} \tag{4.24}$$

where S_γ is a generalized spin as defined in (4.11). After the system has come to equilibrium, the simulation provides a sequence of configurations from which correlation functions can be calculated. The above derivatives can then be obtained from the following relations

$$\frac{\partial\langle S_\gamma^{(m+1)}\rangle}{\partial K_\beta^{(m)}} = \langle S_\gamma^{(m+1)} S_\beta^{(m)}\rangle - \langle S_\gamma^{(m+1)}\rangle\langle S_\beta^{(m)}\rangle \tag{4.25}$$

and

$$\frac{\partial\langle S_\gamma^{(m)}\rangle}{\partial K_\alpha^{(m)}} = \langle S_\gamma^{(m)} S_\alpha^{(m)}\rangle - \langle S_\gamma^{(m)}\rangle\langle S_\alpha^{(m)}\rangle. \tag{4.26}$$

The evaluation of the critical exponents, as well as all the critical characteristics that can be obtained from the transformation matrix —here truncated— is finally done as described at the end of the preceding section.

An interesting fact to note is that this transformation technique leads to two different fluctuation time scales. Indeed, in the majority rule transformation, the value of the cell system can be changed by only one spin. This means that the renormalized system will still contain some of the short-time fluctuations coming from the original system.

Lastly, in view of critical analysis, we note that this procedure requires the knowledge of the critical temperature in advance. This also applies to the recent applications of this method to dynamics, where the critical exponent z is evaluated by a similar space rescaling method that involves time "matching". Before presenting this method, we shall give a brief review of scaling in critical dynamics.

Chapter 5

Critical Dynamics and Scaling

This chapter shall present an overview of critical dynamic phenomena. Scaling laws as well as Monte Carlo investigations will be reviewed. In addition, we shall lastly concentrate on the determination of the critical exponent z for the two-dimensional Ising model.

As seen in the Section 2.4, the range of fluctuation correlations at the critical point is very large. Therefore, any response from the system to a small external perturbation will require the onset of long-range response modes that have a very long relaxation time, mainly because of the large number of particles involved. This is *critical slowing down.*

The study of time-dependent properties is generally more difficult than the study of equilibrium quantities. This is largely because dynamical properties depend crucially on new effects, such as conservation laws. As a result, the study of critical dynamic phenomena is less developed than its static counterpart. Moreover, as we have seen earlier, most of the equations attempting to describe the kinetic processes are phenomenological.

5.1 Conventional theory

The oldest theory trying to explain critical slowing down is based on the thermodynamics of irreversible processes[1] (Kawasaki 1971). Using arguments similar to those used in Section 3.4.2 the rate of change of the order parameter ψ, towards the equilibrium value ψ_o, is related to the thermodynamic difference $\Phi(\psi)$ from the equilibrium value by[2]

$$\frac{\partial \psi}{\partial t} = -\Gamma \frac{\partial \Phi}{\partial \psi} \tag{5.1}$$

where Γ is the kinetic coefficient. The thermodynamic potential Φ can be expanded about the equilibrium value ψ_o

$$\Phi(\psi) = \left(\frac{\partial^2 \Phi}{\partial \psi^2}\right)_{\psi=\psi_o} \frac{(\psi - \psi_o)^2}{2} + \ldots$$

By using the thermodynamic relation

$$\left(\frac{\partial^2 \Phi}{\partial \psi^2}\right) = \left(\frac{\partial h}{\partial \psi}\right) = \frac{1}{\chi},$$

where h is the field coupled with the parameter ψ, and by assuming that the curvature of the potential does not change in the vicinity of its minimum, we then get

$$\frac{\partial \psi}{\partial t} = -\frac{\Gamma}{\chi}(\psi - \psi_o), \tag{5.2}$$

which has an exponential solution associated with a time constant $\tau = \chi/\Gamma$. As seen in Section 2.4, the divergence of χ goes as $|\theta|^{-\gamma}$ near T_c. If Γ remains finite, then the relaxation time τ diverges as χ. However, this argument cannot say anything about possible singularities of Γ at T_c, and indeed some experiments have found it to diverge near the critical temperature (Kawasaki 1976).

It may be instructive to derive the same result from the phenomenological equations of motion presented in Section 3.4.2. For this purpose, suppose we have coarse grained our Ising model, as in equations (3.8) or (3.12), and that we assume that the

[1] This theory is also sometimes called *van Hove theory*

[2] Noise is ignored for simplicity, cf. equation (3.28)

cell Hamiltonian can be described by a Ginzburg-Landau free energy (2.5). That is,

$$\beta\mathcal{H} = \int d^d x \left[\frac{a}{2}\theta\psi^2 + \frac{b}{4}\psi^4 + c(\nabla\psi)^2\right], \tag{5.3}$$

where the continuous variables ψ are obtained from a transformation of the form

$$\psi = \frac{1}{L^{d/2}} \sum_{k<\Lambda} \sigma_k e^{i\boldsymbol{k}\cdot\boldsymbol{x}}.$$

When this last equation is used in (5.3) and the properties of Fourier transforms are used, we obtain (Ma 1976b)

$$\beta\mathcal{H} = \sum_{k<\Lambda}\left[\frac{a}{2}\theta + ck^2\right]|\sigma_k|^2 + \frac{1}{L^d}\sum_{k_1,\ \ ,k_4}\delta(k_1+k_2-k_3-k_4)\sigma_{k1}\sigma_{k2}\sigma_{k3}\sigma_{k4}$$

which can be approximated by

$$\beta\mathcal{H} \simeq \sum_{k<\Lambda}\left[\frac{a}{2}\theta + ck^2\right]|\sigma_k|^2. \tag{5.4}$$

The phenomenological equation of motion for the k^{th} mode is written as (cf. equation (3.28))

$$\frac{\partial\sigma_k}{\partial t} = -\Gamma_k\left[a\theta + 2ck^2\right]\sigma_k + \eta_k \tag{5.5}$$

with η_k subject to the same restrictions as those given by (3.29) and where the driving force has been obtained from $\beta\left(\frac{\partial\mathcal{H}}{\partial\sigma_k}\right)$. This shows that the driving force is parabolic with respect to each mode k. In the limit $k \to 0$ it becomes infinitely small. This is consistent with the fact that the long-range ordering modes are expected to be the ones responsible for critical slowing down. Note that each mode is independent of the others, so that there is no mode-mode coupling. Indeed, if one supposes that the Γ_k are the same for all k then the relaxation time τ will be given by

$$\tau_k = \frac{1}{\Gamma[a\theta + 2ck^2]} \tag{5.6}$$

so that, for small k, near T_c,

$$\tau_k \sim \frac{\theta^{-1}}{\Gamma} = \frac{\chi}{\Gamma} \tag{5.7}$$

where the last equation comes from the fact that $\gamma = 1$ in the mean field theory. This is precisely the same result as the one obtained earlier.

5.2 Dynamic scaling hypothesis

The dynamic scaling hypothesis is expressed as follows

$$\tau_k = \xi^z f(\xi k). \tag{5.8}$$

It could be derived by extending the arguments of static scaling to dynamics. This was done for example by Halperin *et al.* (Halperin and Hohenberg 1969). The exponent z is called the dynamic critical exponent. Note that the argument of the function is a dimensionless quantity. This means that a scale change in the system would lead to rescaling of the characteristic time scale. We will focus attention on z for the two dimensional spin-flip Ising model. We note that there is much general experimental evidence to support the dynamic scaling hypothesis in many systems and a few direct results estimating the value of z have been recently obtained [3] See, for example, (Landau, Tang and Wansleben 1988) and references therein.

We shall now take a look at an explicit example of the scaling form of the conventional theory (Ma 1976b). If we use the mean field value for the correlation length $\xi = \theta^{-1/2}$ in equation (5.6) we can get

$$\tau_k = \frac{1}{\Gamma(\xi^{-2} + 2ck^2)} = \xi^2 \frac{1}{\Gamma(1 + 2c(\xi k)^2)} \qquad \xi^2 f(\xi k) \tag{5.9}$$

from which we find a critical exponent $z = 2$. More correctly, conventional theory gives $z = 2 - \eta$, where $\eta = 0$. However, the above theory does not describe correctly most realistic problems. The main reasons are

- The approximation (Gaussian) of taking the Hamiltonian as in equation (5.1) has already proven to be wrong for the dimensions considered since it leads to mean field theory.

- The assumption that Γ_k is independent of k is also a bad approximation, for the different modes can have different driving mechanisms

[3] The most striking fact about experimental results obtained for two-dimensional systems is that $z < 2$ for all those we are aware of, at the moment.

- The Langevin equation (5.5) did not consider mode-mode coupling.
- Finally, the inclusion of mean field exponents in the theory is not consistent with experimental evidence.

Much literature has been devoted to this subject, for which other notions including hydrodynamics and transport theories are often required. However, a good starting point is Ma's book (Ma 1976b).

5.3 Dynamic quantities and finite-size behaviour

In a finite system, the correlation length will always be bonded by the dimensions of the lattice. Instead of the infinite divergence of the correlation length found at T_c for an infinite system, we rather might expect to have

$$\xi \sim L$$

where L is the linear dimension of the system considered. This is the only argument needed to introduce the finite-size scaling of the correlation length in a finite system, namely

$$\tau \sim L^z. \tag{5.10}$$

This tells us how the relaxation time will scale between systems of different sizes. In fact, this method has been directly used by us to determine the value of z. However, before presenting those results, we shall introduce some of the measured dynamical quantities.

Usual measurements done on a kinetic system encompass the time-displaced spin-spin correlation $C(t)$ and the time-displaced nearest-neighbour correlation $E(t)$. Formally, by assuming we have a hypercubic L^d system, we estimated the following quantities

$$C(L^d, m, t) = \frac{b^{md}}{L^d} \sum_i s_i^{(m)}(t_o) s_i^{(m)}(t_o + t), \tag{5.11}$$

$$E(L^d, m, t) = \frac{b^{md}}{L^d} \sum_{\langle ij \rangle} s_i^{(m)}(t_o) s_j^{(m)}(t_o + t), \tag{5.12}$$

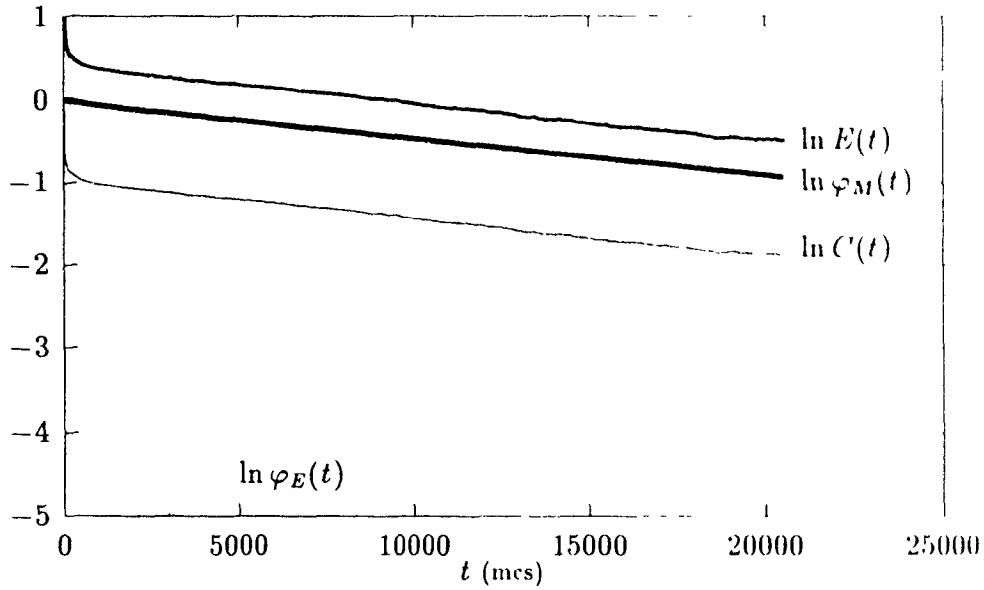

Figure 5.1 Different time-displaced correlation functions for a system of 64×64 sites. Note the large difference between $\varphi_E(t)$ and $\varphi_M(t)$ showing that the energy relaxes much more rapidly than the order parameter. Also note the noise common to $C(t)$ and $E(t)$. We used $\varphi_M(t)$ in our estimations.

where the renormalization iteration number m as well as the RG blocking factor b were explicitly introduced in view of the *matching* technique involved. This latter will be presented below. These two quantities were originally studied because of their computational simplicity.

Other quantities of interest are the general time-displaced correlation functions previously defined by equation (3.13). The advantage of this last quantity over the preceding one is that the product of the fluctuations is subtracted, thus taking care of the specific representativity of the sample taken with respect to the population. The denominator renormalizes the function so as to make it between -1 and 1. Figure 5.1 shows these different time-displaced correlation functions for a given system.

When one selects magnetization as the observable, then the two quantities above (i.e. equations (5.11) and (5.12)) can be shown to be subsets of the resulting time displaced correlation function. For example, the correlation between two sets of magnetization values measured at different times will include equation (5.11) as a

result of the expansion of the sum. That is, by defining $\varphi_M(t)$ as

$$\varphi_M(t) = \frac{\langle M(t_o)M(t_o+t)\rangle - \langle M(t_o)\rangle\langle M(t_o+t)\rangle}{\langle M(t_o) - \langle M(t_o)\rangle^2\rangle^{1/2}\langle M(t_o+t) - \langle M(t_o+t)\rangle^2\rangle^{1/2}}, \tag{5.13}$$

and breaking the product of the two sums M in the first term of the denominator in a sum over sums of self-, first-, second-, third-... neighbour correlations, then the resulting series will contain equation (5.11) as its first term. Moreover, this self- term will be the largest of the sum since a spin is more highly correlated with itself than with any other one. The second term of this expansion is the nearest-neighbour correlation. This is precisely equation (5.12). The expansion coefficients are dependent on the topology of the lattice.

When the energy is used as the observable, the resulting correlation function $\varphi_E(t)$ has a much shorter lifetime mainly due to the fact that this quantity depends on pair-pair correlations over the whole lattice. Therefore the observation of the time evolution of the energy as a measure of the equilibrium of a system is not appropriate. Among the different observables, the order parameter generally has the longest relaxation time.

We shall now present some error analysis in relation to real computer experiments. The independence of the data obtained from a Monte Carlo simulation is a problem of prime importance, especially at T_c where the correlation time τ is relatively large. Zwanzig *et al.* (Zwanzig and Allawadi 1969) derived an expression for the error resulting from the finiteness of the simulation in time. This is done by assuming that the observable is Gaussian and by using relations among different moments, as those found in Landau and Lifshitz (Landau and Lifshitz 1981). By defining the difference between the finite-time average and the ensemble average by

$$\Delta(t) = \langle A(t_o)A(t_o+t)\rangle_{[t_1,t_2]} - \langle A(t_o)A(t_o+t)\rangle_\infty, \tag{5.14}$$

one may equivalently write

$$\Delta(t) = \frac{1}{t_2 - t_1}\int_{t_1}^{t_2} dt_o\,[A(t_o)A(t_o+t) - \langle A(t_o)A(t_o+t)\rangle_\infty].$$

Clearly, the first moment $\langle \Delta(t) \rangle$ goes to zero when the ensemble average is taken out and the statistical error due to finite-time averaging is estimated from the second moment of the distribution. The derivation will not be reproduced here since the clarity of this very good paper can hardly be improved. If one normalizes $\langle A(t_o)A(t_o+t) \rangle$ by the $t = 0$ dispersion, then the relative error on the difference from unity will be found to be

$$\left(\frac{\langle A(t_o)A(t_o+t) \rangle_\infty}{\langle A^2(t_o) \rangle_\infty} - 1 \right) \Big/ \left(\frac{\langle A(t_o)A(t_o+t) \rangle_{[t_1,t_2]}}{\langle A^2(t_o) \rangle_{[t_1,t_2]}} - 1 \right) \sim 1 + \left(\frac{2\tau}{t_2 - t_1} \right)^2 . \quad (5.15)$$

This shows that the error $\Delta(t)$ becomes more and more important as we go away from unity, or equivalently as t gets larger.

We shall now briefly quote the recent developments in the evaluation of the critical exponent z for the two-dimensional spin-flip Ising model case, done with the help of the finite-size scaling hypothesis. Some valuable analyses have been done by Landau *et al.* (Landau, Tang and Wansleben 1988) as well as by Wansleben *et al.* (Wansleben and Landau 1987). The former contains a survey of the estimates for the critical exponent that encompasses the last 10 years and ranges from 1.4 to 2.24 (Landau, Tang and Wansleben 1988; Williams 1985b). By fitting an exponential to the decay of $\varphi_M(t)$ over systems of different sizes, they could fit equation (5.10) quite satisfactorily Thus, the finite-size scaling method yielded a z-value of 2.14.

Because the different methods yielded results that were not consistent within their respective error margins, some authors started to question the systematic errors involved in each of the methods considered. A recent study on statistical and systematic errors on time-displaced correlations with respect to different degree of self-averaging has been presented by Ferrenberg *et al.* (Ferrenberg, Landau and Binder 1990). Moreover there is no *a priori* evidence that a multi-spin coding algorithm will have the same critical behavior. Although both systems are believed to belong to the same universality class, the only formal comparison that we are aware of at this time is the one done by Williams (Williams 1985a), which has some restricted conclusions This hypothesis should definitely be further investigated.

5.4 Dynamic MCRG

We shall now present an extension of the MCRG methods, as described before, to the study of dynamic behaviour at the critical point. This is done partly because the method we propose will have direct applications to this problem and also partly because the study of growth and scaling done by using MCRG methods is a straightforward extension of the present procedure. The application of MCRG methods to growth will be seen in Section 6.4. We note, once more, that the theoretical issues raised by the application of MCRG to such problems can still not be answered at the present time.

Tobochnik, Sarker and Cordery (Tobochnik, Sarker and Cordery 1981) were the first to extend the MCRG methods to the study of dynamical critical behaviour. The central idea, proposed by Wilson to Tobochnik *et al.* , is *matching*. Starting with two lattices differing by a factor b in their linear dimensions, a sequence of configurations is generated for each of them with the standard Monte Carlo techniques discussed earlier. We shall consider a zero field Ising model with its Hamiltonian given by

$$\mathcal{H}(T) = K \sum_{\langle ij \rangle} \sigma_i \sigma_j \tag{5.16}$$

where we used $\langle ij \rangle$ to denote the sum over all nearest-neighbour pairs. From these two sequences of configurations, a majority rule MCRG transformation is iterated in order to generate other sequences each smaller by a blocking factor b. Again, the $m+1$ iterated largest system will be compared with the m iterated smallest one. However, the blocking procedure will have reduced the correlation length by a factor b. In view of equation (5.8), this means that the characteristic time of the system will have been changed by a factor b^z, since the dimensionless argument of the function will stay invariant.

The matching condition mentioned above can be expressed in terms of the two observables introduced by equations (5.11) and (5.12) as follows

$$C(L, m, t) = C(bL, m+1, b^z t) \tag{5.17}$$

and similarly for E. This means, given two systems having the same finite-size effects, we are interested in how the characteristic time scale has changed if one of these has been renormalized once more than the other. The answer is given by the above scaling relation.

Most of the simulations performed with the help of this technique have been done on a two-dimensional Ising model (Yalabik and Gunton 1982; Katz, Gunton and Liu 1982; Williams 1985b). A complete review can be found in a paper by Williams (Williams 1985b). Simulations implying different lattice sizes have been done, although the sizes used were still relatively small compared to the ability of today's computers. In relation to this problem, a nice and promising analysis of a real space time-dependent RG applied to a one-dimensional Ising model was made by Achiam (Achiam 1978).

The previous idea could also be exploited in an interesting way which involves the temperature. We know that the correlation length will change under a RG transformation. That is, for two *equilibrium* systems, one of which being iterated once more than the other, we have

$$\xi(T_1) = b\xi(T_2). \tag{5.18}$$

Clearly, this equality will hold with the special condition $T_1 = T_2$ at the critical point. However, we can use the asymptotic form of the correlation length near T_c thus giving

$$\frac{\theta_2}{\theta_1} = b^{1/\nu} \tag{5.19}$$

from which the value of the critical exponent should be obtained as a verification.

Lastly, we should mention that apart from MCRG, a pleiad of other techniques have been used in order to study critical dynamics. The so-called ϵ-expansions, and other direct theoretical approaches will not be described here. We shall however briefly describe a MC approach which consists in studying *damage spreading* in a given system. This computer experiment involves the study of time development of differences between two almost identical systems evolving under the same MC dynamics. The critical exponent is then extracted by finite-size analysis of the relaxation

constants. A recent contribution to this approach can be found in (Poole and Jan 1990).

Chapter 6

Growth—Theories and Review

Domain growth is intimately related to topology. This was recognized by Gibbs who first tried to calculate the reversible work required to form a cluster from the supersaturated vapour by developing a thermodynamic theory of curved surfaces. But, as mentioned earlier, phase transitions are a dynamic problem and a kinetic approach only came much later ($\sim$ 1940) with the work of Zeldovich, Farker, Becker, Döring, Frenkel, and others, on steady state nucleation theories. For a review, see, for example, (Abraham 1974; Gunton, San Miguel and Sahni 1983) and references therein. More recently (1960 to now) an explosion of activity, fired by metallurgic applications, occurred in this field and the following pages will only try to give the part relevant to our problem.

6.1 Some different approaches

Among the theories proposed at this time, the two main approaches of growth theories were highly influenced by the existing stable-unstable relaxation dichotomy. One of these, the older, consists in considering the dynamics of clusters. This is appropriate, for example, for the relaxation process involved in the decay of a metastable state. This forms the core of homogeneous nucleation theory.

The major ingredient of this theory is the concept of a critical droplet. Imagine,

for example, an Ising model in which the magnetic field h has been momentarily reversed. Then, some "droplets" of some size n will start to form in the homogeneous background. Each of these will generate an energy difference ΔE according to

$$\Delta E = 2hn + \sigma n^{(d-1)/d},$$

where σ is a surface tension term[1] and d is the dimension. The process thus involves a competition between a more stable bulk component and an energy costing surface term. This defines a critical droplet size from which the whole process of creating a droplet starts to liberate energy. Most of these theories consider a Boltzmann distribution of the droplets and involves differential equations on which various physical boundaries conditions have been imposed.

This model, however, is limited to low densities and temperatures far from the critical point since the droplets are usually taken as non-interacting. This clearly breaks down near the critical point where large regions of space become correlated.

Another approach consists in concentrating on the interfaces. Some information can be predicted with the help of very simple arguments. Assume, for example, a two-component mixture. It is expected that the driving force of a moving boundary will come from the excess of its free energy. Although the displacement of an interface implies microscopic analysis and diffusion properties, we simply assume that the speed of the interface responds linearly to the driving force.[2] We expect that the excess in free energy will be proportional to the surface tension times the mean curvature. The latter, from geometrical arguments, is proportional to the reciprocal of the size R of the domains. We get, after integrating,

$$R^2 \propto t. \tag{6.1}$$

This result is precisely the Allen-Cahn law which will be derived more formally in the next section. However, contrary to this "intuitive" approach, the following derivation

[1] Note that the Ising model is misleading with respect to the surface tension term since it comes from the coupling interaction between the background phase and the spins on the surface. For an actual droplet, the effect is rather due to the geometrical fact that a molecule on the surface is less tightly bound than a molecule inside. It is a surface effect

[2] The proportionality constant is sometimes referred to as the mobility

does not consider the surface tension directly[3] . We also note that Lifshitz (1962) previously derived the same result on the basis of diffusion arguments.

Lastly, we note that the numerical solutions of the relaxational TDGL presented in Section 3.4.2 are consistent with the value of $\frac{1}{2}$ (Valls and Mazenko 1986) for the growth exponent n in $R \sim t^n$.

6.2 Antiphase boundary motion theory

Theories to explain the motion of grain boundaries, in polycrystalline metals for example, have been proposed in recent years. Among these different approaches, Allen and Cahn (1979) proposed a theory based on the motion of the antiphase boundary.[4] For this, they considered the antiphase boundary as a surface having its own characteristics such as geometrical properties (including thickness), free energy, velocity, etc...It is also recognized that phase boundaries have an excess free energy Note that the energy of this interface should vanish continuously near T_c since the two phases converge accordingly.

The starting equation for this theory is the Ginzburg-Landau free energy density as defined by equation (2.5). Moreover, it is assumed that the order parameter is driven by an equation similar to (3.28) but without the random noise term.[5] Thus, in terms of an order parameter ψ defined over a small region of space, we have

$$\frac{\partial \psi}{\partial t} = -\Gamma \frac{\delta F[\psi]}{\delta \psi}. \tag{6.2}$$

This last functional derivative can be evaluated as follows. For a change $\delta\psi$ at x then we can write, from equation (2.5) and by using $\psi' = \psi(\boldsymbol{x}')$,

$$\delta F = \int \left[\frac{\partial f_o}{\partial \psi'} + c \frac{\partial}{\partial \psi'} (\nabla' \psi')^2 \right] \delta(\boldsymbol{x} - \boldsymbol{x}') \, \delta\psi' \, d\boldsymbol{x}' \tag{6.3}$$

[3]Some coefficient can indeed be related to a surface tension

[4]In a binary alloy for example, the antiphase is the interface at $\boldsymbol{BB}$ in the sequence $ABABBABABA$. . Generally speaking, it is the interface between two identical domains differing by a displacement that shifts the domains from one superlattice to another.

[5]The effect of random noise has been studied by Kawasaki and Otha (1982a, 1982b) However, a more accessible description as well as the influence of the temperature is presented in (Grant and Gunton 1983).

$$= \frac{\partial f_o}{\partial \psi}\,\delta\psi + 2c\int \nabla'\psi'\,\nabla'\delta(\boldsymbol{x}-\boldsymbol{x}')\,\delta\psi'\,d\boldsymbol{x}'. \tag{6.4}$$

By using properties of the delta function, finally get[6]

$$\frac{\delta F}{\delta \psi} = \frac{\partial f_o}{\partial \psi} - 2c\,\nabla^2\psi. \tag{6.5}$$

Note that by the fundamental theorem of integral calculus, the stationary point of the free energy functional, representing the equilibrium situation, will be given when, at any point $\boldsymbol{x}$,

$$\frac{\partial f_o}{\partial \psi} = 2c\,\nabla^2\psi. \tag{6.6}$$

By equation (6.5), equation (6.2) can be rewritten as

$$\frac{\partial \psi}{\partial t} = -\Gamma\frac{\partial f_o}{\partial \psi} + M\,\nabla^2\psi \tag{6.7}$$

where $M = -2\Gamma c$ has dimensions of a diffusion constant. Allen and Cahn have shown that this last equation does not have a spherically symmetrical solution.

Since $\psi(\boldsymbol{x})$ is analytic everywhere, it is possible to define a curvilinear set of coordinates using the family of iso-ψ planes perpendicular to the gradient of $\psi(\boldsymbol{x})$. In a natural way, the gradient is the derivative with respect to the normal, say q_1, and we have, according to Arfken's notation (1985) for a Laplacian defined over coordinates (q_1, q_2, q_3) with metrics (h_1, h_2, h_3) ,

$$\nabla^2\psi = \frac{1}{h_1h_2h_3}\left[\frac{\partial}{\partial q_1}\left(\frac{h_2h_3}{h_1}\frac{\partial\psi}{\partial q_1}\right)\right].$$

The element dn along the normal coordinate is given by $h_1\,dq_1$ so that

$$\nabla^2\psi = \frac{1}{h_2h_3}\frac{\partial}{\partial n}\left(h_2h_3\frac{\partial\psi}{\partial n}\right) = \frac{\partial^2\psi}{\partial n^2} + \frac{\partial\psi}{\partial n}\frac{1}{h_1h_2h_3}\left[\frac{\partial}{\partial q_1}(h_2h_3)\right].$$

In the same coordinate system it is possible to express the divergence of a unit vector along the normal as

$$\nabla\cdot\hat{n} = \frac{1}{h_1h_2h_3}\left[\frac{\partial}{\partial q_1}(h_2h_3)\right].$$

[6]Note that c can be seen to be proportional to the surface tension.

Moreover, differential geometry can relate the divergence of a normal unit vector to the mean of the mean curvature $(K_1 + K_2)$ along the iso-ψ surfaces. We then have

$$\frac{\partial \psi}{\partial t} = -\Gamma \left\{ \frac{\partial f_o}{\partial \psi} - 2c \left[\frac{\partial^2 \psi}{\partial n^2} - (K_1 + K_2)_{\psi = \text{cst}} \frac{\partial \psi}{\partial n} \right] \right\}. \tag{6.8}$$

Suppose the system had time to separate in two distinct regions that coexist between gently curved interfaces. Indeed, the local ordering of very small volume elements in two equivalent coexisting regions, of order parameter near the values $\pm \psi_e$, will be formed almost instantaneously when observed from a macroscopic point of view. Therefore, if (6.6) is assumed to hold at "medium" time phase separation, then equation (6.8) reads

$$\left(\frac{\partial \psi}{\partial t} \right)_n = -M(K_1 + K_2) \left(\frac{\partial \psi}{\partial n} \right)_t. \tag{6.9}$$

The velocity v of an iso-ψ plane will be given by

$$v = \left(\frac{\partial n}{\partial t} \right)_\psi = -\left(\frac{\partial \psi}{\partial t} \right)_n \Big/ \left(\frac{\partial \psi}{\partial n} \right)_t \tag{6.10}$$

where we used the relation $\left(\frac{\partial x}{\partial y}\right)_z \left(\frac{\partial y}{\partial z}\right)_x \left(\frac{\partial z}{\partial x}\right)_y = -1$. Hence, the velocity of the planes will be described by

$$v = \left(\frac{\partial n}{\partial t} \right)_\psi = M(K_1 + K_2). \tag{6.11}$$

Since the mean curvature of smooth and thin interfaces is directly related to the size of the domains, we get equation (6.1),

$$v \simeq \frac{\partial R}{\partial t} \simeq \frac{1}{R} \tag{6.12}$$

meaning that

$$R \sim t^{1/2}. \tag{6.13}$$

6.3 Growth measurement

From an experimental point of view, the measurement of domain size, at early times, is done almost exclusively by scattering methods. In the first Born approximation, the scattering cross section is equal to the matrix element

$$\Gamma_{fi} \propto \langle \int d\boldsymbol{x}\ e^{-i\boldsymbol{p}_f \boldsymbol{x}} \sigma(\boldsymbol{x}) e^{i\boldsymbol{p}_i \boldsymbol{x}} \rangle,$$

where $\sigma(\boldsymbol{x})$ can now be seen as the electronic probability density. If $\boldsymbol{k}$ is defined as the momentum transfer $\boldsymbol{p}_f - \boldsymbol{p}_i$, then, in view of the Fourier transformations (3.9) and (3.10), the cross section can be expressed as

$$\Gamma_{fi} = \langle |\sigma_{\boldsymbol{k}}|^2 \rangle \tag{6.14}$$

giving a direct relation with the order parameter density.

At later times, electron microscopy is available but the analysis of the results is then much less obvious (Doremus 1985). In the context of surface sciences (e.g. adsorption measurements), the techniques involved are various and sophisticated. From the viewpoin of numerical simulations, there exist three common methods of "measurement" for the various models. One of these, involving the first moment of the structure factor, has not been used in the course of this work and will therefore not be presented here. We shall present the two other ones.

6.3.1 The inverse perimeter density

We first want to determine the perimeter density of a given model. For this purpose, assume a N site Ising model on which we define $B_{\uparrow\uparrow}, B_{\downarrow\downarrow}$ and $B_{\uparrow\downarrow}$ as the number of bonds in the configuration indicated by their subscripts and $N_\uparrow, N_\downarrow$ the number of spind up or down, respectively. If we use u as the energy per site, the Hamiltonian (3.2) can be rewritten, in this new notation, as [7]

$$u = \frac{\epsilon}{N}(B_{\uparrow\uparrow} + B_{\downarrow\downarrow} - B_{\uparrow\downarrow}). \tag{6.15}$$

For a γ neighbour model we must also have, counting the total number of bonds,

$$\frac{\gamma N}{2} = B_{\uparrow\uparrow} + B_{\downarrow\downarrow} + B_{\uparrow\downarrow}.$$

These two last equations can be used to derive the mean perimeter density, i. e. the average number of "broken bond" per spin. Note that this terminology implies a ferromagnetic model. Thus we have

$$\frac{B_{\uparrow\downarrow}}{N} = \frac{\gamma N}{4} - \frac{u}{2\epsilon}.$$

[7] It is given by (3.3) for a two-dimensional system at equilibrium.

We then define $\bar{R}(t)$ as the mean radius of the domain by

$$\bar{R}(t) = \frac{1}{2}(R_\uparrow(t) + R_\downarrow(t)),$$

where

$$R_\uparrow(t) = C_d \frac{N_\uparrow(t)}{B_{\uparrow\downarrow}(t)}$$

is the mean radius of the '↑' domains and similarly for the '↓' domains. The factor C_d is the proportionality constant in dimension d. We assume that C_d is not a function of R so that the distribution of the shape of the domains must remain constant as they grow. Clearly, this is true in view of self-similarity discussed earlier. By combining these last equations, using $N_\uparrow + N_\downarrow = N$,

$$\bar{R}(t) \propto \frac{N}{B_{\uparrow\downarrow}(t)} = \frac{4}{\gamma - \frac{2u(t)}{\epsilon}}. \tag{6.16}$$

This parameter is the easiest to use since it follows directly from the value of the energy, which is usually straightforwardly obtained.

6.3.2 The squared magnetization

Consider now the ensemble average for the square of the magnetization $\langle M^2(t) \rangle$. Since the magnetization is defined as

$$M = \frac{1}{N}\sum_{i=1}^{N} \sigma_i,$$

therefore

$$\begin{aligned} \langle M^2(t) \rangle &= \frac{1}{N^2}\langle \sum_{i=1}^{N}\sum_{j=1}^{N} \sigma_i(t)\sigma_j(t) \rangle = \frac{1}{N^2}\sum_{i=1}^{N}\sum_{j=1}^{N} \langle \sigma_i(t)\sigma_j(t) \rangle, \\ &= \frac{1}{N}\sum_{i} \langle \sigma_i(t)\sigma_0(t) \rangle. \end{aligned}$$

The summand in the last equation is just the definition of the spin correlation function. This thus says that the mean squared magnetization is equivalent to the mean of the correlation of one spin with respect to all the others. If the form of the correlation function remains the same,[8] it would possible to relate the measure of the spin

[8] Self-similarity supports this idea

correlation to the size of the domains by some parameter of the curve. The parameter above is just a system-normalized integral of this function over all space. Another demonstration, that the average squared magnetization is related to the domain size, can be found in (Sadiq and Binder 1984). It is argued in this paper that, for intermediate times, the main contribution to the product $\langle \sigma_i \sigma_j \rangle$ will average to the value of the order parameter at equilibrium M_{eq}^2, if i and j are in the same domain, and to zero if they are in different domains. Therefore, since

$$\langle M^2(t) \rangle = \frac{1}{N^2} \sum_i \sum_j \langle \sigma_i(t) \sigma_j(t) \rangle$$

we can break the sum in a sum over the $n(t)$ domains composed of a number of sites proportional to $R^d(t)$, and get

$$\langle M^2(t) \rangle \sim \frac{1}{N^2} n(t) \sum_i' \sum_j' M_{eq}^2 \sim \frac{1}{N^2} n(t) R^{d2}(t) M_{eq}^2$$

where primes have been put on the sums in order to represent summing so that i and j are in the same domain. If furthermore one assumes that the interfaces are negligible so that $n(t)R^d(t) \sim N$ we then get

$$\langle M^2(t) \rangle \propto \frac{1}{N} R^d(t) M_{eq}^2$$

from which we define

$$R^d(t) \propto \frac{N \langle M^2(t) \rangle}{M_{eq}^2} \propto \langle M^2(t) \rangle. \tag{6.17}$$

The inverse perimeter density generally gives better results. The square of the magnetization seems to be more unstable so that an average over more systems is required to get valuable data.

6.4 MC growth and scaling studies

With the tools presented so far, we are now able to give a general review of Monte Carlo studies of growth. Monte Carlo simulations on antiferromagnetic (Phani et al. 1980; Sahni, Dee and Gunton 1981; Kaski et al. 1983) as well as ferromagnetic

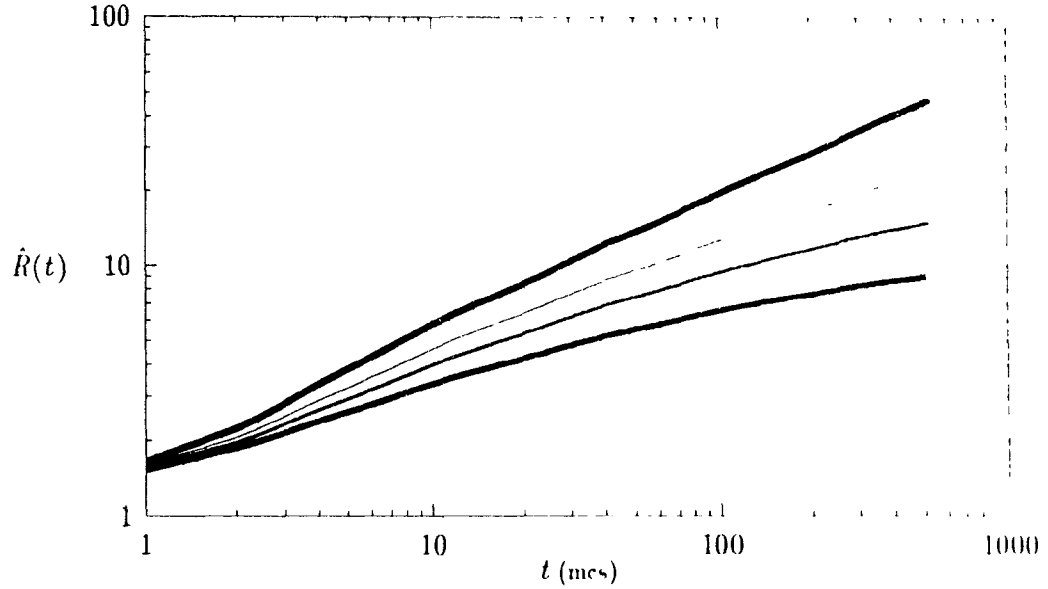

Figure 6 1. The dependence of the quench temperature on the time evolution of the domain size The different curves represent a system of 128 × 128 quenched at temperatures going, from top to bottom, from 0 0T_c to 0 9T_c in steps of 0 1T_c The final state temperature has a non trivial effect on the velocity of the interfaces

(Gawlinski et al. 1985) two-dimensional Ising models unanimously gave the $n = \frac{1}{2}$ growth exponent. The effect of the temperature of the heat bath is not negligible Indeed, the final state drives the process so that a direct effect is to be expected from the final state temperature. Figures 6.1 and 6.2 represent the evolution of the inverse perimeter density and the energy per spin in time. The closer the final state to T_c, the slower will be the growth. This is due to large relaxation times required for the low k modes near T_c.

Moreover, all the dynamic measurements of the structure factor were found to scale according to the form

$$S(k,t) = \langle R(t) \rangle^d f(k\langle R(t) \rangle)$$

As shown earlier, RG methods have been proven to be very useful in the context of second-order phase transitions. The same technique has also been extended to the study of growth dynamics. For example, some real space RG analysis has been done in a series of papers by Mazenko *et al.* . See (Viñals et al. 1985) and references therein Combined with the standard MC simulation techniques, MCRG methods have been

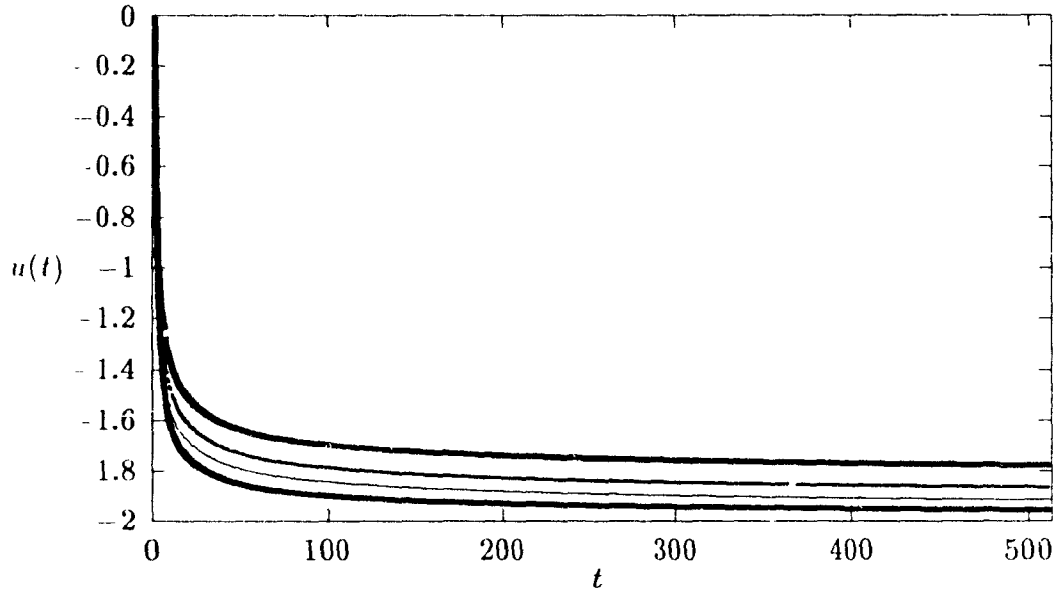

Figure 6.2 The curves represent a system of 128 x 128 quenched at temperatures going, from bottom to top, from $0.0T_c$ to $0.9T_c$ in steps of $0.1T_c$. Note that the driving force goes asymptotically slower and slower as closer to T_c. Because of the very weak slope, it can be found to fit a power law as well as an exponential

further extended to study the non-equilibrium dynamics of the Ising model.

The method exploits the self-similarity that the system bears in time. The RG transformation will therefore be used to rescale the linear dimensions of the system, thus transforming the coupling constants and also time in a non-trivial way. Indeed, the main idea is that a transformed system, at a temperature T_1 and time t_1, may be found equivalent, after renormalization, to a system at temperature T_2 and time t_2.

A quench is done from a high temperature system to a finite $T < T_c$. In view of RG formalism, the equilibrium states corresponding to times $t = 0$ and $t = \infty$ will be characterized, after m iterative transformations, by coupling constant vectors $\boldsymbol{K}_i^{(m)}$ and $\boldsymbol{K}_f^{(m)}$ respectively. We know, however, that such an Ising model has an unstable fixed point $\boldsymbol{K}^*$ at T_c, from which a RG transformation flows towards either of the two stable fixed points $\boldsymbol{K}_o^*$ and $\boldsymbol{K}_\infty^*$. Therefore, as $m \to \infty$, the RG transformations applied on a configuration sequence of a given quench would end up by giving two sets of systems at two different temperatures $\boldsymbol{K}_i^{(m)} = 0$ and $\boldsymbol{K}_f^{(m)} = \infty$. Therefore, the application of RG transformations to a given quench, done at a certain T, will

yield a phenomenon driven by a lower T. In contrast to critical phenomena, this transformation thus involves stable attractive fixed points.

The details of the method are as follows. An infinite temperature (random) configuration of a N-site Ising model is put in contact with a cold heat bath (a cold Hamiltonian) at a temperature $T < T_c$. Then, a time sequence of configurations is produced by storing the system configurations at each, say, δt mcs. For such a procedure, the overall time range is generally of the order of few hundreds mcs, depending on the system size, and of a few unities for δt. We then perform a MCRG majority rule transformation on each of the configurations, thus reducing the linear dimensions by a factor b. We note here that the master equation for the renormalized sequence of configurations will not be Markovian any more.

Meanwhile, the same procedure is applied to a similar system of size Nb^d. We want to match systems of the same linear dimension, but different iteration numbers, such that the domain size is the same. That is, we want to have, assuming a hypercubic system,

$$R(L,m,t) = R(Lb,m+1,t') \tag{6.18}$$

which is expected to hold for different iteration numbers m. This matching condition is used to obtain the growth exponent. In fact, we must have

$$\begin{aligned} \ln R &\sim n \ln t \\ \ln \frac{R}{b} &\sim n \ln t', \end{aligned}$$

so that

$$\frac{t}{t'} = b^{1/n}. \tag{6.19}$$

The success of this method is that, indeed, matching occurs for a whole range of t after only a few iterations. Moreover, it also remains consistent for the subsequent iterations. An effect of the RG process in this case is to smooth out the irrelevant fluctuations in the domains. Since those are not part of the scaling regime of R, the scale change iterates them away so that the remaining part of the system is expected to be consistent with further iterations. As a result, a translation in time should be

equivalent to a scale change in all proportions in the scaling regime. We can expect that the latter is characterized by long-range ordering modes. Reference (Kumar, Viñals and Gunton 1986) contains a more complete discussion on the effect of MCRG on such systems. More theoretical work is required to establish clearly the nature of RG in these non-equilibrium problems.

This process was successfully applied to the kinetic Ising model first by Viñals *et al.* (1985) and then by others (Kumar, Viñals and Gunton 1986). It has also been applied to the problem of spinodal decomposition (Roland and Grant 1988; Roland and Grant 1989; Roland 1989) in order to derive the controversial growth exponent $\frac{1}{3}$, for the problem where the order parameter is conserved.

Chapter 7

Results and Discussion

This chapter will present the original contribution of this thesis. The proposed MCRG method will be given in terms of the formalism already presented. The method will be applied to the kinetic Ising model with spin-flip dynamics in order to evaluate the growth exponent and results at various temperatures will be presented. Application to critical dynamics will then be described. Some preliminary results will be given and corroborated with results obtained from the different methods introduced in the previous chapters, particularly finite-size scaling.

7.1 The idea

The original idea of the method we propose is to consider time as being a variable that can be treated in the same way space is. Indeed, the dynamic MCRG methods presented earlier take advantage of self-similarity by allowing a scale change in space, thus generating a non-trivial relation with time. We now ask: Would it be possible to design a Monte Carlo method that would do an effective scale change in time? This is what this chapter will try to answer.

In view of what has been said before, a real space RG transformation will change the Hamiltonian $\mathcal{H}(\boldsymbol{K})$ by moving the parameter $\boldsymbol{K}$ to some other point in K space. Moreover, the probability independence characterizing the time steps of the original

evolution sequence of the system will not hold after a real space RG transformation, thus yielding a non-Markovian process over some renormalized time scale.

We now try to analyze what would be the effect of a similar majority rule "blocking" process applied on *one* spin in different consecutive time steps. First, we remark that a transformation of this kind will wipe out the high frequencies of fluctuations in time. In this case as well, it is clear that the time evolution of the configuration will not be Markovian any more, since the history of the spin is determined by the blocked cell value.

The advantage of blocking in time is two-fold. First, because the high-frequency fluctuations in time are wiped out, the resulting curve will be much smoother as we renormalize. Since a real space MCRG method does not renormalize the fluctuations in time, the simultaneous application of renormalizing space and time can take care of this point. Second, the time blocking factor can be adjusted so as to balance the effects resulting from blocking in space. Consider for example the growth relation $R(t) \sim t^{1/2}$ found in the scaling regime of a spin-flip growth phenomenon. A standard blocking operation performed on space would reduce the mean domain size by a factor b. If one keeps the same time scale, the process would seem to be much slower since the reduction of domain size can be thought of as a backward movement in time. Formally, this process has been exploited by the matching condition (6.18), namely

$$R(L, m, t, T) = R(Lb, m + 1, t', T'), \tag{7.1}$$

where t is clearly larger than t' and T is larger than T'. In fact, we found earlier (6.19) that $t - b^{1/n}t'$ is a direct consequence of the growth power law, when one assumes that the quenching temperature has reached a fixed point. Indeed, the temperature of the final driving state will end up being the zero temperature if one renormalizes times enough. Now suppose one chooses a *time blocking* factor such that $t'' = t$; i.e., a rescaled time t'' so that the growth process remains unchanged. This is done with the transformation $t'' = b^{-1/n}t'$, so for $b = 2$ and $n = 1/2$ this requires a transformation of the time scale by compressing it by a factor of 4. The discrepancy between the original system and the transformed system could then be used in order to evaluate

the exactness of n.

Things are not that simple, however. In this analysis, we assumed that the RG transformations had already brought the final state driving temperature to the zero temperature fixed point. Indeed, as RG iterations goes on, the whole sequence of configurations will behave as if it occurred at a lower quench temperature. If one assumes that the asymptotic regime will eventually be reached, despite the transient critical behaviour that would start to be felt as T approaches T_c ($T \gtrsim 0.7T_c$), then the coefficient α of $R(t) = \alpha(T)t^{1/2}$ will converge to $\alpha(0)$ from one iteration to another.

One can still hope that after only a few iterations, T will be equal to T' in equation (7.1). This is already true for any process at $T \gtrsim 0.3T_c$, as can be seen from figure 7.2 (page 88), but as $T \gtrsim 0.7$, the iterations needed are larger than those that can be done on systems ran on standard size computers. A way to take care of this difficulty has already been described in the literature. It consists in choosing two temperatures T_1 and T_2 such that $T_2' = T_1$, with $T_2 > T_1$. Since RG works consistently, we must also have $T_2^{(m+1)} = T_1^{(m)}$, where m is any renormalization iteration number. This has been verified in some work done by Gawlinsky *et al.* (1985). The same matching procedure can also be extended to spinodal decomposition of a binary alloy, by choosing a time dilation factor of 8. This still remains to be done.

On the other hand, the study of critical dynamics directly involves a scaling law including time. The latter assumes that a scale change in space will induce a scale change in the specific characteristic times of the system. Those are generally represented by the relaxation times. This hypothesis thus assumes that all the relaxation times of the system will respond in the same manner to the applied scale change in space, no matter which observable is considered. This assumption is perfectly consistent with the scaling hypothesis that says that the diverging correlation length is the only relevant length. It is also consistent with all the results obtained from different simulations.

Critical dynamics is sometimes best understood when one compares it with diffusion. As a reference, a standard isotropic diffusive process obeying Fick's law will

have an "order parameter" then obeying the following relation

$$\psi(\mathbf{r},t) = \frac{A}{\sqrt{t}} e^{-\mathbf{r}^2/4Dt}, \tag{7.2}$$

where D is the diffusion constant and A is related to the initial diffusing quantity located at the origin. One can easily show[1] that a scale compression by a factor b in space will be equivalent to a scale compression of b^2 in time, thus showing that $z = 2$ for a purely diffusive process. Cardy (1985) showed, by using conformational invariance arguments in order to map a two-dimensional system, represented by the mode-mode uncoupled van Hove equation (model A, cf. equation (5.5)), to a one-dimensional one, that the correlation function in two dimensions is of the form

$$g(r,t) = t^{\frac{2-d-\eta-1}{z}} e^{-r^z/t}. \tag{7.3}$$

It is interesting to note that the mean field values $\eta = 0$ and $z = 2$ give an equation of the form equation (7.2).

7.2 Description of the method

A sequence of configurations produced by a growth phenomenon and a sequence coming from the analysis of critical dynamics are equivalent in terms of how they are generated. The main difference resides in system preparation. For critical dynamics, it is patiently brought to equilibrium at the critical temperature. On the other hand, for the study of growth, the system is prepared in a random fashion and the quench temperature is determined appropriately ($T < T_c$). The description of the proposed MCRG method will be equally applicable to these two processes although different observables will be involved.

On a sequence of configurations, separated by a time δt, blocking is done on a set of 16 spins coming from 4 different lattices at 4 contiguous times. These numbers come from a choice of a $b = 2$ space blocking factor. The new cell spin is produced by using the majority rule. Because the blocked variable is mapped to the time corresponding

[1] Note that the quantity A also has to be rescaled by the same factor.

to the earlier time involved divided by b^{2m}, such a procedure will induce a shift of the origin in the case of growth phenomena. Meanwhile, as mentioned previously, a real space RG procedure generates a growth process describing a system quenched at a lower temperature, since $T = 0$ is the only fixed point of the problem for late times. Our program will consist in determining the degree of consistency of our results with the Allen-Cahn predictions.

For critical dynamics, the method mainly consists in extracting the dynamic critical exponent from the matching relation

$$\varphi_M(L, m, t, T) = \varphi_M(b^j L, m + j, \frac{t'}{b^{jz}}, T') \tag{7.4}$$

where j is the difference in MCRG iteration number. The choice $b = 2$ has been made for this part of our work. Since the process is undergone at T_c, it is clear that the temperature will stay invariant, so that $T = T'$. The relaxation of the observed quantity turns out to fit an exponential decay so well that matching at any point yields the same value. Instead, we shall use the time constants obtained from the relaxation of time-time correlation functions. As seen in the previous section, a purely diffusive process would stay invariant under the application of the proposed MCRG method. The discrepancy δ between diffusion and critical slowing down can be obtained from

$$\delta = \frac{\ln(\tau(L, m)) - \ln(\tau(b^j L, m + j))}{j \ln b} \tag{7.5}$$

where the variables still have the same meaning. The critical exponent z is then obtained directly from δ since

$$z = 2 + \delta. \tag{7.6}$$

7.3 Simulations and results

Simulations were performed on a two-dimensional Ising model with periodic boundary conditions defined on a square lattice, with system sizes ranging from $N = 16 \times 16$

to $N = 128 \times 128$ [2] and with a dynamic algorithm as the one defined by (3.21). The initial states of all the quenches were random configurations of spins, thus representing a system at infinite temperature. The algorithm used bitwise coding in order to limit the memory requirement and to improve the speed of the program. The periodic boundary conditions were put in a look-up table thus minimizing `if` statements. The calculation of the energy of the selected spin, as well as flipping the spin, was done using Boolean algebra so that the algorithm could be more easily vectorized. A complete description of the computational aspects as well as the listings of the programs can be found in the Appendix.

7.3.1 Domain growth

There are some comments we have to make before starting the interpretation of our results. First, we have to note that the average $\langle R(t) \rangle$ is not directly evaluated for it would diverge. Indeed, for a zero temperature configuration — accessible at all T with different probabilities — the denominator of (6.16) vanishes. This means that $\bar{R}(t)$ has to be redefined as

$$\bar{R}(t) = \frac{2}{2 + \langle u(t) \rangle}. \tag{7.7}$$

However, because of the broader probability distribution arising from a finite system, $\langle u(t) \rangle$ should contain in proportion more configurations at zero temperature than an infinite system. In addition, one must deal with the finite-size effect discussed earlier involving the fact that a droplet of a certain size will start interacting with itself through the periodic boundary conditions. Therefore, finite-size effects will tend to accelerate growth. The last effect can be seen in figure 7.1.

We also note that relation (6.18), matching growth size between MCRG iterations, will hold only if the time origin remains fixed. This is not the case for the transformation involved. Indeed, the MCRG will tend to shift the origin in a way

[2] This means, for the largest system, 16,384 spins forming a configuration space of $\sim 10^{4932}$ elements! Some 32 such systems could be run simultaneously. Each of the simulations could be done on a SUN 3/50 and a DEC 5000 within a reasonable amount of time.

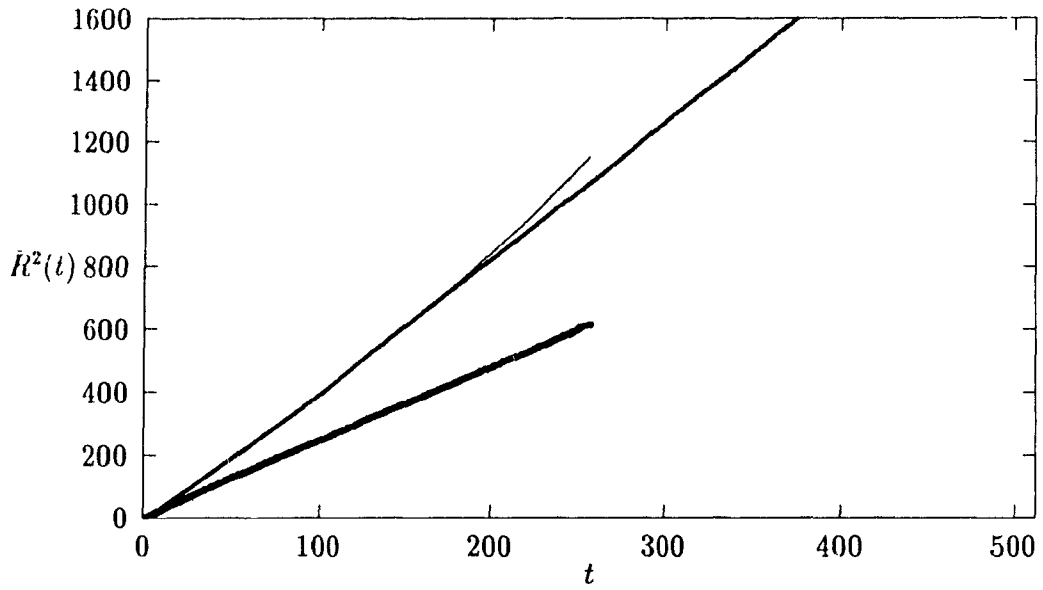

Figure 7.1. A comparison of two quenches done at the same temperatures but in systems of different sizes. The size of the systems are 64 and 128 and the data has been averaged over 3200 and 1600 runs respectively. The temperatures were 0.2, 0.5 and $0.6T_c$, from top to bottom. The discrepancy occurs at $R \gtrsim 0.4L$. There is no difference for the 0 $6T_c$ curve.

depending on the choice of the value of t' given to the obtained blocked configurations. This choice is relatively unimportant, and an approximate time origin can be recovered by deliberately shifting the data in a way to get the reference point $(0, 1)$. This way of proceeding, however, gives too much importance to the origin, especially when one considers the asymptotic behaviour towards the power law growth at higher T. Moreover, the scaling regime will be related to the origin in a non-trivial way for high temperatures. In addition, the inhomogeneity of time, characteristic of a growth process, is one more reason to allow the time origin to drift. The consecutive time steps to be blocked do not have the same weight in time, although we consider these as such.

The temperature plays an important rôle in a quench. Data obtained at very low temperatures seem to indicate a growth exponent slightly larger than 1/2, and this can partly be explained by the reasons above, although some correction term might exist. In order to distinguish possible transition regimes, the instantaneous derivative of the inverse perimeter density has been taken with respect to time. It allows us to

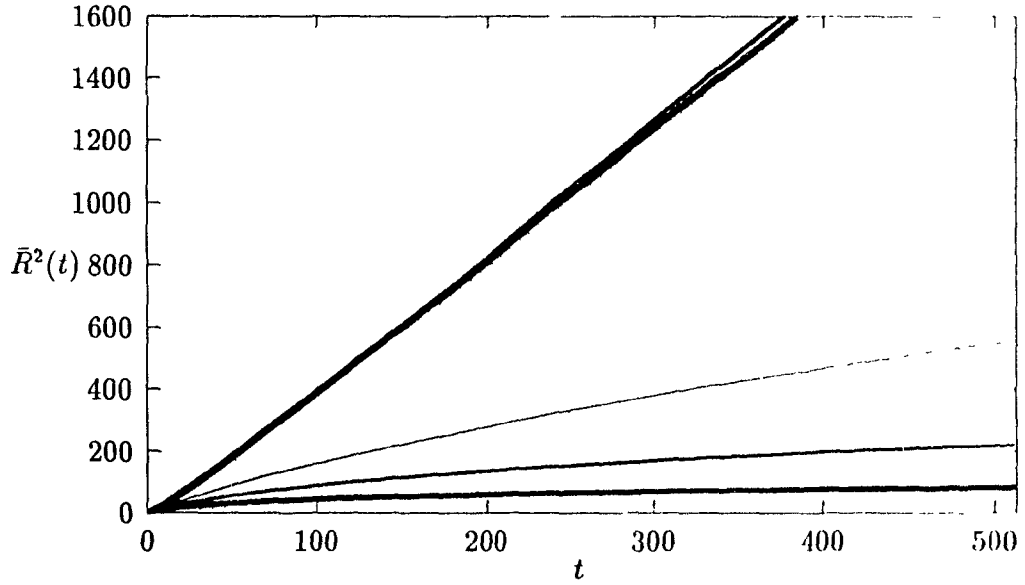

Figure 7.2: A system of 128 x 128 has been quenched at temperatures ranging from 0 to $0.9T_c$ every 0.1, from top to bottom. The curves at 0.0, 0.1 and $0.2T_c$ overlap. The domain size, estimated by the inverse perimeter density, has been averaged over 1600 quenches.

distinguish a systematic change of regime at very early times, as can be seen from figures 7.4 to 7.16. Compare with the first part of figure 6.1 on page 77.

On the other hand, quenching a system at a temperature close to T_c will involve non-trivial effects implicating some different scaling regimes and transient. Some aspects of this problem have been described in (Tartas 1988). These effects get worse as one is closer to T_c. The effect of temperature can be seen from figure 7.2.

As we pointed out earlier, the effect of RG brings the temperature of the quench down to the zero temperature fixed point. Therefore, a zero temperature quench should be invariant under MCRG. This is what can be seen from figure 7.3 which has, as m goes, the same coefficient $\alpha(T)$ within experimental error, as can be seen from figure 7.4.

The situation is not the same for quenches at higher temperature. It would be much simpler if one could determine the function $\alpha(T)$ for then, a flow graph of α with respect to m and T could be built from the value of the discrete derivative of

$\alpha(T,m)$ with respect to m, given a temperature. Indeed, self-consistency implies

$$\frac{\partial\alpha(L,T',m)}{\partial m} = \frac{\partial\alpha(b^j L,T,m+j)}{\partial m}, \tag{7.8}$$

where T and T' are such that

$$\alpha(L,T',m) = \alpha(b^j L,T,m+j). \tag{7.9}$$

One last remark concerning the system sizes involved in the matching condition. As mentioned earlier, systems of the same size but different m's should be compared in order to minimize finite-size effects. However, the correlation length for a growth problem is much smaller than the system size. Therefore no finite-size effect is apparent when comparing growth in systems of different size, as far as $\bar{R} \lesssim 0.4L$, like figure 7.1 has demonstrated.

Figure 7.3 to figure 7.16 show the application of the proposed method to quenches at higher temperatures. For all quenches, the system was prepared randomly and then analyzed at each few mcs. Similar data series have been produced for smaller system sizes, but they will not be reproduced here, since they lead essentially to the same results.[3] As figure 7.2 has already shown, the curves obtained contain a relatively low amount of noise[4] and that our data set can be considered as the best ever obtained in MC growth problem related studies. Accordingly, as a more rigourous and severe analysis of our data, the derivatives of most of the quench curves have been taken in order to possibly distinguish different scaling regimes. We emphasize that derivatives are very sensitive to any kind of noise, and that they usually cannot be applied on poor quality data. As can be seen from figure 7.4, the derivatives of the curves obtained from a low temperature quench study behave as expected; i.e., they all converge to the same constant value, within their respective error. Also note the distinct scaling regimes at very early times. The very first part of the curves behaves as if it was independent of the temperature, although high temperatures saturate this process more rapidly. Indeed, the growth process has a $t = 0$ derivative of ~ 0.5 for all

[3] Apart from finite-size effects of course.

[4] Note that there are 512 data points for each curve of figure 7.2.

the cases below $\sim 0.8T_c$. Above this temperature, this first mechanism seems to be hindered and, rather, the derivative starts to decay from that same value. It is also interesting to note how MCRG works on the high temperature curves. Figure 7.2, for example, shows that although the growing mechanism is relatively slow as time goes on, the fact of renormalizing bring the whole process to a lower temperature, thus making it growing more rapidly. Even for very high temperatures, this change of growth activity is observed.

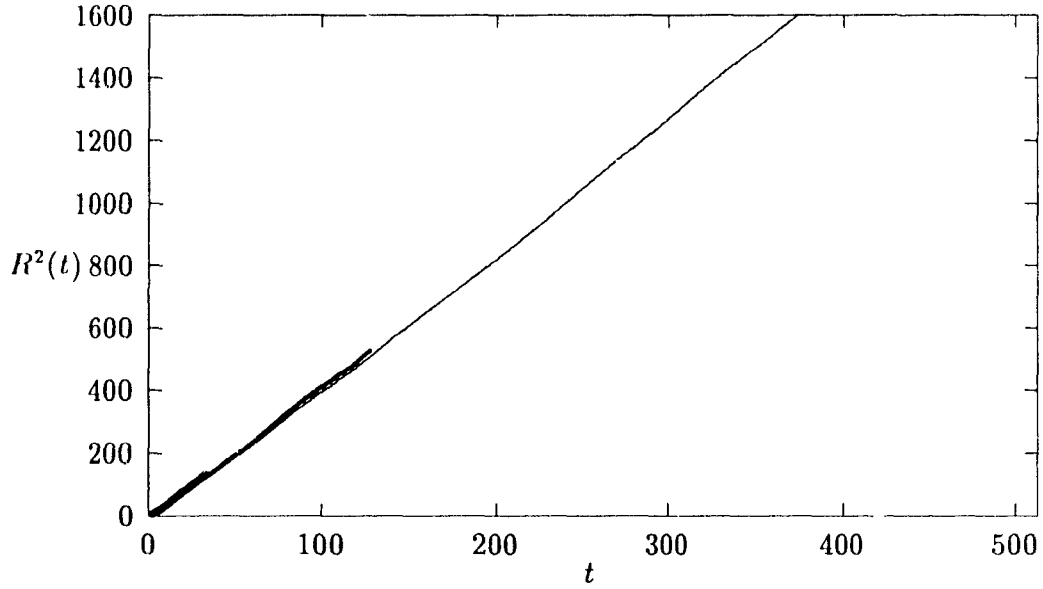

Figure 7.3. MCRG on a $10^{-5}T_c$ quench. Similar curves are obtained for $T \lesssim 0.3T_c$. The value of the linear coefficient $\alpha(T)$ is invariant as m goes. Note the drifting origin as explained in the text. System size of 128×128, over 1600 quenches. Shorter curve as $m = 0, 1, 2$.

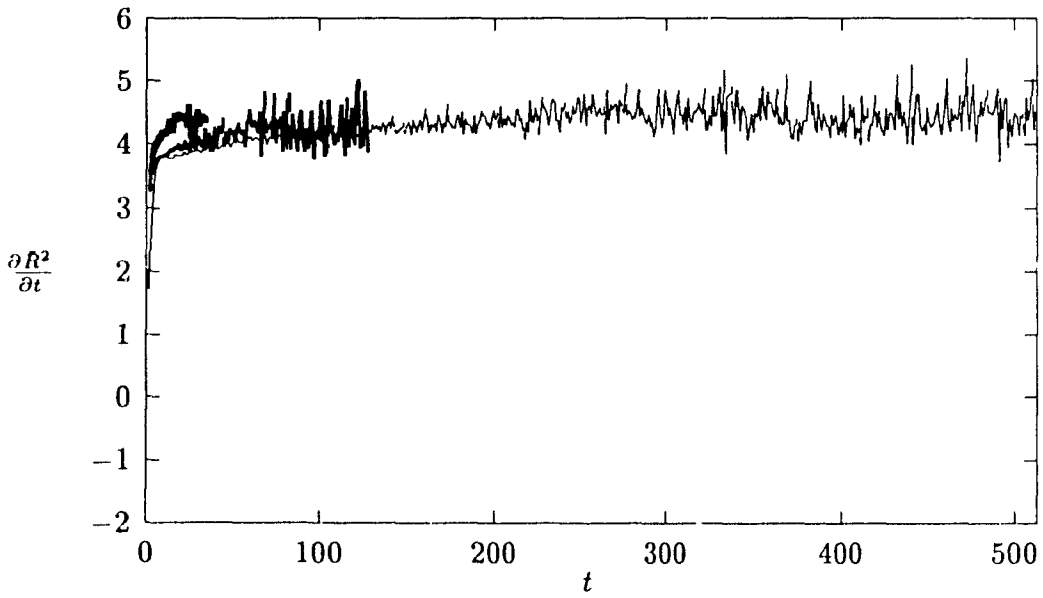

Figure 7.4: The derivative of the curves of figure 7.3 has been taken for $m = 0, 1, 2$. It shows that the scaling regime is reached at earlier times in the renormalized system. The value of coefficient α converges to the same final value for all curves. Shorter curves as $m = 0, 1, 2$.

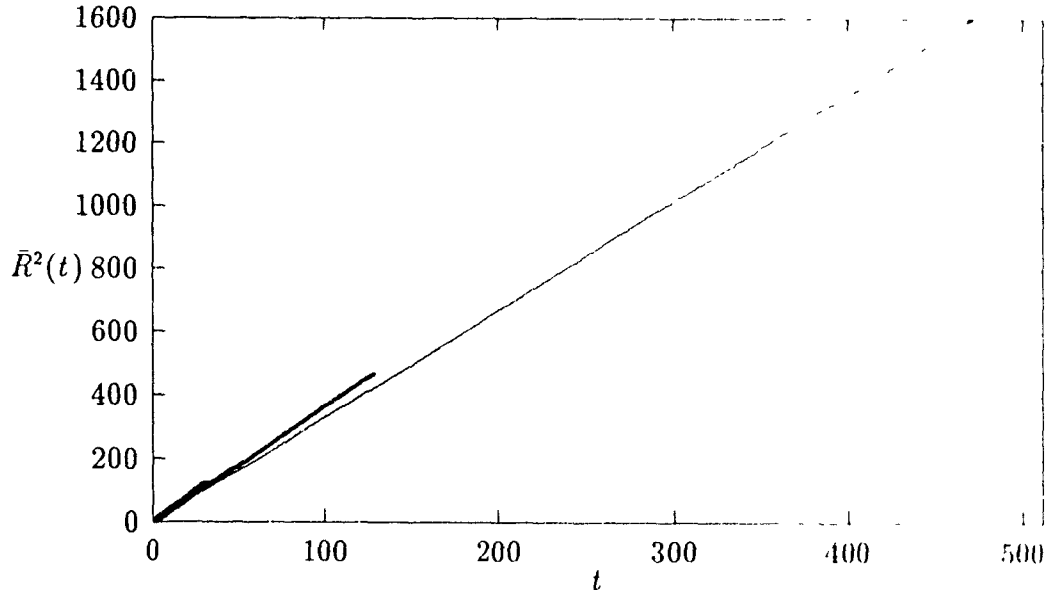

Figure 7 5. Quench for a 128 × 128 system. The quench temperature is 0 47T_c and the number of averages is the same as in fig. 7.3. Note how the coefficient α converges to the slopes obtained in the preceding figure. The same scale has been kept throughout in order to have a direct comparison Curves as in figure 7.3.

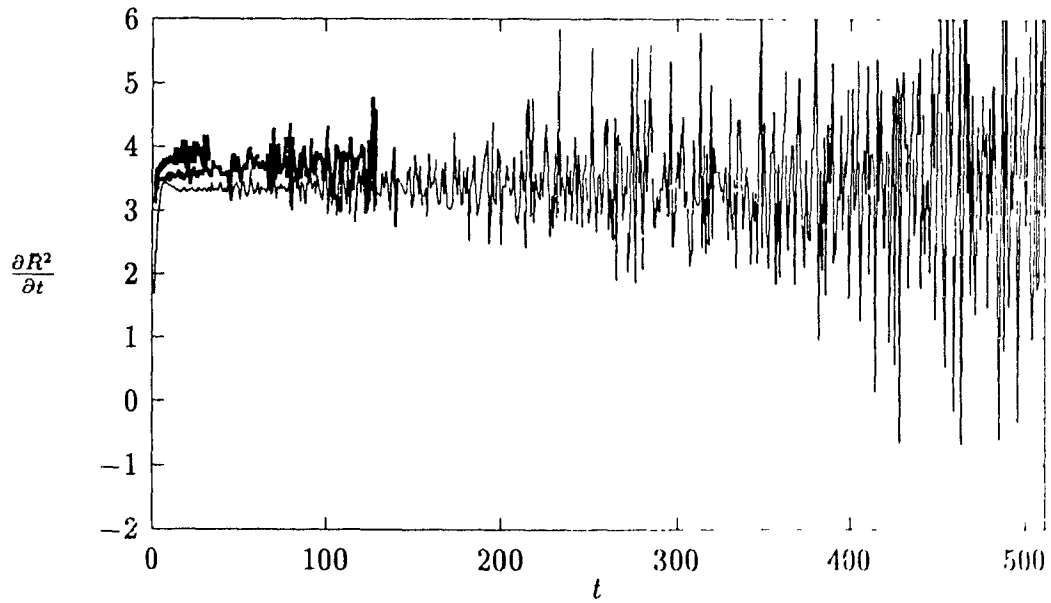

Figure 7.6: The derivative of the curves of the preceding figure has been taken for m 0, 1, 2 Compare the convergence value of the $m = 2$ curve with the one obtained from a low temperature quench (cf. fig. 7.4). Curves as in figure 7.4.

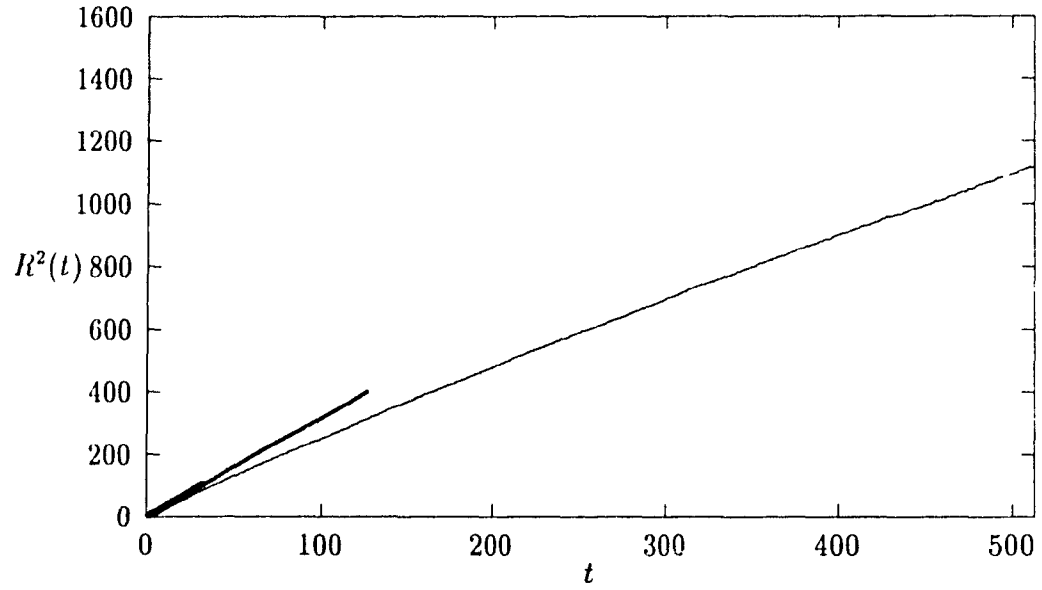

Figure 7 7: Quench for a 128 × 128 system. The quench temperature is $0.5T_c$ and the number of averages, as well as the meaning of the curves, are the same as in fig. 7.3.

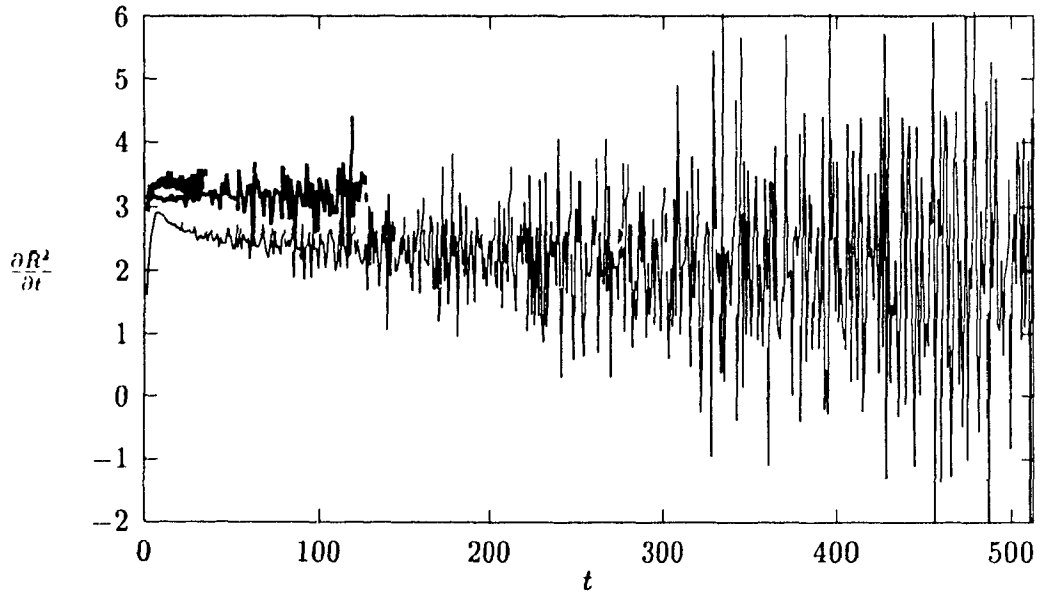

Figure 7 8: The derivative of the curves of the preceding figure has been taken for $m = 0, 1, 2$. Although the number of averages is the same here, the data is much noiser. Curves as in figure 7.4.

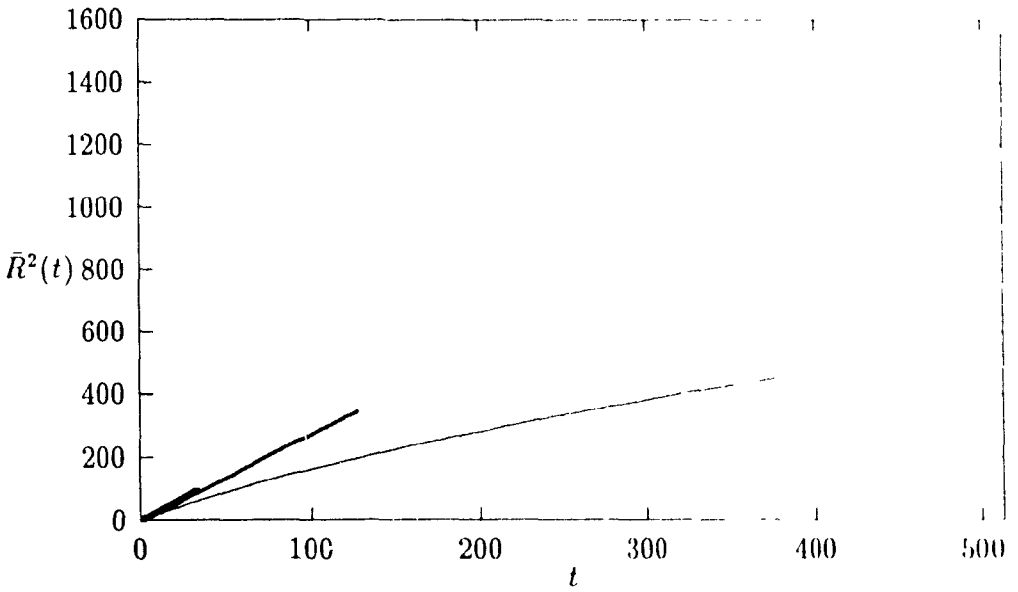

Figure 7 9: Quench for a 128 × 128 system The quench temperature is $0\ 6T_c$ and the number of averages, as well as the meaning of the curves, are the same as in fig 7 3.

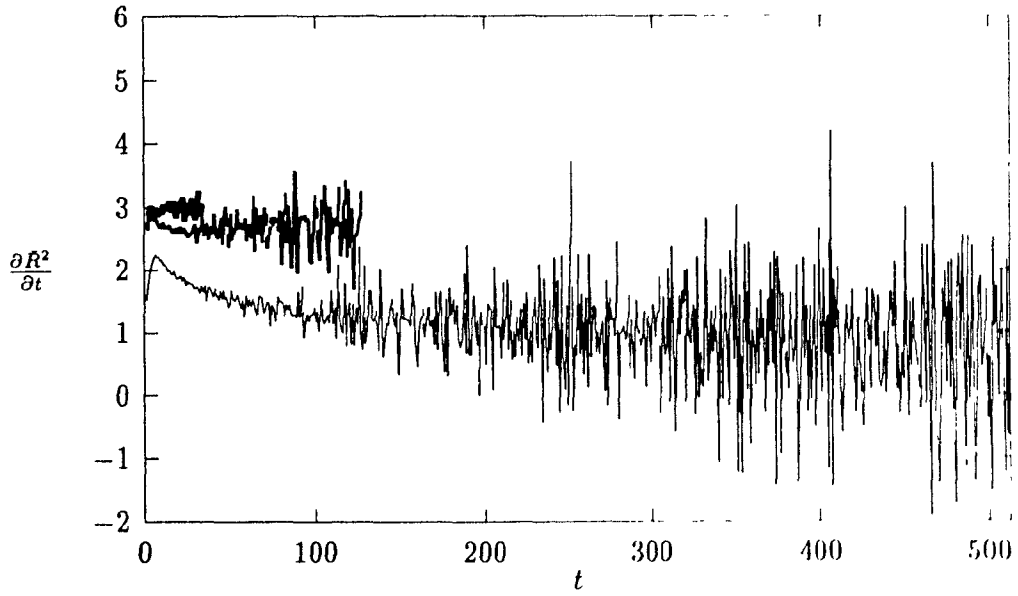

Figure 7.10: The derivative of the curves of the preceding figure has been taken for m 0, 1, 2 Curves as in figure 7 4.

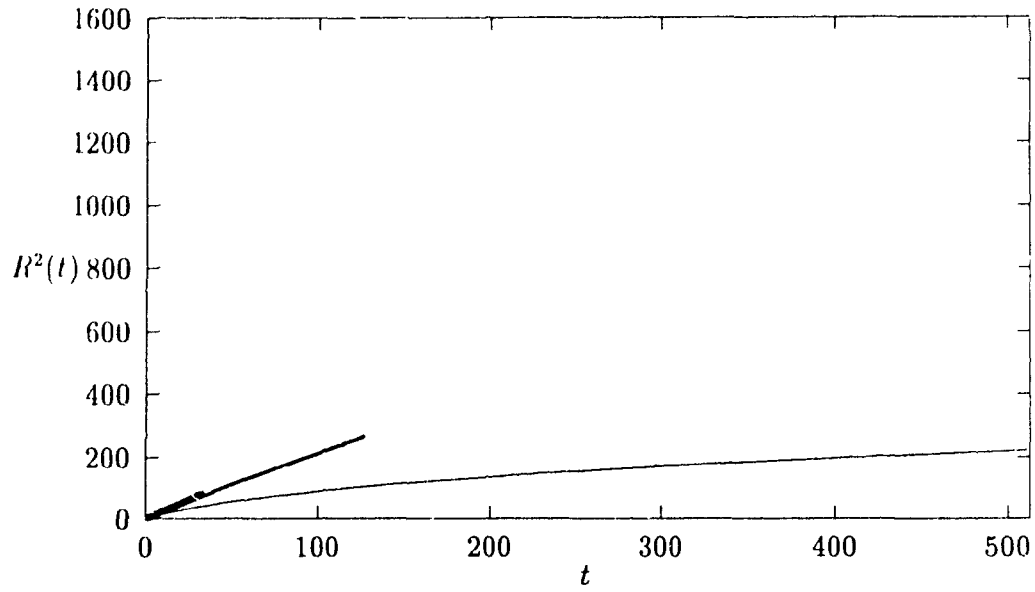

Figure 7 11: Quench for a 128 × 128 system. The quench temperature is 0 $7T_c$ and the number of averages, as well as the meaning of the curves, are the same as in fig 7.3.

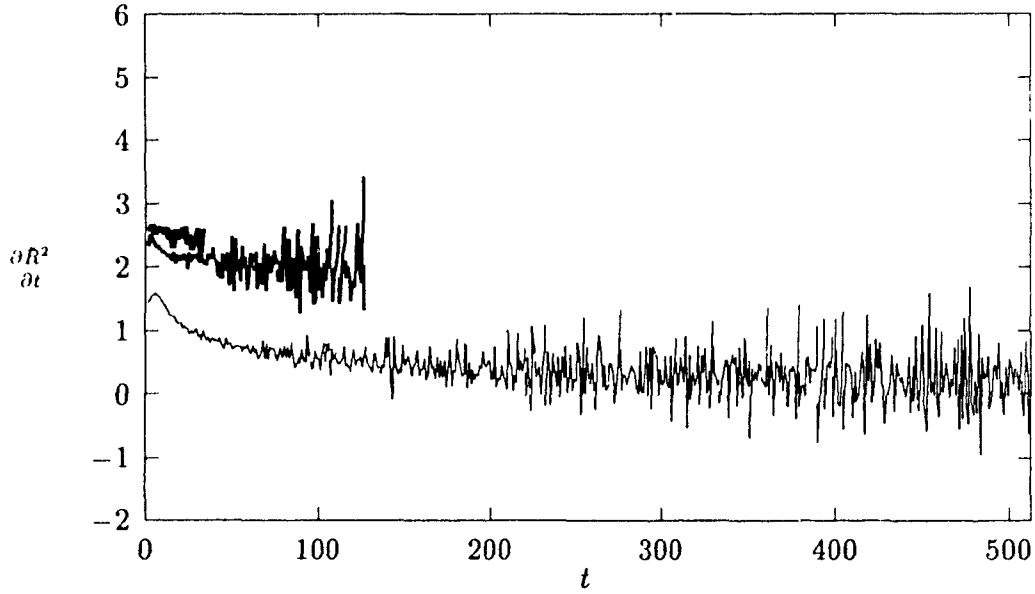

Figure 7 12 The derivative of the curves of the preceding figure has been taken for $m = 0, 1, 2$ Curves as in figure 7.4.

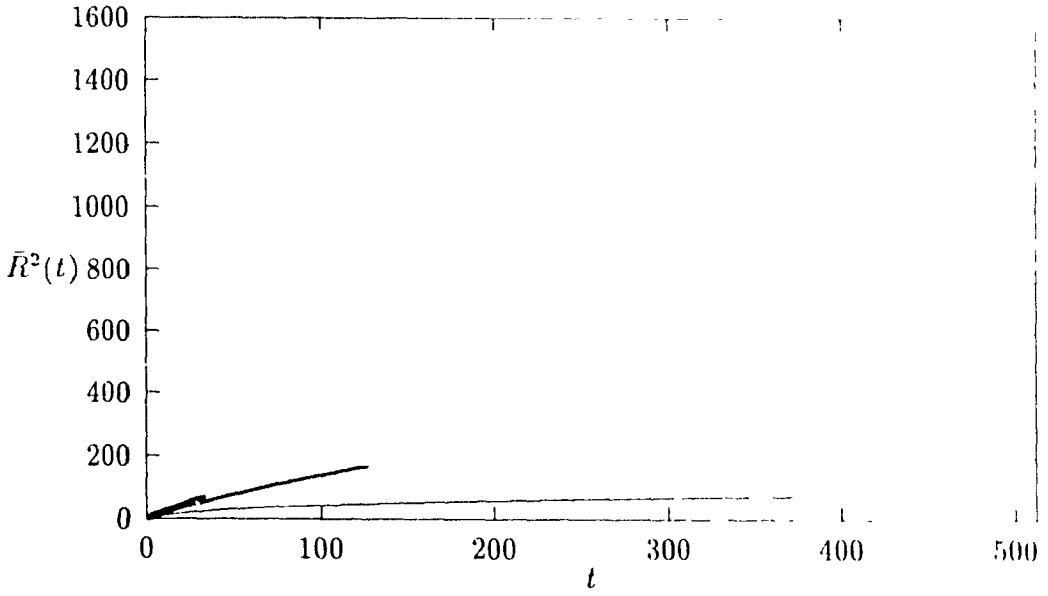

Figure 7 13: Quench for a 128 × 128 system The quench temperature is 0 8T_c and the number of averages, as well as the meaning of the curves, are the same as in fig 7 3

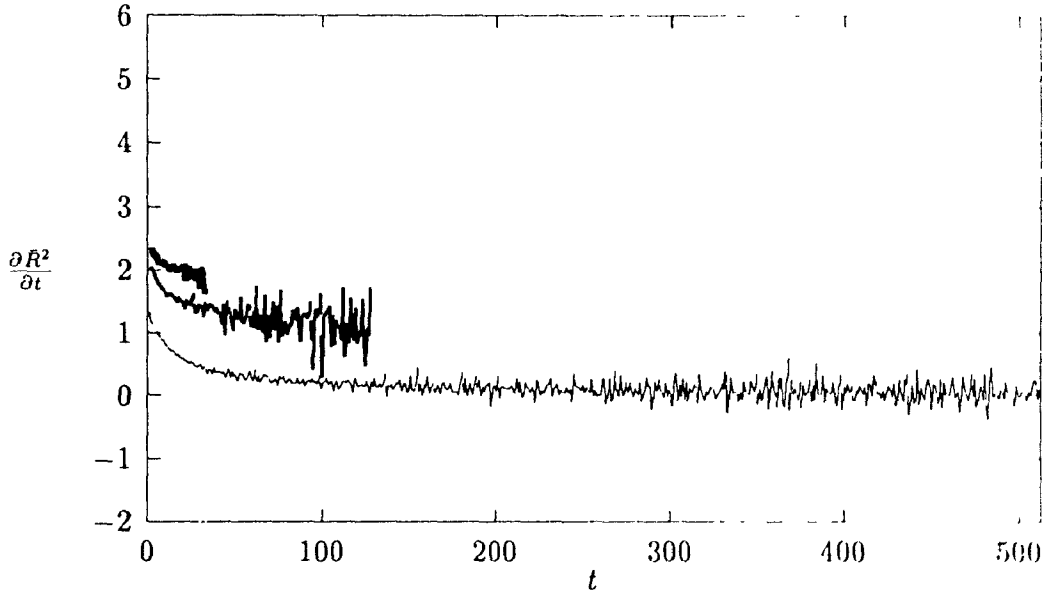

Figure 7 14: The derivative of the curves of the preceding figure has been taken for m 0, 1, 2 Curves as in figure 7.4

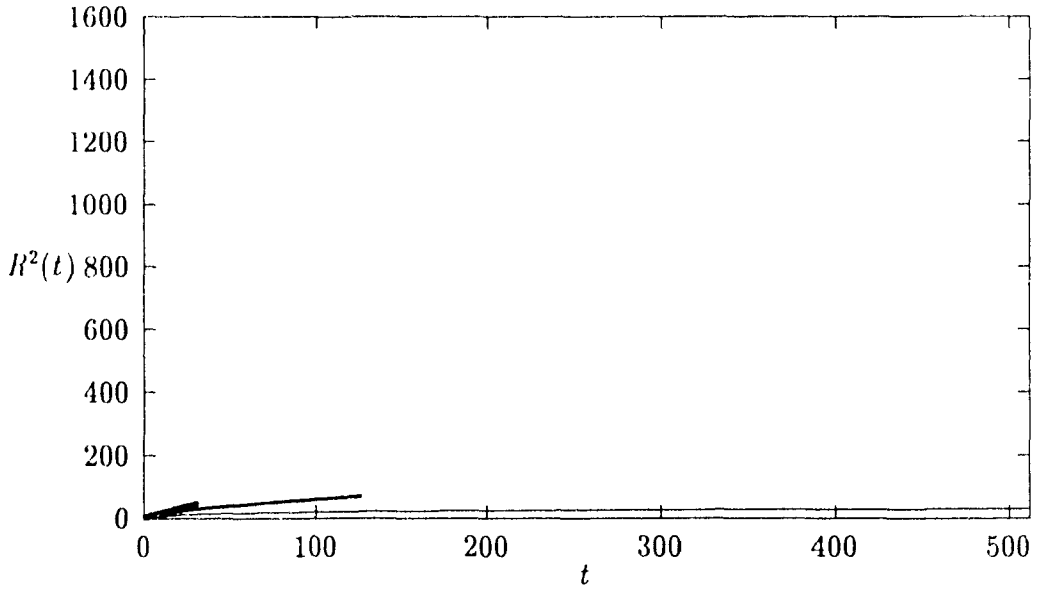

Figure 7.15: Quench for a 128 × 128 system. The quench temperature is $0.9T_c$ and the number of average, as well as the meaning of the curves, are the same as in fig. 7.3.

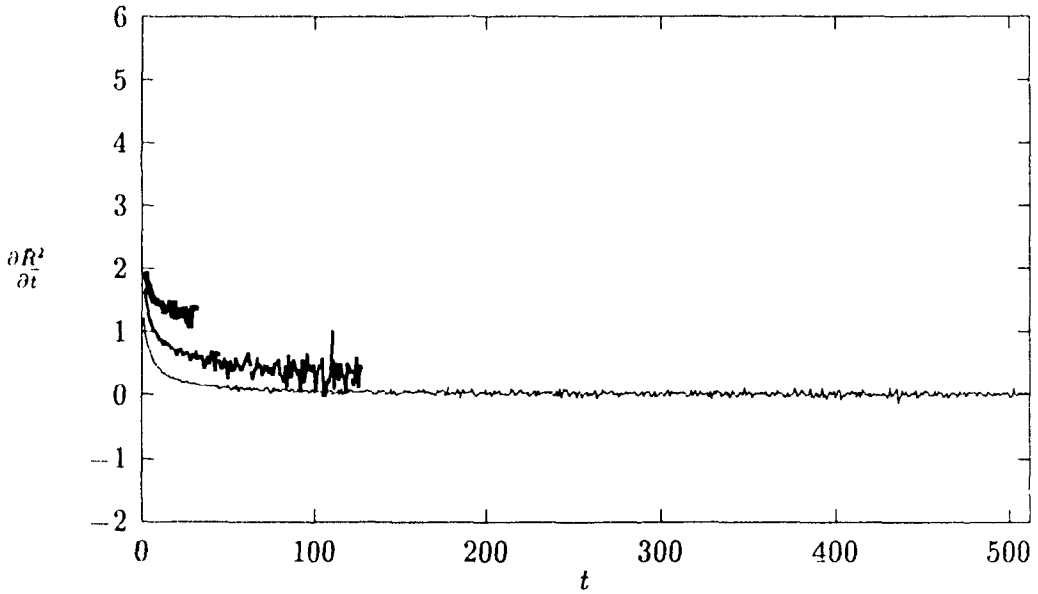

Figure 7.16 The derivative of the curves of the preceding figure has been taken for $m = 0, 1, 2$. The slow down of growth is remarkable after a few mcs only. Curves as in figure 7.4.

7.3.2 Critical dynamics

The analysis of the data obtained for critical dynamics differs from growth in a few aspects. First of all, we note that time is homogeneous for the present case, so that the previous possible drifting problem now becomes irrelevant. On the other hand, finite-size effects are much stronger for critical dynamics since the correlation length is of the order of the system size. Matching will therefore require systems of different sizes. Lastly, we note that the dynamical critical exponent can also be obtained from finite-size scaling analysis and this other method will provide us a direct test for the validity of our present technique.

The characteristics of the simulations were as follows. The initial states were random configurations on which an equilibrating simulation of 9, 17 and 44 times the relaxation time constants for system size of 64, 32 and 16 respectively, had been previously performed. The numerical implementation consisted in building pointer rings of size of the order of a few τ in order to store the values of the magnetization and its deviation, and then, to calculate the mathematical correlation of the ring values with themselves displaced by a time lag t. With this same algorithm, 32 systems were run and averaged in parallel. A more detailed description of the computational aspects of this work, as well as the code listings have been inserted in the appendix.

As shown by figures 7.17 to 7.19, the results fit a simple exponential surprisingly well, even at early times. For reasons of precision, as it is unequivocally shown by figure 5.1, the time-displaced correlation function $\varphi_M(t)$ will be the only one to be used here. Section 5.3 defines this quantity as well as other time-displaced correlation functions. The relaxation time constant were extracted from these graphs and matching is summarized in table 7.1. Our results are consistent with $z \approx 2.21$ 2.24.

Each MCRG matching result was compared with a finite-size scaling analysis and both were found to yield the same value within the interval of confidence of the data. The value of z was found to be larger when doing matching with smaller systems, but this effect was also observed from finite-size scaling analysis, thus proving that this

effect is not particular to our method. The values of τ were collected for $m = 0$ and plotted on a log-log scale in order to find a global exponent from finite-size scaling as defined by equation (5.10) (page 62). This is done in figure 7.20. This yields an exponent of $z = 2.29 \pm 0.05$, which is quite consistent with our estimate from the new RG method of $z \simeq 2.21$–2.24. The large value of the error is mainly due to the low number of points. Some further investigations are still needed to generate points for larger system size. The previous estimation of Landau *et al.* (1988) for example, used a collection of two-dimensional systems ranging from $L = 12$ to $L = 96$ only. Their best estimate is 2.14 ± 0.05, obtained from a multi-spin coding algorithm. While this value is clearly not contained in the error we have, further statistics may be required for us to definitely exclude their estimate. Furthermore, the updating scheme they used might have a non-negligible systematic effect on the value of the critical exponent obtained. We note that other estimated values of 2.24 (Achiam 1980; Poole and Jan 1990), and 2.23 (Katz, Gunton and Liu 1982), are consistent with the value we have here.

In conclusion, the analysis of φ has demonstrated unambiguously that the decay of time-time correlation functions can be very well described by a simple exponential, thus showing that critical relaxation is purely exponential in finite-size systems. Second, the method we proposed turns out to be efficient as well as self-consistent, and offers a promising way for evaluating the critical exponent z with still more precision. Finally, in the framework of testing this original technique, we generated data of a higher quality compared to any other existing data.[5]

[5] *Checher board* algorithms clearly have more mcs/site statistics, but the quality of the data obtained from such algorithms still remains questionable.

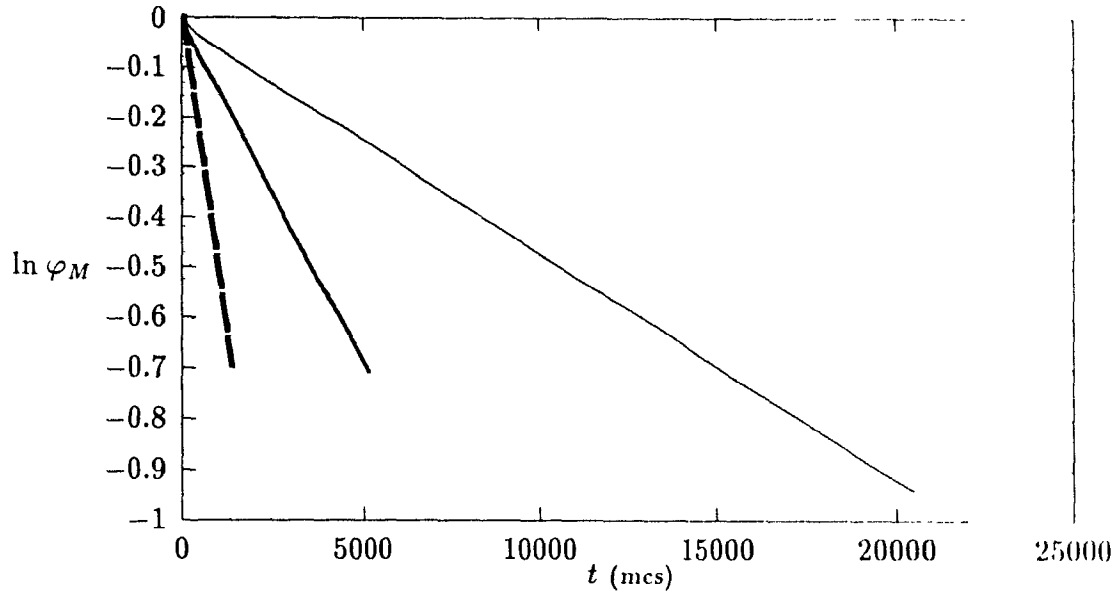

Figure 7.17: Critical dynamics MCRG on a 64 × 64 system. Curves are for $m = 0, 1, 2, 3, 4$, from top to bottom. Averaged over 32 independent systems observed for 8 806 400 mcs. The equilibrating time of 204 800 mcs and φ_M calculated every 16 mcs.

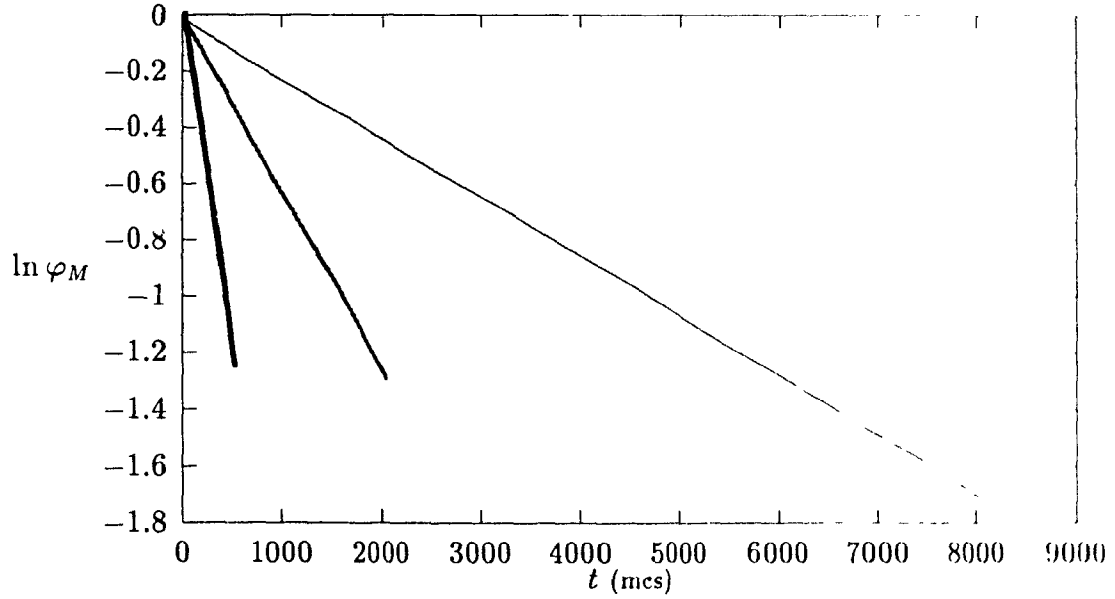

Figure 7.18: Critical dynamics MCRG on a 32 × 32 system Curves are for $m = 0, 1, 2, 3$, from top to bottom. Averaged over 32 independent systems each observed for 8 192 000 mcs. Equilibrating time of 81 920 mcs and φ_M calculated every 16 mcs.

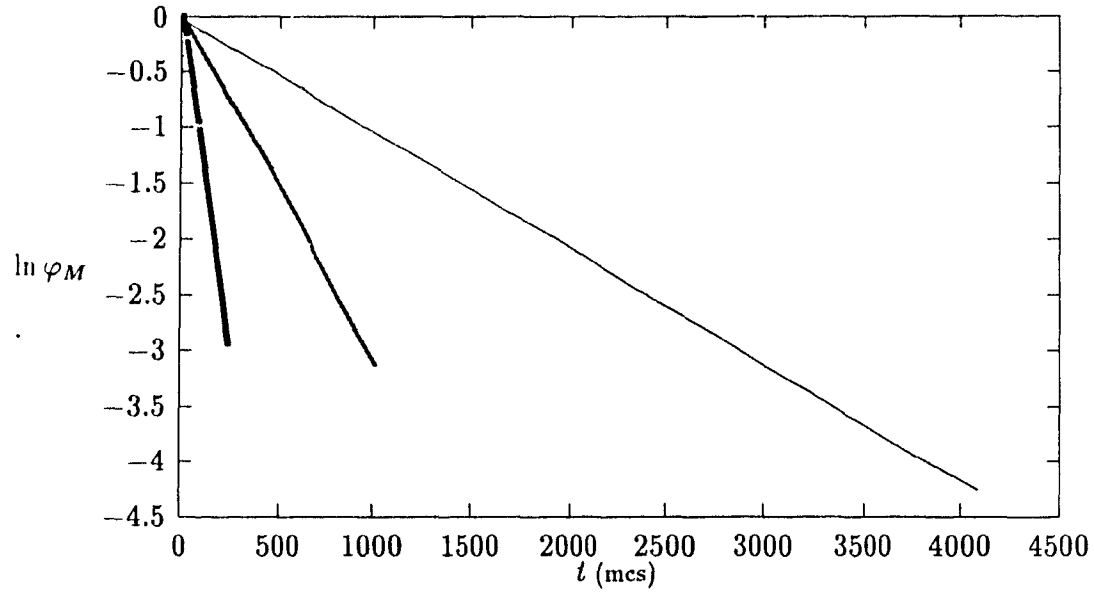

Figure 7.19: Critical dynamics MCRG on a 16 × 16 system. The observation time, for 32 systems ran in parallel, was 15 511 552 mcs, and equilibrating time 40 960 mcs. Other features are as those in figure 7.18.

$b^{-m}L$	τ_{64}	z_{64-32}	τ_{32}	z_{32-16}	τ_{16}
64	22151(5) $(m=0)$				
32	7329(4) $(m=1)$	2.623(1)	4759(1) $(m=0)$		
16	1833(2) $(m=2)$	2.208(2)	1587(1) $(m=1)$	2.725(2)	960(1) $(m=0)$
8	461(1) $(m=3)$	2.21(2)	397.7(4) $(m=2)$	2.30(2)	322.0(2) $(m=1)$
4	120(3) $(m=4)$	2.24(5)	101(1) $(m=3)$	2.3(1)	80.9(3) $(m=3)$

Table 7.1: This table is the result of matching curves of figures 7.17 to 7.19. The error, as shown in parenthesis for the last digit, is calculated from the goodness of the fit, so it is not useful for the estimation of the real error when $m = 0$, since the RG method has not yet converged.

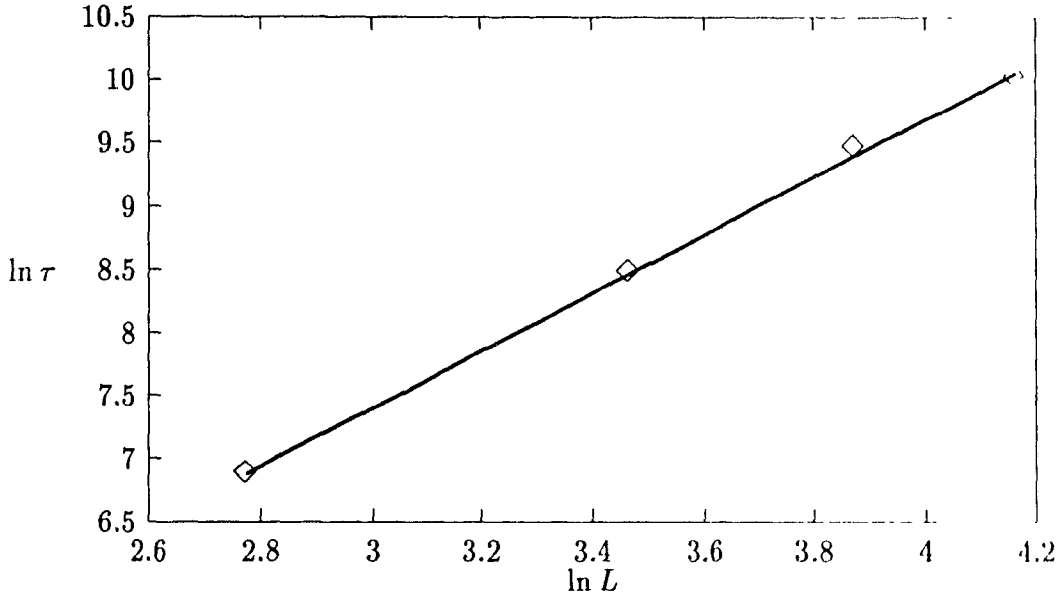

Figure 7.20: The value of the exponent z can be extracted from finite-size scaling as described by equation (5.10). The system sizes were 16, 32, 48, 64 with statistics as described earlier The value of the slope is 2.29(5).

Chapter 8

Conclusion

This last chapter will first summarize the results obtained in the preceding chapter and then suggest new avenues for both problems considered in this thesis.

8.1 Evaluation of the method

For reasons of clarity, the two problems will be separated and treated accordingly.

8.1.1 Growth dynamics

As shown in the last chapter, the proposed method has yielded results in agreement with the Allen-Cahn law. Instead of extracting a specific growth exponent, the approach taken was to test the degree of compatibility of our results with the Allen-Cahn growth law. However, the results do not exclude the possibility of the existence of correcting factors at very high and very low temperatures, mainly because of transient regimes and crossover effects. At high temperatures, for example, critical slowing down effects rule out some of the basic hypotheses needed for the derivation of the antiphase boundary motion. Indeed, as one gets closer to T_c, one must consider the fact that the thickness of the interfaces becomes larger and larger, and the very notion of an interface no longer has a clean definition.

Moreover, related to the inhomogeneity of time and to the algorithm used, some

drifting effects were found during time renormalization. Those effects were not important with respect to the approach taken here, but they prevent us from extracting a complete description of the problem since the choice of the new origin has to be made in an arbitrary way.

8.1.2 Critical dynamics

For the case of critical dynamics, the success of the method is, however, undeniable. Because of the complete homogeneity of time, due to the presence of equilibrium, the time scale renormalization has not lead to any complicating effects. Moreover, the fact that all the matching could perfectly agree with finite-size scaling done on the two systems considered is very encouraging. The need to investigate larger systems is evident from our data. Finite-size effects are much too strong when RG has brought the system size down to $L \lesssim 8$, and the results shown by table 7.1 are very conclusive. Moreover, larger systems would permit convergence to a better value for z, since our results tend to indicate a smaller value for the critical exponent as the system size increases. Furthermore, the observation of the data indicated that the time relaxation constants were not yet stable at their present values. A serious analysis of the behaviour of the results in time is still lacking. Any further development should consider this aspect before judging of the quality of the data.

The main advantage of our technique over finite-size scaling methods is the extraction of more results from the same simulations. Moreover, if the simulations were done on larger systems, self-consistency would allow the convergence of the data to better results, out of the same simulations. Therefore, not only has the feasibility been proven, but the superiority of this technique has been clearly demonstrated by simulation on systems of slightly larger sizes.

On the other hand, the values obtained from finite-size scaling are somewhat inconclusive, mainly because of the low number of data points. However, the relatively large error value encompasses a good range of dynamic critical exponents obtained in the literature and the production of more data points would eventually lead to com

parable results. Again, simulation of larger systems would permit a better estimation of the critical exponent. As a check of our technique, it would always be possible to verify our results by direct comparison via a finite-size scaling analysis. As shown by the preceding chapter, however, the error would be much smaller from a consistent MCRG process than from finite-size scaling.

8.2 New approaches

This very last section will try to indicate further avenues of investigation related to that problem. First, we stress the lack of a sound theoretical background for renormalization techniques in general. The inclusion of time as an extra parameter in our renormalization scheme is certainly not an improvement to the understanding of this problem. Second, the influence of real computer simulation parameters on the expected behaviour of the system has to be further investigated. Indeed, as previously mentioned, there is no *a priori* evidence that a multi-spin algorithm should lead to the same critical exponent. Moreover, one would be justified in expecting that the observation of a dynamical quantity should be much more sensitive to the random number generator and the related updating schemes than an equilibrium one.

The representation of the system in terms of Langevin equations should be further investigated. The domain of application, as well as more formal derivations from basic principles, would surely help the understanding of non-equilibrium statistical mechanics. The solution of the strong non-linearities found in these problems is not an easy task, however. Finally, the system can be investigated in terms of estimating homogeneous transition probabilities. This method should yield some novel dynamical results for the growth dynamics from a quench, as well as the critical problem. The solution of these equations for transition probabilities is not expected to be easy, but they would surely have the advantage of expressing the system in terms of a relatively smaller number of variables.

In conclusion, the new method, presented in this thesis, has brought new light to

two challenging problems, and permitted the generation of numerical results of better quality than any previous study. The availability of more powerful computers will certainly allow this technique to yield further useful results for related problems.

Appendix A

Description of the Code

The following will briefly describe the algorithms used for the problem of critical dynamics. The algorithms used for the previously described problem of domain growth are almost the same apart from the fact that (1) the system is not allowed to equilibrate before we start the measurements, (2) energy, instead of magnetization, is measured in order to determine the mean domain size (note that no time-time correlation function is involved in this case) and (3) an average is made over different quenches done on randomized systems instead of continuing with the same system in time as it is the case for critical dynamics.

The algorithms have been written in both *C* and *FORTRAN* but only a *C* version will be presented here. The following version is one of the most complete ones which still contains a clear representation of the algorithms in spite of having fancy features such as taking care of the history of results and allowing the reading of a previous set of configurations already equilibrated at T_c for example. The source code has been subdivided into separated files in order to take advantage of `static` *C* declarations. It comprises a header file containing declaration of macros and machine dependent variables, a utility file containing various functions used to allocate memory, to copy, read and save matrices, and to initialize lookup tables for a two-dimensional-periodic-boundary-condition Ising model, an analysis file containing an algorithm computing the magnetization of the different systems ran in parallel and storing these results for

subsequent calculations of time-time correlation functions, a MCRG routine file which renormalizes the systems using a majority rule blocking algorithm, a main program file which will be explained in more details below, and finally, a makefile which has been included in view of completeness.

The general idea is to run a simulation on a $M \times N$ integer matrix. Each bit of the integer is used as a spin. The bit size[1] of the integer allows to run from 16 to 64 systems in parallel, depending on the architecture of the hardware used. When an integer is visited, all of the systems are visited so that the systems all share the same visiting history, although the probabilistic outcome, as well as the initial conditions, will be different for each of them. Due to the Hamiltonian of the two-dimensional Ising model, the state of a spin has a degeneracy 10, depending of whether it is "up" or "down", and depending on the number (0–4) of parallel neighbours it has. In order to use Boolean algebra, the state of a spin will be represented by ten integers having a bit set "on" for each corresponding system having the visited spin site being in the state represented by the given integer. For a 32 bit integer hardware for example, 32 bits will thus be distributed among ten 32 bit integers, each bit having no equivalent in any other state integer, since a spin can only be found in one of its ten states. We shall not go into the detailed description of the Boolean algebra involved, but the reader will find the details in the *lturn()* function below. It uses the Metropolis algorithm on a matrix passed as an argument and runs for a given number of *mcs* also obtained from the argument stack. After selecting a matrix integer (a site) at random, the "flipping" procedure is done systematically on any visited spin having two and less parallel neighbours, and with a Boltzmann probability for any visited spin having three or four parallel neighbours. The Boltzmann distributed probabilities are stored bitwise in two integers that then operate, using Boolean algebra, systematically on the two integers representing the sites in the situation of having three and four parallel neighbours and this for the, say 32, parallel systems at the same time.

Anyone, who has done such simulations before, would know that the generation

[1] Defined as *THICK* in the header file.

of random number is the procedure forming the major bottleneck of the algorithm. A tentative to use socket I/O programming in order to use other slave machines in parallel turned out to be disappointing in terms of the overall speeding up of the process. There still remains some other tricks to try though...

The configurations thus generated, by the Metropolis algorithm, are analyzed and temporarily stored until we accumulate four of them. At this point, the four matrices are renormalized in both space and time as described in Chapter 7. Still, the resulting $M/2 \times N/2$ matrix is analyzed and temporarily stored until four similar ones have been accumulated. The same process continues until the size of the original system permits.

This whole process generates different levels of results and analyses. Level 0 is the original matrix on which the Monte Carlo simulation is performed. Each next RG level has the size of its corresponding system matrix divided by two and the number of data points in time divided by four. Our goal is to compute the time-time correlation functions as determined by equation (3.13) (page 33). This has to be done for all the levels involved. Because the process will be running for a long time, saving the complete history of each system is not realistic. This suggests the idea of "rings". For each parallel system, and each level of RG, a ring of a size such that a few τ of data can be saved will be constructed. To fill each ring, every time a new system matrix is obtained —from the raw Monte Carlo generator or from the MCRG process— the values of magnetization are computed for all systems in parallel and then saved in their respective ring. Each new magnetization data set obtained will be saved around this ring and the correlation of the present values with the magnetization values obtained at previous times will be computed.

This way, the function $\varphi_M(t)$ can be constructed for each of the, say 32, systems in parallel, and for each of the RG level. The time t will run from 0 to some value[2] usually taken as a few relaxation times τ. Each of the correlation functions forming the time-time correlation function $\varphi_M(t)$ (cf. equation (3.13) on page 33) is averaged in time

[2] Defined as *WINDOW* in the header file. Note that this value depends on τ which in turn depends on the system size.

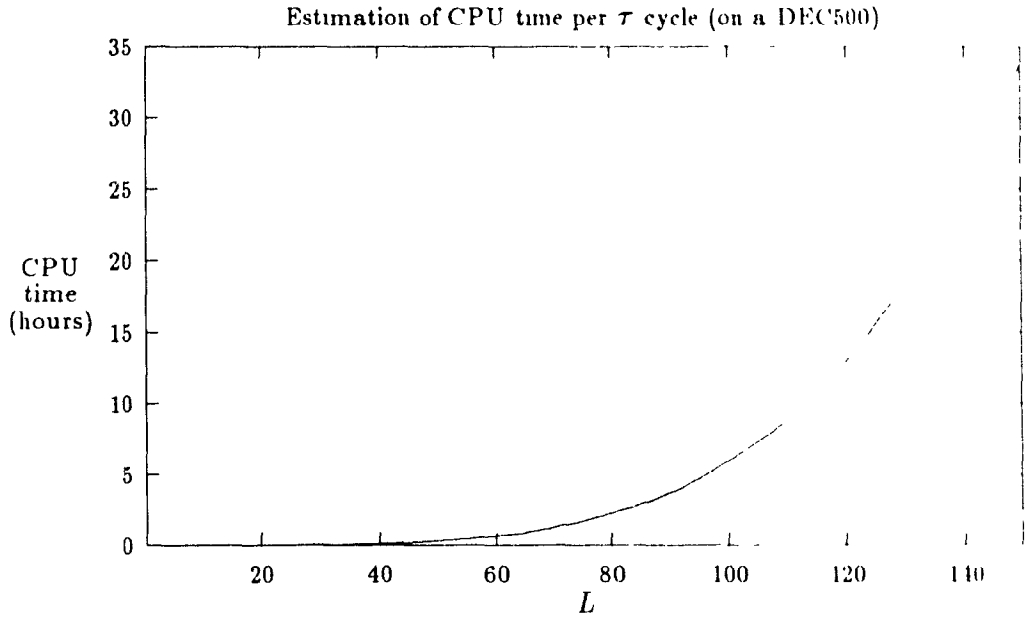

Figure A.1: Estimated CPU time for one τ cycle as a function of the system size L. The increase is due to (1) the increase of CPU time needed to process larger systems and (2) to the increase of τ as the system size increases. This makes it evident that larger systems are not technically accessible for now. This curve has been estimated from a DEC5000 workstation running the code found in this Appendix. No more than one order of magnitude improvement could be obtained from a supercomputer.

as the process goes on. At print time, an other average is made over all the systems in parallel.

The value τ is then extracted by fitting an exponential to $\varphi_M(t)$. This is done by using a least square fitting algorithm over a semi-log representation of the function. The extraction of the critical exponent z is then done according to the description given in Chapter 7.

Up to now, the major problem in obtaining data has been related to CPU time limitations. As figure A.1 shows, the estimated CPU time required to run a system of linear size L becomes incredibly large for $L \gtrsim 100$. This curve has been estimated from benchmarks obtained from running the code below on a DEC5000 workstation

Appendix B

C Listings

B.1 The makefile and header files

FILENAME MAKEFILE JAN 10 1991: 14:27

```
# Macro definitions
#
# parameters
# SIZE can be overidden by "make lcrin4 SIZE=64" for example
SIZE = 32
PAR = -DS$(SIZE)
CFLAGS = -O $(PAR)
LDFLAGS = -lm
CC = cc
# objects                                                          10
LCRIN4_OBJ = lutil.o lturn.o lana.o lctsrg.o

default
        @echo "Use to make lcrin4, clean"

lcrin4: $(LCRIN4_OBJ) lcrin4.c
        $(CC) $(CFLAGS) -o lcrin4 $(SIZE) lcrin4.c $(LCRIN4_OBJ) $(LDFLAGS)

$(LCRIN4_OBJ): lparam.h makefile
                                                                   20

clean
        @/bin/rm -f *.o test core
```

FILENAME LPARAM.H JAN 14 1991: 23:52

```
/* parameter file */
#ifdef S24 /* the size is 24 by 24 */
#define M 24
#define N 24
#define WINDOW 16384 /* observe for 2 $\tau$ Monte Carlo steps */
#define MCSTEP 16    /* analyse every 16 mcs */
```

```
#define AVG 1000    /* run for a thousand averages */
#endif
#ifdef S32
#define M 32
#define N 32
#define WINDOW 16384
#define MCSTEP 16
#define AVG 1000
#endif
#ifdef S48
#define M 48
#define N 48
#define WINDOW 32768
#define MCSTEP 16
#define AVG 500
#endif
#ifdef S64
#define M 64
#define N 64
#define WINDOW 65536
#define MCSTEP 32
#define AVG 500
#endif
#ifdef S96
#define M 96
#define N 96
#define WINDOW 98304
#define MCSTEP 32
#define AVG 500
#endif

#define SKIP 25    /* the number of averages between history function files */
#define WARMUP (10 * WINDOW) /* It says it all */
#define T 1 0  /* temperature in terms of Tc  */
#define LEVEL 5   /* This means 4 RG + 0   */

#define MAXRAND 2147483648 0  /* machine dependent  */
#define Tc  2 269185314213  /* from Onsager solution  */
#define MAXNAME 80
#define DATUM (WINDOW/MCSTEP)  /* number of raw data in time */
#define TNS (M*N)  /* total number of sites  */
#define THICK (8*sizeof(unsigned))  /* number of bit in an integer */
#define MFAC ((float)((float)M/MAXRAND)) /* speed up factors */
#define NFAC ((float)((float)N/MAXRAND))

#define ERROR (-1)
```

B.2 Utility functions

```
/* Utility file */
/* Last modification time 91/01/14 */
#include "lparam.h"


/* Lookup tables initialization for up right down left neighbours.
   This can be simplified to only two function, but I left four
   for sake of clarity. */

void umit(ulat, m)                                                    10
unsigned *ulat;
int m;
{
   int i,

   ulat[0] = m-1,
   for (i=1,i<m;i++) {
      ulat[i] = i-1;
   }
   return;                                                            20
}

void rmit(rlat, n)
unsigned *rlat,
int n;
{
   int j,

   for (j=0,j<n-1;j++) {
      rlat[j] = j+1;                                                  30
   }
   rlat[n - 1] = 0;
   return;
}

void dmit(dlat, m)
unsigned *dlat;
int m,
{
   int i;                                                             40

   for (i=0,i<m - 1,i++) {
      dlat[i] = i+1,
   }
   dlat[m - 1] = 0,
   return;
}

void lmit(llat, n)
unsigned *llat;                                                       50
int n;
{
```

```
    int j;

    llat[0] = n-1;
    for(j=1;j<n;j++) {
        llat[j] = j-1;
    }
    return;
}

#include <stdio.h>
/* required on certain systems  */
/************************
#include <stdlib.h>
************************/
/* Allocation routines for speeding up access to the matrix
   as well as for more flexibility on the sizes and indices  */

unsigned **alloc_uint_mat(m, n)
int m, n;
{
    unsigned **ptr;
    int i;

    ptr = (unsigned **)calloc((unsigned)m, sizeof(unsigned *));

    if (ptr == (unsigned **)NULL) {
        fprintf(stderr,"Error 1 in unsigned matrix allocation\n");
        exit(1);
    }

    for (i=0;i<m;i++) {
        ptr[i] = (unsigned *)calloc((unsigned)n, sizeof(unsigned));
        if (ptr[i] == (unsigned *)NULL) {
            fprintf(stderr,"Error 2 in unsigned matrix allocation\n");
            exit(1);
        }
    }
    return(ptr);
}

int **alloc_int_mat(m, n)
int m, n;
{
    int **ptr;
    int i;

    ptr = (int **)calloc((unsigned)m, sizeof(int *));

    if (ptr == (int **)NULL) {
        fprintf(stderr,"Error 1 in int matrix allocation\n");
        exit(1);
    }
```

```
    for (i=0,i<m;i++) {
        ptr[i] = (int *)calloc((unsigned)n, sizeof(int));
        if (ptr[i] == (int *)NULL) {
            fprintf(stderr,"Error 2 in int matrix allocation\n");
            exit(1);
        }
    }
    return(ptr);
}


float **alloc_float_mat(m, n)
int m, n;
{
    float **ptr,
    int i;

    ptr = (float **)calloc((unsigned)m, sizeof(float *));

    if (ptr == (float **)NULL) {
        fprintf(stderr,"Error 1 in float matrix allocation\n");
        exit(1);
    }

    for (i=0;i<m,i++) {
        ptr[i] = (float *)calloc((unsigned)n, sizeof(float));
        if (ptr[i] == (float *)NULL) {
            fprintf(stderr,"Error 2 in float matrix allocation\n");
            exit(1);
        }
    }
    return(ptr),
}


int *alloc_int_vec(n)
int n,
{
    int *ptr;

    ptr = (int *)calloc((unsigned)n, sizeof(int));

    if (ptr == (int *)NULL) {
        fprintf(stderr,"Error in vector allocation\n");
        exit(1);
    }

    return(ptr),
}

float *alloc_float_vec(n)
```

```
int n,
{
   float *ptr;

   ptr = (float *)calloc((unsigned)n, sizeof(float)),

   if (ptr == (float *)NULL) {
      fprintf(stderr,"Error in vector allocation\n");
      exit(1);
   }

   return(ptr);
}

/* Generate a random configuration */
void ranit(slat)
unsigned** slat;
{
   register int i, j,
   long random();

   for (i=0;i<M;i++) {
      for (j=0;j<N;j++) {
         slat[i][j] = random() * random();
      }
   }
   return;
}

/* At RG level l, copy matrix old onto matrix new */
void lcp_mat(l, old, new)
unsigned **old, **new; /* from and to matrices */
int l; /* RG level, required to determine the size */
{
   register int i, j;
   extern int *msize, *nsize,

   for (i=0;i<msize[l];i++) {
      for (j=0;j<nsize[l];j++) {
         new[i][j] = old[i][j];
      }
   }

   return;
}


/* A subroutine saving the matrix */

savemat(avg, mat)
int avg;
unsigned int **mat;
```

```
{
        int i, j,                                                          210
        char filename[MAXNAME],
        FILE *fp,
        extern char *prog;

        sprintf(filename, "%s.mat", prog);
        if ((fp = fopen(filename, "w")) == NULL) {
                fprintf(stderr, "Could not open %s file.\n", filename);
                return (-1);
        }
        fprintf(fp, "Effective mcs:   %d\n", avg * WINDOW);                220
        for (i=0;i<M;i++) {
                for (j=0;j<N;j++) {
                        if (fprintf(fp, "%ud ", mat[i][j]) != 1) {
                                fprintf(stderr, "Error occured when saving configuration\n"),
                                return (-1);
                        }
                }
        }

        return;                                                            230
}

/* a subroutine reading the saved matrix */

readmat(filename, mat)
char *filename;
unsigned int **mat,
{
        int i, j;
        FILE *fp;                                                          240

        if ((fp = fopen(filename, "r")) == NULL) {
                fprintf(stderr, "Could not open %s file.\n", filename);
                return (-1);
        }
        for (i=0;i<M;i++) {
                for (j=0;j<N;j++) {
                        if (fscanf(fp, "%ud ", &mat[i][j]) != 1) {
                                fprintf(stderr, "Error occured when loading configuration\n");
                                return (-1);                               250
                        }
                }
        }

        return;
}
```

B.3 The magnetization analysis file

FILENAME: LANA.C JAN 9 1991 17 19

```
/* Analysis of the configurations */

#include "lparam.h"

static int *mvec; /* used to save results from the 32 configurations */
static int **prev, **next; /* 5 RG level lookup tables for the rings */
static int ***mring; /* the ring itself with 5 RG levels */
static int *rn; /* pointer to current ring position in each level */

/* Initializes the data rings used for saving the values
   of the magnetization kept in order to calculate the time- time
   correlation functions. There is no point in keeping data
   from very early configurations since these are not correlated
   any more. This is why a ring (a loop) is used, which allows
   overwriting on results obtained from early configurations.
   This thus save computer space The following function
   only allocates this structure */

void init_rings()
{
   int ll, i, n;
   extern int *mvec;
   extern int **prev, **next;
   extern int ***mring;
   extern int *alloc_int_vec(),
   extern int **alloc_int_mat(),
   extern int *rn,
   extern int *datum;

   rn = alloc_int_vec(LEVEL);
   mvec = alloc_int_vec(THICK);

   mring = (int ***)calloc((unsigned)LEVEL, sizeof(int **)),

   prev = (int **)calloc((unsigned)LEVEL, sizeof(int *)),
   next = (int **)calloc((unsigned)LEVEL, sizeof(int *)),

   for (ll=0;ll< LEVEL;ll++) {
      n = datum[ll];
      mring[ll] = alloc_int_mat(THICK, n),
      prev[ll] = alloc_int_vec(n);
      next[ll] = alloc_int_vec(n),
      for(i=0;i<n,i++) {
         prev[ll][i] = i-1;
         next[ll][i] = i+1,
      }
      prev[ll][0] = n - 1;
      next[ll][n-1] = 0;
```

```
    }

    return,
}

/* This function calculates the magnetization out
   of the configuration. Each integer is treated as
   THICK (32 for a dec5000) bits, each of which being
   in an indepenident system. The only thing these systems
   have in common is the spin update history  */

void lana(ll, s)
int ll,        /* the RG level  */
unsigned **s,  /* pointer to the configuration matrix */
{
    register int tmp,
    register int i, j, k,
    extern int *mvec,
    extern *msize, *nsize;  /* size as a function of RG level  */
    extern int *tnsv; /* defined in main, total number of sites  */
    void store_m();

    tmp = -tnsv[ll];
    for (i=0,i < THICK; i++) {
        mvec[i] = tmp;
    }

    for (i=0, i < msize[ll]; i++) {
        for (j=0;j < nsize[ll];j++) {
            tmp = s[i][j];
            for (k=0,k<THICK;k++) {
                mvec[k] += 2 * (tmp&01),
                tmp >>= 1,
            }
        }
    }

    store_m(ll, mvec),

    return,
}

/* This function stores the magnetization in the proper
   RG level ring  It increments the position pointer to
   the next position found from the lookup table. */

void store_m(ll, m)
int ll,    /* the RG level  */
int *m;    /* a vector containing the THICK magnetization values */
{
    int k, n;
    extern int ***mring;
```

```
    extern int *rn,

    rn[ll] = next[ll][rn[ll]],
    n = rn[ll];

    for (k=0,k< THICK,k++) {
        mring[ll][k][n] = m[k],
    }

    return;                                                    110
}


/* Calculates the time–time correlation function for
   the ll RG level. Actually it finds three minimal sums
   of the definition of φ_M(t)   */

void lcorr_m(ll, sum1, sum2, sum3)
int ll;
float **sum1, **sum2, **sum3;                                  120
{
    extern int ***mring,
    extern int *datum;  /* contains the size of the rings */
    int i, k, t, n;
    int nn, **p;

    p = mring[ll];
    n = rn[ll];

    for (k=0;k <THICK;k++) {                                   130
        nn = n;
        for (t=0;t<datum[ll],t++) {
            sum1[k][t] += (float) (p[k][n] * p[k][nn]);
            sum2[k][t] += (float)  p[k][nn];
            sum3[k][t] += (float) (p[k][nn] * p[k][nn]);
            nn = prev[ll][nn];
        }
    }

    return,                                                    140
}
```

B.4 The *Metropolis* algorithm

FILENAME. LTURN.C JAN 9 1991 17 19

```
/* the Monte Carlo Metropolis algorithm */
#include "lparam.h"

static int *up, *rt, *dn, *lt;  /* the neighbour lookup tables */
```

```
/* Allocates and initializes the lookup tables */
void init_lturn()
{
    extern int *alloc_int_vec(),
    extern int *up, *rt, *dn, *lt,
    extern void uinit(), rinit(), dinit(), linit(),

    up = alloc_int_vec(M),
    rt = alloc_int_vec(N),
    dn = alloc_int_vec(M),
    lt = alloc_int_vec(N);

    uinit(up, M);
    rinit(rt, N);
    dinit(dn, M),
    linit(lt, N);

    return;
}


/* The one that makes it all */
void lturn(s,mcs,pro)
unsigned **s;  /* the matrix */
int mcs,       /* the number of mcs to run for */
long pro[2],   /* the Boltzmann factors (2 in 2 D is enough) */
{
    int ranvec3, ranvec4;  /* vector of bits generated with a
                              probability equal to the one of
                              flipping a spin when 3 or 4 of its
                              neighbours are parallel to it. */
    static int tns = TNS;   /* total number of sites in level 0 */
    static float mfac = MFAC; /* random # generator dependent factors */
    static float nfac = NFAC;
    int i, j, k;  /* utility integers */
    int a, b,
    register unsigned n1, n2, n3, n4;
    register unsigned c3pu, c4pu;  /* case n parallel neighbours up */
    register unsigned c0pd, c1pd, c2pd, c3pd, c4pd; /* case n par. nei. down */
    register unsigned nalla, nallo, site, wsite; /* all_and, all_or */
    register unsigned odd, n1a2, n3a4, n1o2, n3o4; /* 1and/or2, ... */
    register unsigned used3, used4, /* which random number used */
    long random(),

    ranvec3 = 0,
    ranvec4 = 0;
    used3 = 0,
    used4 = 0;

    for(k=0,k<THICK,k++) {  /* generate the Boltzmann distributed bits */
        if (random() <= pro[0]) {
```

```
            ranvec3 |= 01<<k;
        }
        if (random() <= pro[1]) {
            ranvec4 |= 01<<k;
        }
    }

    for (a=0;a<mcs;a++) {  /* turn' */
        for (b=0,b<tns;b++) {
            i = random() * mfac;  /* choose a i from 0 to M  */
            j = random() * nfac;  /* choose a j from 0 to N */

            for(k=0;k<THICK;k++) {  /* refresh the used bits  */
                if (used3&01) {
                    if (random() <= pro[0]) {
                        ranvec3 |= 01<<k;  /* turn or leave it on  */
                    }
                    else {
                        ranvec3 &= ~(01<<k); /* turn or leave it off */
                    }
                }
                used3 >>= 1;
                if (used4&01) {
                    if (random() <= pro[1]) {
                        ranvec4 |= 01<<k;
                    }
                    else {
                        ranvec4 &= ~(01<<k),
                    }
                }
                used4 >>= 1;
            }

            site = s[i][j];  /* the site */
            n1 = s[up[i]][j];  /* the four neighbours */
            n2 = s[i][rt[j]];
            n3 = s[dn[i]][j];
            n4 = s[i][lt[j]];

            wsite = ~site;  /* to make it legible  */
            odd = n1 ^ n2 ^ n3 ^ n4, /* oddness */
            n1o2 = n1 | n2;
            n3o4 = n3 | n4;
            nallo = n1o2 | n3o4,
            n1a2 = n1 & n2;
            n3a4 = n3 & n4;
            nalla = n1a2 & n3a4;

            /* the different cases  */
            c3pu = (n1a2 ^ n3a4) & odd & site,
            c4pu = site & nalla;
```

```
        c0pd = wsite & nalla,
        c1pd = (n1a2 ^ n3a4) & odd & wsite,
        c2pd = ~(odd | nalla | site) & nallo;
        c3pd = wsite & (n1o2 ^ n3o4) & odd,
        c4pd = ~(site | nallo);

        /* remember those bits we will use */
        used3 = c3pd|c3pu;
        used4 = c4pd|c4pu;

        /* random flip for these cases only */
        c4pd &= ranvec4;
        c4pu &= ~ranvec4;
        c3pd &= ranvec3;
        c3pu &= ~ranvec3;

        /* this choice takes care of flipping automatically the others */
        s[i][j] = c0pd|c1pd|c2pd|c3pd|c4pd|c3pu|c4pu;
      }
    }
    return;
}
```

B.5 The MCRG algorithm

FILENAME: LCTSRG.C JAN 9 1991 17:19

```
/* majority rule space-time MCRG */
#include "lparam.h"

/* Takes 16 spins from 4 systems at contiguous times and does
   a majority rule blocking in order to generate a renormalized
   system of half the size of the original ones. */

void lctsrg(ll, old, new)
int ll,  /* the current RG level */
unsigned ***old, **new;  /* the level ll and ll+1 matrices */
{
    int i, j, k,
    register unsigned b1, b2, b3, b4, b5, b6, b7, b8;
    register unsigned b9, b10, b11, b12, b13 b14, b15, b16;
    unsigned word, result;
    extern int *msize, *nsize;
    extern long random(),

    for (i=1;i< msize[ll];i+=2) {
        for (j=1,j< nsize[ll];j+=2) {
            word = 0;
            b1 = old[0][i][j];
            b2 = old[1][i][j];
            b3 = old[2][i][j],
```

```
b4 = old[3][i][j],
b5 = old[0][i][j-1],
b6 = old[1][i][j-1];
b7 = old[2][i][j-1],
b8 = old[3][i][j-1];
b9 = old[0][i-1][j],
b10 = old[1][i-1][j];
b11 = old[2][i-1][j],
b12 = old[3][i-1][j];
b13 = old[0][i-1][j-1],
b14 = old[1][i-1][j-1],
b15 = old[2][i-1][j-1];
b16 = old[3][i-1][j-1];
for (k=0;k< THICK,k++) {
   result = (b1&01)+(b2&01)+(b3&01)+(b4&01)+(b5&01)+(b6&01)+
         (b7&01)+(b8&01)+(b9&01)+(b10&01)+(b11&01)+
         (b12&01)+(b13&01)+(b14&01)+(b15&01)+(b16&01),

   if (result > 8) {
      result = 1,
   }
   else if(result == 8) {
      result = 0,
      if (random() > MAXRAND/2.0) {
         result = 1;
      }
   }
   else {
      result = 0;
   }

   b1 >>=1;
   b2 >>=1;
   b3 >>=1;
   b4 >>=1;
   b5 >>=1;
   b6 >>=1,
   b7 >>=1;
   b8 >>=1;
   b9 >>=1;
   b10 >>=1;
   b11 >>=1;
   b12 >>=1;
   b14 >>=1;
   b13 >>=1,
   b14 >>=1;
   b15 >>=1;
   b16 >>=1;
   result <<= k;
   word |= result,
}
new[(i-1)/2][(j-1)/2] = word;
```

```
    }
  }

}
```

B.6 The main program file

FILENAME LCRIN4 C JAN 15 1991 01 28

```
/* The main program */
/* lcrin4b c version with a history */
/* Last modification time 91/01/14 */
#include <math.h>
#include <stdio h>
#include "lparam.h"

                /* utility allocation functions */
int *alloc_int_vec();
unsigned **alloc_uint_mat();
float **alloc_float_mat();
void lamio();

char *prog,              /* the program name */
int *up, *rt, *dn, *lt,   /* neighbours lookup vectors */
int *tnsv;              /* total number of sites f(RG) */
int *datum,              /* number of time data points */
int *msize, *nsize,      /* m X n matrix */

main(argc, argv)
int argc;
char **argv,
{
   long pro[2],   /* the Boltzmann factor in terms of MAXRAND */
   int avg;      /* the current number of averages */
   int l, t, m, n,  /* utility integers */
   int n0, n1, n2, n3; /* RG level 0-4 counters */
   unsigned ***s0, ***s1, ***s2, ***s3, **s4; /* the 5 RG level systems */
   float ***msum1, ***msum2, ***msum3; /* minimal sums required to
                                  compute φ_M(t) */
   int time(), srandom();
   void lcp_mat(), ranit();
   void lana(), lturn();
   void init_lturn(), init_rings();

   prog = argv[0];

        if (argc >2) {
                fprintf(stderr, "Usage:  %s [saved_matrix_file]\n", prog);
                exit(1),
```

```
    }

/* allocation and initialization of all the variables */
msum1 = (float ***)calloc((unsigned)LEVEL, sizeof(float **)),
msum2 = (float ***)calloc((unsigned)LEVEL, sizeof(float **)),
msum3 = (float ***)calloc((unsigned)LEVEL, sizeof(float **)),
/* each s? fills up to four matrices and then renormalizes */
s0 = (unsigned ***)calloc((unsigned)4, sizeof(unsigned **)),
s1 = (unsigned ***)calloc((unsigned)4, sizeof(unsigned **)),
s2 = (unsigned ***)calloc((unsigned)4, sizeof(unsigned **)),
s3 = (unsigned ***)calloc((unsigned)4, sizeof(unsigned **)),

tnsv = alloc_int_vec(LEVEL);
msize = alloc_int_vec(LEVEL),
nsize = alloc_int_vec(LEVEL);
datum = alloc_int_vec(LEVEL);

t = DATUM;
m = M;
n = N,
for (l=0;l<LEVEL,l++) {
   datum[l] = t;
   msize[l] = m;
   nsize[l] = n;
   tnsv[l] = m*n;
   msum1[l] = alloc_float_mat(THICK, t);
   msum2[l] = alloc_float_mat(THICK, t),
   msum3[l] = alloc_float_mat(THICK, t),

   t /=4;   /* RG divides time by 4  */
   m /=2,   /* and divides space by 2 */
   n /=2;
}
for (t=0;t< 4;t++) {
   s0[t] = alloc_uint_mat(M, N);
}
for (t=0;t< 4;t++) {
   s1[t] = alloc_uint_mat(M/2, N/2),
}
for (t=0;t< 4,t++) {
   s2[t] = alloc_uint_mat(M/4, N/4),
}
for (t=0;t< 4,t++) {
   s3[t] = alloc_uint_mat(M/8, N/8),
}

s4 = alloc_uint_mat(M/16, N/16);

init_rings();
init_lturn(),

/* computes the Boltzmann from the Temperature in Tc units */
```

```
pro[0] = (long) (exp(-4.0/(T * Tc)) * MAXRAND),
pro[1] = (long) (exp(-8.0/(T * Tc)) * MAXRAND),

srandom(time((long *)NULL)),   /* seed the generator with time */

      if (argc == 2) {  /* read the previously prepared matrix file  */
            if (readmat(argv[1], s0[3]) == ERROR) {
            fprintf(stderr, "%s:  Error occured while reading file %s.\n", prog, argv[1]);
            exit(1);
            }
      }
      else {
   ranit(s0[3], M, N);    /* generate a random configuration */
   lturn(s0[3], WARMUP, pro);  /* bring it to T */
      }


n0 = n1 = n2 = n3 = 0;  /* this first loop fills the data rings */                    110
for (avg=1;avg<=4;avg++) { /* do it 4 times to fill all ring levels  */
   for (t=0;t<DATUM;t++) {
      lturn(s0[3], MCSTEP, pro);
      lana(0, s0[3]),
      if (n0 < 3)
         lcp_mat(0, s0[3], s0[n0]);
      if (++n0 == 4) {
         lctsrg(0, s0, s1[n1]),
         lana(1, s1[n1]);
         n0 = 0,                                                                    120
         if(++n1 == 4) {
            lctsrg(1, s1, s2[n2]),
            lana(2, s2[n2]),
            n1 = 0;
            if(++n2 == 4) {
               lctsrg(2, s2, s3[n3]),
               lana(3, s3[n3]),
               n2 = 0,
               if(++n3 == 4) {
                  lctsrg(3, s3, s4);                                                130
                  lana(4, s4);
                  n3 = 0;
               }
            }
         }
      }
   }
}

/* here is the real stuff  */                                                       140
for (avg=1;avg<=AVG;avg++) {
   for (t=0;t<DATUM,t++) {
      lturn(s0[3], MCSTEP, pro),
      lana(0, s0[3]),
```

```
        lcorr_m(0, msum1[0], msum2[0], msum3[0]);
        if (n0 < 3)
            lcp_mat(0, s0[3], s0[n0]),
        if (++n0 == 4) {
            lctsrg(0, s0, s1[n1]);
            lana(1, s1[n1]);
            lcorr_m(1, msum1[1], msum2[1], msum3[1]);
            n0 = 0;
            if(++n1 == 4) {
                lctsrg(1, s1, s2[n2]),
                lana(2, s2[n2]);
                lcorr_m(2, msum1[2], msum2[2], msum3[2]),
                n1 = 0;
                if(++n2 == 4) {
                    lctsrg(2, s2, s3[n3]);
                    lana(3, s3[n3]);
                    lcorr_m(3, msum1[3], msum2[3], msum3[3]),
                    n2 = 0;
                    if(++n3 == 4) {
                        lctsrg(3, s3, s4);
                        lana(4, s4);
                        lcorr_m(4, msum1[4], msum2[4], msum3[4]),
                        n3 = 0;
                    }
                }
            }
        }
    }

    /* saves the correlation function at each average */
    lanio(avg, msum1, msum2, msum3);
                /* saves the matrix at each average */
                if (savemat(avg, s0[3]) == ERROR) {
                        fprintf(stderr, "%s:  Error occured while saving matfile\n", prog),
                }
}

    return;
}

void lanio(avg, gsum1, gsum2, gsum3)
int avg,    /* the current average number */
float ***gsum1, ***gsum2, ***gsum3;  /* the minimal sums */
{
    FILE *fp;
    char fname[MAXNAME];
    float tmp2, tmp20;
    float num, denom1, denom2;
    float **sum1, **sum2, **sum3;
    int ll, t, k,
    float phi;
    float n,
```

```
    for (ll=0,ll< LEVEL;ll++) { /* do it for each level */
        sum1 = gsum1[ll];
        sum2 = gsum2[ll],                                          200
        sum3 = gsum3[ll];
        n = avg * datum[ll];

                    /* in order to keep a time history of the function */
        if (avg%SKIP) { /* give a different name every SKIP averages */
            sprintf(fname, "landm.%d", ll),
        }
        else {
            sprintf(fname, "landm%d.%d", avg, ll),
        }                                                          210


        if ((fp = fopen(fname, "w")) == (FILE *)NULL) {
            fprintf(stderr, "%s:  Could not open file %s\n", prog, fname);
            exit(1);
        }

        fprintf(fp, "RG level:  %d\n", ll);
        fprintf(fp, "avg:  %d\n", avg);
        fprintf(fp, "original system size:  %d X %d\n", M, N),     220
        fprintf(fp, "T (Tc):  %f\n", T);
        fprintf(fp, "Window size:  %d\n", MCSTEP*datum[ll]),
        fprintf(fp, "Analysed every:  %d\n\n", MCSTEP);
        fprintf(fp, "time\tphi(t)\n");

        for (t=0,t< datum[ll],t++) {
            phi = 0.0;
            for (k=0,k<THICK;k++) {
                tmp20 = sum2[k][0];
                tmp2 = sum2[k][t],                                 230
                num = n * sum1[k][t] - (tmp20 * tmp2),
                denom1 = sqrt(n * sum3[k][0] - (tmp20 * tmp20)),
                denom2 = sqrt(n * sum3[k][t] - (tmp2 * tmp2)),
                phi += num /(denom1*denom2);
            }
            phi /= (float) THICK;

            fprintf(fp, "%d\t%f\n", t*MCSTEP, phi),
        }
                                                                   240
        fclose(fp),
    }

    return,
}
```

References

Abraham, F. F. 1974. *Homogeneous Nucleation Theory.* Academic Press, New York

Achiam, Y. 1978. *J. Phys. A*, **11**, 975.

Achiam, Y. 1980. *J. Phys. A*, **13**, 1355.

Allen, S. M. and Cahn, J. W. 1979. *Act. Meta.*, **27**, 1085.

Andreev, A. F. 1964. *Soviet Physics JETP*, **18**, 1415.

Arfken, G. 1985. *Mathematical Methods for Physicists.* Academic Press, New York, third edition.

Bhanot, G. 1988. *Rep. Prog. Phys.*, **51**, 429.

Binder, K. 1974. *Advan. Phys.*, **23**, 917.

Binder, K. 1979. In Binder, K., editor, *Monte Carlo Methods in Statistical Physics*, volume 7 of *Topics in Current Physics.* Springer-Verlag, Berlin.

Binder, K. and Heermann, D. W. 1988. *Monte Carlo Simulation in Statistical Physics*, volume 80 of *Solid State Science.* Springer Verlag, Berlin, third edition.

Binder, K. and Stauffer, D. 1984. In Binder, K., editor, *Applications of the Monte Carlo Method in Statistical Physics.* Springer-Verlag, Berlin

Brout, R. 1965. *Modern Theory of Critical Phenomena.* Frontiers in Physics. The Benjamin/Cummings Publishing Co, Inc., Reading, Massachussets.

Brush, S. G. 1967. *Rev. Mod. Phys.*, **39**, 883.

Cahn, J. W. and Hilliard, J. E. 1958. *J. Phys. Chem.*, **28**, 258.

Cardy, J. L. 1985. *J. Phys. A*, **18**, 2771.

Doremus, R. H. 1985. *Rate of Phase Transformations.* Academic Press, Orlando.

Ferrenberg, A. M., Landau, D. P., and Binder, K. 1990 To be published.

Fisher, M. E. 1967. *Rep. Prog. Phys* , **30**, 615.

Gawlinski, E. T., Grant, M., Gunton, J. D., and Kaski, K. 1985. *Phys. Rev B*, **31**, 281.

Glauber, R. J. 1963. *J. Math. Phys.*, **4**, 294.

Grant, M. and Gunton, J. D. 1983. *Phys. Rev. B*, **28**, 5496.

Griffith, R. B. 1981. *Physica*, **106A**, 59.

Gunton, J. D. 1984. In Bowler, K. C. and McKane, A. J., editors, *Statistical and Particle Physics*, Edinburgh. A NATO Advanced Study Institute, Scottish Universities Summer School in Physics.

Gunton, J. D. and Droz, M. 1983. *Introduction to the Theory of Metastable and Unstable States.* Lecture Notes in Physics. Springer-Verlag, Berlin.

Gunton, J. D., San Miguel, M., and Sahni, P. S. 1983. In Domb, C. and Lebowitz, J. L., editors, *Phase Transition and Critical Phenomena*, volume 8. Academic Press, New York.

Halperin, B. I. and Hohenberg, P. C. 1969. *Phys. Rev.*, **177**, 952.

Halperin, B. I. and Hohenberg, P. C. 1977. *Rev. Mod. Phys.*, **49**, 435.

Heermann, D. W. 1984. *Z. Phyz. B*, **55**, 309.

Heller, P. 1967. *Rep. Prog. Phys.*, **30**, 731.

Hemmer, P. C. and Lebowitz, J. L. 1976. In Domb, C. and Green, M. S., editors, *Phase Transition and Critical Phenomena*, volume 5B. Academic Press, New York.

Hilhorst, H. J., Schick, M., and van Leeuwen, J. M. J. 1979. *Phys. Rev. B*, **19**, 2749.

Huang, K. 1987. *Statistical Mechanics.* Wiley, New York, second edition.

Ising, E. 1925. *Z. Physik*, **31**, 253.

Kadanoff, L. P., Götze, W., Hamblen, D., Hecht, R., Lewis, E. A. S., Palciaukas, V. V., Rayl, M., Swift, J., Aspnes, D., and Kane, J. 1967. *Rev. Mod. Phys*, **39**, 395.

Kaski, K., Yalabik, M. C., Gunton, J. D., and Sahni, P. S. 1983. *Phys. Rev. B*, **28**, 5263.

Katz, S. L., Gunton, J. D., and Liu, C. P. 1982. *Phys. Rev. B*, **25**, 6008.

Kawasaki, K. 1971. In Green, M. S., editor, *Fenomeni Critici*, New York. Scuola internazionale de fisica 'Enrico Fermi', Academic Press.

Kawasaki, K. 1972. In Domb, C. and Lebowitz, J. L., editors, *Phase Transition and Critical Phenomena*, volume 2. Academic Press, New York.

Kawasaki, K. 1976. In Domb, C. and Lebowitz, J. L., editors, *Phase Transition and Critical Phenomena*, volume 5B. Academic Press, New York.

Kawasaki, K. and Ohta, T. 1982a. *Prog. Theo. Phys.*, **67**, 147.

Kawasaki, K. and Ohta, T. 1982b. *Rep. Prog. Phys.*, **68**, 129.

Kennedy, A. D., Kuti, J., Meyer, S., and B.Pendelton 1986. *J Comp Phys*, **64**, 133

Kumar, S., Viñals, J., and Gunton, J. D. 1986. *Phys. Rev B*, **34**, 1906.

Landau, D. P., Tang, S., and Wansleben, S. 1988. *J. Phys.*, C-8, 1525.

Landau, L. and Lifshitz, E. 1981. *Physique Statistique*. Éditions Mir, Moscow, fourth edition.

Langer, J. S. 1971. *Annals of Physics*, **65**, 53.

Léontovitch, M. 1986. *Physique Statistique*. Éditions Mir, Moscow.

Lifshitz, I. M. 1962. *Soviet Physics JETP*, **15**, 939.

Ma, S.-K. 1976a. *Phys. Rev. Lett.*, **37**, 461.

Ma, S.-K. 1976b. *Modern Theory of Critical Phenomena*. Frontiers in Physics The Benjamin/Cummings Publishing Co, Inc., Reading, Massachussets.

Maris, J. M. and Kadanoff, L. P. 1978. *Am. J. Phys.*, **46**, 652.

Metropolis, N., Rosenbluth, A. W., Rosenbluth, M. N., Teller, A. H., and Teller, E. 1953. *J. Chem. Phys.*, **21**, 1087.

Müller-Krumbhaar, H. and Binder, K. 1973. *J. Stat. Phys.*, **8**, 1.

Niemeijer, T. and van Leeuwen, J. M. J. 1976. In Domb, C. and Lebowitz, J. L., editors, *Phase Transition and Critical Phenomena*, volume 6. Academic Press, New York.

Onsager, L. 1944. *Phys. Rev.*, **65**, 117.

Phani, M. K., Lebowitz, J. L., Kalos, M. H., and Penrose, O. 1980. *Phys Rev Lett*, **45**, 366.

Pippard, A. B. 1957. *Classical Thermodynamics*. Cambridge University Press, Cambridge.

Pippard, A. B. 1985. *Response and Stability*. Cambridge University Press, Cambridge.

Plischke, M. and Bergersen, B. 1989. *Equilibrium Statistical Physics*. Prentice Hall Advanced Reference Series. Prentice Hall, Englewood Cliffs, New Jersey.

Poole, P. H. and Jan, N. 1990. *J. Phys. A*, **23**, L453.

Press, W. H., Flannery, B. P., Teukolsky, S. A., and Vettering, W. T. 1988. *Numerical Recipes in C.* Cambridge University Press, Cambridge.

Roland, C. and Grant, M. 1988. *Phys. Rev. Lett.*, **60**, 2657.

Roland, C. and Grant, M. 1989. *Phys. Rev. B*, **39**, 11971.

Roland, C. M. 1989. *Growth and Scaling in First Order Phase transitions.* PhD thesis, McGill University.

Sadiq, A. and Binder, K. 1984. *J. Stat. Phys.*, **35**, 517.

Safran, S. A., Sahni, P. S., and Grest, G. S. 1983. *Phys. Rev. B*, **28**, 2693.

Sahni, P. S., Dee, G., and Gunton, J. D. 1981. *Phys. Rev. B*, **24**, 410.

Schmid, E. W., Spitz, G., and Lösch, W. 1988. *Theoretical Physics on a Personal Computer.* Springer-Verlag, Berlin.

Siggia, E. D. 1979. *Phys. Rev. A*, **20**, 595.

Stanley, H. E. 1971. *Introduction to Phase Transition and Critical Phenomena.* Oxford University Press, Oxford.

Swendsen, R. H. 1979. *Phys. Rev. Lett.*, **42**, 859.

Swendsen, R. H. 1984. In Bowler, K. C. and McKane, A. J., editors, *Statistical and Particle Physics,* Edinburgh. A NATO Advanced Study Institute, Scottish Universities Summer School in Physics.

Tartas, J. 1988. Domain growth in the ferromagnetic spin-flip ising model. Master's thesis, McGill University.

Tobochnik, J., Sarker, S., and Cordery, R. 1981. *Phys. Rev. Lett.*, **46**, 1417.

Valls, O. T. and Mazenko, G. F. 1986. *Phys. Rev. B*, **34**, 7941.

Viñals, J. 1990. Private communication.

Viñals, J., Grant, M., San Miguel, M., Gunton, J. D., and Gawlinski, E. T. 1985. *Phys. Rev. Lett.*, **54**, 1264.

Viñals, J. and Gunton, J. D. 1986. *J. Phys. A*, **19**, L933.

Wansleben, S. 1987. *Comp. Phys. Com.*, **43**, 315.

Wansleben, S. and Landau, D. P. 1987. *J. App. Phys.*, **61**, 3968.

Wegner, F. J. 1976. In Domb, C. and Green, M. S., editors, *Phase Transition and Critical Phenomena*, volume 6. Academic Press, New York.

Williams, J. K. 1985a. *J. Phys. A*, **18**, 1781.

Williams, J. K. 1985b. *J. Phys. A*, **18**, 49.

Wilson, K. 1971. *Phys. Rev. B*, **4**, 3174.

Yalabik, M. C. and Gunton, J. D. 1982. *Phys. Rev. B*, **25**, 531.

Zwanzig, R. and Allawadi, K. 1969. *Phys. Rev.*, **182**, 280.